University of Alberta

Soil aggregate turnover and the physical protection of soil organic matter as measured using Dy-labelled tracer spheres.

By

Alain François Plante

A thesis submitted to the Faculty of Graduate Studies and Research in partial fulfillment of the requirements for the degree of Doctor of Philosophy

in

Soil Science

Department of Renewable Resources

Edmonton, Alberta

Spring 2001

National Library of Canada
Acquisitions and Bibliographic Services
395 Wellington Street
Ottawa ON K1A 0N4
Canada

Bibliothèque nationale du Canada
Acquisitions et services bibliographiques
395, rue Wellington
Ottawa ON K1A 0N4
Canada

Your file Votre référence

Our file Notre référence

The author has granted a non-exclusive licence allowing the National Library of Canada to reproduce, loan, distribute or sell copies of this thesis in microform, paper or electronic formats.

L'auteur a accordé une licence non exclusive permettant à la Bibliothèque nationale du Canada de reproduire, prêter, distribuer ou vendre des copies de cette thèse sous la forme de microfiche/film, de reproduction sur papier ou sur format électronique.

The author retains ownership of the copyright in this thesis. Neither the thesis nor substantial extracts from it may be printed or otherwise reproduced without the author's permission.

L'auteur conserve la propriété du droit d'auteur qui protège cette thèse. Ni la thèse ni des extraits substantiels de celle-ci ne doivent être imprimés ou autrement reproduits sans son autorisation.

0-612-60334-2

Canada

University of Alberta

Library Release Form

Name of Author: Alain François Plante

Title of Thesis: Soil aggregate turnover and the physical protection of soil organic matter as measured using Dy-labelled tracer spheres.

Degree: Doctor of Philosophy

Year this Degree Granted: 2001

Permission is hereby granted to the University of Alberta Library to reproduce single copies of this thesis and to lend or sell such copies for private, scholarly or scientific research purposes only.

The author reserves all other publication and other rights in association with the copyright in the thesis, and except as herein before provided, neither the thesis nor any substantial portion thereof may be printed or otherwise reproduced in any material form whatever without the author's prior written permission.

Alain Plante

207-9915 88th Avenue
Edmonton AB T6E 2R4

Date: Jan 2, 2001

University of Alberta

Faculty of Graduate Studies and Research

The undersigned certify that they have read, and recommend to the Faculty of Graduate Studies and Research for acceptance, a thesis entitled "Soil aggregate turnover and the physical protection of soil organic matter as measured using Dy-labelled tracer spheres" submitted by Alain François Plante in partial fulfillment of the requirements for the degree of Doctor of Philosophy in Soil Science.

Dr. Denis Angers (External Examiner)

Dr. Lesley Fuller

Dr. William McGill (Supervisor)

Dr. Yongsheng Feng

Dr. Noorallah Juma

Dr. Jacob Masliyah

Date: Jan. 2, 2001

Dedication

for Mom, Dad and Jess

Abstract

Several studies have hypothesized that turnover of soil aggregates promotes soil organic matter losses under cultivation. Other studies suggest that the protection of organic matter requires occlusion into aggregates. However, few observations or quantifications of aggregate turnover are reported. We selected ceramic spheres for use as tracers and dysprosium as a label for detection by instrumental neutron activation analysis. From characterization of the tracers we concluded that mass and diameter variability was insufficient to affect their quantification. Tracer spheres were applied to field plots to measure aggregate turnover in contrasting field soils. Soil aggregation was cyclical and reset by the over-winter period and spring tillage. Tracers were rapidly incorporated into macroaggregate size fractions, demonstrating rapid soil aggregate turnover. Data from the field study were used to generate a quantitative model of aggregate dynamics consisting of four macroaggregate size fractions and first-order flows between them. Mean residence times of aggregate size compartments ranged from 4 to 95 days, and were generally shorter in the Breton versus Malmo soils. Higher aggregate turnover, higher relative soil respiration, and lower soil organic matter content in the Breton soil all suggest a lower capacity to physically protect organic matter, leaving more C available for mineralization. However, observations of aggregate turnover in Malmo soil suggest that turnover may also provide the opportunity for organic matter occlusion. A laboratory study measuring the decomposition of added particulate organic matter and aggregate dynamics under differing frequencies of simulated tillage supported the findings of the field study. Total soil respiration in incubated soils was higher in a once-tilled treatment, suggesting that more frequent tillage promoted the retention of organic matter. While

aggregate MWD was lower, frequently tilled samples showed greater incorporation of tracer spheres. We hypothesized that there may exist threshold rates of aggregate turnover that will occlude, rather than release organic matter. The work reported in this study represents a first attempt to observe and quantify gross soil aggregate turnover. Quantification of soil aggregate turnover is essential to testing hypotheses that aggregate turnover controls the accrual or loss of soil organic matter.

Acknowledgements

Many thanks are extended to my advisor Dr. Bill McGill for his sage advice and encouragement in the area of my research, for his financial support, for his encouragement to attend various conferences and meetings. Bill's reputation as a great academic supervisor preceded him, and is certainly well justified.

Thanks also to the other members of my advisor committee: Dr. Noorallah Juma for his support along way as a teaching mentor, Dr. Yongsheng Feng for his criticism of the kinetic analysis of the data, and Dr. Jacob Masliyah for his input and for his interest in a topic that drifted far away from his own expertise.

The development of the tracer sphere method could not have been possible without Mr. Jim Stensrud of Kinetico Inc. in Nashwauk MN. His supportive approach to the production of research-scale batches of tracers was instrumental to the work.

Who would have thought I'd end up working at a nuclear reactor? Dr. John Duke's assistance in developing the neutron activation protocol was "instrumental" to the tracer approach. His enthusiasm, support and assistance are greatly appreciated.

Elston Solberg, Jill deMulder and Alberta Agriculture, Food & Rural Development are thanked for their maintenance of, and access to the field plots used in the field experiment.

Thanks are extended to those who have provided technical support: Dr. Doug Craig for the tracer particle size analysis, Rashmi Sinha and Allison McLean for summer field assistance, and Sumithrai Vasanthan for lab assistance. Particular thanks to Clive Figueriedo for help with instrumentation and somehow always supplying the equipment I couldn't find.

A warm thanks goes out to all those in the Renewable Resources Department who shared my stay; Jeff, Sean, Heather and the numerous others who have made the past years memorable indeed.

A final thanks to Jessica for believing in me through thick and thin.

Table of Contents

CHAPTER 1:
Introduction: Soil aggregate dynamics and the dynamics of soil organic matter

1.0 Definition of terms 1
2.0 Models of soil aggregation 2
2.1 Random particle model 3
2.2 Microaggregate model 3
2.3 Hierarchical model 4
2.4 Concentric model 7
2.5 Aggregate formation models 7
3.0 Soil organic matter dynamics 8
4.0 Soil organic materials as aggregate binding agents 11
5.0 Soil aggregate dynamics: formation and degradation 14
6.0 Soil organic matter and aggregate interactions 22
6.1 SOM and aggregate associations 22
6.2 Soil aggregation controls on organic matter dynamics 26
7.0 Conclusions 30
References 34

CHAPTER 2:
Development of an inert tracer particle method for the study of soil aggregate dynamics

1.0 Introduction 41
1.1 Objectives 42
2.0 Materials and methods 42
2.1 Tracer sphere development 42
2.1.1 Tracer particle selection 42
2.1.2 Tracer detection 44
2.1.3 Tracer labelling 46
2.2 Tracer sphere characterization 48
2.2.1 Surface characteristics 48
2.2.2 Mass and size variability 49
2.2.3 Dysprosium concentration 49
2.2.4 Label leaching and tracer integrity 50
2.2.5 Detection limit 51

2.3 Quantification of tracer spheres by INAA 52
3.0 Results 53
3.1 Surface characteristics 53
3.2 Mass and size variability 53
3.3 Dysprosium concentration 54
3.4 Label leaching and tracer integrity 54
3.5 Detection limit 55
4.0 Discussion 56
5.0 Conclusion 58
References 69

CHAPTER 3:
A particle tracer and wet sieving approach to the study of soil aggregate dynamics

1.0 Introduction 72
1.1 Objectives 73
2.0 Materials and methods 73
2.1 Pre-treatments applied 73
2.2 Wet sieving procedure 74
2.3 Tracer content 74
2.4 Mean-weight diameter calculations 75
3.0 Results 75
4.0 Discussion 77
5.0 Conclusions 78
References 84

CHAPTER 4:
Intra-seasonal turnover of soil aggregates in two contrasting field soils using a labelled tracer particle

1.0 Introduction 85
1.1 Objectives 86
2.0 Materials and methods 86
2.1 Experimental field sites 86
2.2 Water-stable aggregate size distribution 88
2.3 Tracer content 89
2.4 Statistical analyses 89
3.0 Results and Discussion 90
3.1 Patterns of soil aggregation 90

3.2 Tracer sphere incorporation 91
3.3 Spatial fate of incorporated tracer spheres 93
3.4 Dynamics of tracer sphere incorporation 94
4.0 Conclusions 95
References 105

CHAPTER 5:
A quantitative compartmental model of soil macroaggregate dynamics

1.0 Introduction 108
1.1 Objectives 109
2.0 Theory 109
3.0 Model development 111
3.1 Model calibration 112
3.2 Prediction of tracer sphere dynamics 113
4.0 Results and Discussion 114
4.1 Model structure 114
4.2 Kinetic parameters 115
4.3 Prediction of tracer sphere dynamics 117
4.4 Limitations of the model 118
5.0 Conclusions 119
References 128

CHAPTER 6:
Linking active organic matter dynamics and soil aggregate dynamics in two contrasting field soils

1.0 Introduction 131
1.1 Objectives 132
2.0 Materials and methods 132
2.1 Experimental field sites 132
2.2 Soil biochemical analyses 133
2.2.1 Total soil organic C 133
2.2.2 Soil respiration 133
2.2.3 Soil microbial biomass C 133
2.3 Soil physical analyses 134
2.4 Statistical analyses 134
3.0 Results 135
3.1 Soil physical analyses 135

3.2 Soil biochemical analyses 135
4.0 Discussion 136
4.1 Active organic matter dynamics 136
4.2 Linking aggregate dynamics and C dynamics 136
5.0 Conclusions 138
References 144

CHAPTER 7:
Soil aggregate dynamics and active organic matter dynamics in laboratory-incubated soil with differing simulated tillage frequencies

1.0 Introduction 146
1.1 Objectives 147
2.0 Materials and methods 148
2.1 Simulation of tillage energy 148
2.2 Soil respiration and stable C isotope ratio of CO_2 148
2.3 Water-stable aggregation 151
2.4 Tracer content 151
2.5 Stable isotope ratio of C in aggregate fractions 151
3.0 Results 152
3.1 Soil respiration and stable C isotope ratio of CO_2 152
3.2 Water-stable aggregation and tracer content 152
3.3 Stable isotope ratios of C in aggregate fractions 152
4.0 Discussion 153
4.1 Mineralization of added POM 153
4.2 Retention of SOM under differing frequencies of tillage 154
5.0 Conclusions 158
References 167

CHAPTER 8:
General Discussion and Conclusions

1.0 Synthesis 170
2.0 Summary of findings 170
2.1 Chapter 2: A tracer particle method for the study of soil aggregate dynamics 170
2.2 Chapter 3: Calibration of a wet sieving procedure to study aggregate dynamics 171
2.3 Chapter 4: Soil aggregate turnover in two contrasting field soils 171

2.4 Chapter 5: A quantitative model of soil macroaggregate dynamics 171
2.5 Chapter 6: Linking active organic matter dynamics with aggregate dynamics 172
2.6 Chapter 7: Physical protection of organic matter under simulated tillage 172
3.0 Implications and speculations 173
3.1 Measuring aggregate and organic matter turnover 173
3.2 Soil aggregate turnover and the protection of organic matter 174
3.3 The potential for tillage-enhanced physical protection of organic matter to maximize C sequestration 176
4.0 Future research.....177
4.1 Observing tracer particle dynamics from initially complete incorporation ..177
4.2 Simultaneous observations of different sized particle tracers.....178
4.3 Comparing particle tracer dynamics in tilled versus no-till soils 178
References 180

APPENDIX A:
Trace sphere application rates to field plots. 182

List of Tables

Table 1-1. Aggregate distribution (% retained) after wet sieving an aggregated clay soil. 32

Table 1-2. Kinetic parameters of decomposition of some organic compounds in soil. 32

Table 1-3. CENTURY model parameters used to describe soil organic matter dynamics. 32

Table 1-4a. Initial glass bead distribution in aggregate size fractions. 33

Table 1-4b. Final measured (A) and expected (B) glass bead distribution in aggregate size fractions. 33

Table 2-1. Tracer sphere mass and variability in composite samples from pilot-scale batch. 59

Table 2-2. Tracer sphere mass ($\mu g\ sphere^{-1}$) and variability in single sphere samples. 59

Table 2-3. Mean sphere sizes determined from image analysis data. 59

Table 2-4. Calculated and measured sphere densities (n = 4, average CV < 1%) 60

Table 2-5. Concentration of Dy label in single spheres (% wt). 60

Table 2-6. INAA counts from 2 mL water aliquots taken from sphere integrity tests. 60

Table 2-7. Dy content of soil samples with and without spheres from pilot-scale batch and associated calculated numbers of spheres. 61

Table 2-8. Pair-wise comparisons of means and variances of sphere characteristics between manufactured batches. 62

Table 2-9. Pair-wise comparisons of mean and variance of Dy concentration between sphere size fractions within batches. 62

Table 3-1. Mean soil aggregate and dysprosium mean weight diameters (mm). 79

Table 3-2. Statistical significance (*p*-values) of pre-treatment comparisons of soil MWD. 79

Table 3-3. Statistical significance (*p*-values) of pre-treatment comparisons of Dy MWD. 80

Table 4-1. Selected site characteristics and surface layer (0-15 cm) properties of field soils used (from Solberg et al. 1997). 97

Table 4-2. Selected properties of tracer particles applied to field plots. 97

Table 4-3. Mean tracer sphere recovery based on applied rates and detected Dy for the 1998 subplots (%). 98

Table 5-1. First-order constants and associated mean residence times of model aggregate size components. 120

Table 5-2. Statistical diagnostics of model predictions of tracer sphere dynamics. 120

Table 6-1. Selected properties of surface layer (0-15 cm) of field soils used in experiment 139

Table 6-2. Microbial biomass C from 1998 subplots (mg C kg^{-1} OD soil) 140

Table 7-1. Stable isotope ratio, $\delta^{13}C$ (‰), of reference samples and atmospheric CO_2-corrected soil respired CO_2. 159

Table 7-2. Proportion of soil respired CO_2 attributable to the mineralization of added POM (%). 159

Table 7-3. Stable isotope ratios of C, $\delta^{13}C$ (‰), in the pooled >1 mm aggregate fraction at the end of 8-week incubation. 159

List of Figures or Illustrations

Figure 2-1: Scanning electron micrograph of tracer spheres, showing (a) sealed exterior surface and (b) honeycombed interior. 63

Figure 2-2: Correction calculations to µg Dy determined by INAA. 64

Figure 2-3: Calibration curve relating deadtime to the pulse pile-up correction factor. 65

Figure 2-4: Cumulative particle size distributions of (a) large, (b) medium, and (c) small size fractions of Dy-labelled tracer spheres. 66

Figure 2-5: Tracer sphere Dy concentration as a function of sphere mass for the (a) pilot-, (b) 1998 field-, and (c) 1999 field-scale batches. 67

Figure 2-6: Typical gamma-ray spectra of (a) tracer spheres only, (b) soil only, and (c) soil and sphere mixture. 68

Figure 3-1. Water-stable aggregate size distribution of (a) Malmo, and (b) Breton samples. 81

Figure 3-2. Distribution of tracer Dy in water-stable aggregate size fractions of (a) Malmo, and (b) Breton samples. 82

Figure 3-3. Water-stable soil aggregate mean weight diameter as a function of antecedent soil moisture content in air-dried samples from field study reported in Chapter 4. 83

Figure 4-1. Water-stable soil aggregate size distribution in straw amended (T8) plots from (a) Malmo and (b) Breton soils. 99

Figure 4-2. Water-stable soil aggregate mean weight diameter (MWD). 100

Figure 4-3. Normalized tracer sphere Dy content of the pooled "aggregated" fraction (1 to >4 mm). 101

Figure 4-4. Tracer sphere Dy distribution in aggregate size fractions of straw amended (T8) plots from (a) Malmo and (b) Breton soils. 102

Figure 4-5. Tracer sphere Dy mean weight diameter (MWD). 103

Figure 4-6. Comparison of soil aggregate versus Dy MWD in straw amended (T8) plots from (a) Malmo and (b) Breton soils. 104

Figure 5-1. Schematic representation of (a) a fully developed model structure, and (b) an oversimplified model structure for aggregate dynamics. 121

Figure 5-2. Compartmental soil aggregate dynamics model fit for the Malmo soil. (■, calibration data from field study, –, model output) 122

Figure 5-3. Compartmental soil aggregate dynamics model fit for the Malmo soil. (■, calibration data from field study, –, model output) 123

Figure 5-4. Model structures for Malmo and Breton soils. (Numbers next to flow arrows represent proportion of material leaving compartment.) 124

Figure 5-5. Model predictions of tracer sphere dynamics in Malmo soil. (■, tracer sphere data from field study, –, model prediction) 125

Figure 5-6. Model predictions of tracer sphere dynamics in Malmo soil. (■, tracer sphere data from field study, –, model prediction) 126

Figure 5-7. Measured and predicted tracer Dy mean weight diameters for (a) Malmo and (b) Breton soils. 127

Figure 6-1. Carbon dioxide evolution in 10-day laboratory incubations on a per gram of soil basis. 141

Figure 6-2. Carbon dioxide evolution in 10-day laboratory incubations on a per gram of organic carbon basis. 142

Figure 6-3. Carbon dioxide evolution in 10-day laboratory incubations on a per gram of microbial biomass carbon basis. 143

Figure 7-1. Rate of CO_2 evolution from samples incubated under differing tillage frequencies. (Vertical lines represent timing of tillage events.) 160

Figure 7-2. Cumulative CO_2 evolved from samples incubated under differing tillage frequencies. (Vertical lines represent timing of tillage events.) 161

Figure 7-3. Soil respiration from POM and non-POM sources of organic C. 162

Figure 7-4. Water-stable soil aggregate mean weight diameters. 163

Figure 7-5. Tracer sphere Dy mean weight diameters. 164

Figure 7-6. Tracer Dy enrichment of water-stable aggregates >1 mm. 165

Figure 7-7. Conceptual representation of the relationships between soil aggregate turnover and organic matter mineralization for (a) incoming, initially free organic matter, and (b) native, protected organic matter. 166

List of Symbols, Nomenclature, or Abbreviations

INAA, instrumental neutron activation

MWD, mean weight diameter

POM, particulate organic matter

SOM, soil organic matter

Chapter 1:

Introduction: Soil aggregate dynamics and the dynamics of soil organic matter

1.0 Definition of terms

The term *soil structure* has been used extensively in the study of soils, and although its concept is generally understood, the use of many definitions for the term has perhaps created uncertainty about its application.

Brewer (1976) defines soil structure in the following terms:

> "the physical constitution of a soil material is expressed by the size, shape and arrangement of the solid particles and voids, including both the primary particles to form compound particles, and the compound particles themselves; fabric is the element of structure which deals with the arrangement".

In a philosophically styled article, Letey (1991) extended this definition to include a broader range of elements and processes. The definition presented was:

> "soil structure is the size, shape and arrangement of the solid particles and voids which is highly variable and associated with a complex set of interactions between mineralogical, chemical and biological factors".

Dexter (1988) provided an even broader definition for soil structure as: "the spatial heterogeneity of the different components or properties of soil". This definition certainly encompasses all possible elements, processes and resulting effects involved in structure, but is perhaps too broad to be useful. Kay (1990) used several terms to include both elements and processes to define soil structure. Kay defined *structural form* as "the heterogeneous arrangement of solid and void space that exists in soil at a given time", *structural stability* as "the ability of a soil to retain its arrangement of solid and void space when exposed to different stresses", and *structural resiliency* as "the ability of a soil to recover its structural form through natural processes when the applied stresses are reduced or removed". According to these definitions, soil structure is both a static and dynamic soil property.

The terms *soil structure* and *soil aggregation* are not interchangeable. The classic definition of a soil aggregate is often attributed to Martin et al. (1955) as:

> "naturally occurring cluster or group of soil particles in which the forces holding the particles together are much stronger than the forces between adjacent aggregates"

While soil structure implies a certain reference to architecture and thus refers to the physical arrangement of both particles and pores, soil aggregation refers only to composite soil particles (aggregates, peds or clods), and the processes creating the composite particles. The distinction between structure and aggregation was well expressed by Allison (1969), when he pointed out that a soil may have "good structure … when few aggregates are present".

Soil aggregation as a process includes both the formation and stabilization processes that create composite soil particles. During aggregation, the processes of formation and stabilization can be independent and sequential, or simultaneous. The terms *aggregate formation* and *structure formation* can be used interchangeably, noting that aggregate formation will result in, but does not make reference to changes in the soil porosity.

Aggregate degradation refers to the breakdown of large aggregates to release smaller aggregates or primary particles as a result of the input of disruptive energy. The process of aggregate breakdown makes no reference to chemical or biological degradation, or to the decomposition of organic materials.

2.0 Models of soil aggregation

As methods of soil dispersion and electron microscopy have improved, the view of soil as an aggregation of primary particles has developed. The need to explain how soil particles interact to form aggregates of various sizes has prompted the development of a series of models of soil aggregation.

2.1 Random particle model

The simplest of such models are soil as a solid mass with a random distribution of failure planes[1], or aggregates as random assemblages of primary particles. This concept is reflected in the manner by which some researchers have approached aggregation in their experimental methods. In a study examining the stability of soil aggregates, Kemper et al. (1987) sonically dispersed soil into the primary sand, silt and clay fractions and recombined the fractions to create soils with increasing clay contents. The created soil pastes were passed through a 2 mm sieve to create "aggregates". This methodology suggests that macroaggregates are formed by direct, random interactions between primary particles.

2.2 Microaggregate model

Using ultrasonic dispersion methods, Edwards and Bremner (1967) developed their "microaggregate theory". The authors found that macroaggregates are easily disrupted and that most of the dispersion energy is expended in disrupting stable microaggregates. Hence, they propose that the fundamental structural units in soil are silt-size microaggregates (< 250 μm), which they represented as a compound particle of clay particles bound together by humified organic matter and polyvalent metals. Macroaggregates are thus a combination of microaggregate sub-units. The processes of macro- and microaggregate formation and dispersion are proposed to be the same process occurring in different directions. The reversible process was represented as:

$$[(\text{C-P-OM})_x]_y \leftrightarrow y(\text{C-P-OM})_x \leftrightarrow xy(\text{C-P-OM}) \qquad (1)$$

where (C-P-OM) may be viewed as an organo-mineral complex, $(\text{C-P-OM})_x$ as a microaggregate, and $[(\text{C-P-OM})_x]_y$ as a macroaggregate.

The hypothesis that aggregate formation is a reversal of dispersion was supported by experiments showing increases in fine sand-size and silt-size aggregation after drying dispersed soil solutions. In addition to proposing and evaluating their model, Edwards

---

[1] B.D. Kay, 1996, personal communication.

and Bremner concluded by stating some of the implications of their model in reference to the accumulation of organic materials in aggregates. Many of these implications have been tested continuously over the past thirty years. Although the authors themselves recognized that their model might be overly simplified, the microaggregate theory has become a fundamental concept used in our understanding of soil mineral and organic matter associations.

2.3 Hierarchical model

Building on the implications of the microaggregate model, several researchers have proposed soil aggregation as a hierarchy (Williams et al. 1967; Dexter 1988; Oades and Waters 1991). The hierarchical model proposes that soil aggregates are not necessarily composed of a random arrangement of primary soil particles (i.e. sand, silt and clay). Rather, larger aggregates are composed of smaller aggregates, which in turn comprise clusters of primary particles. As a matter of illustration, the hierarchical model would suggest that a large aggregate of 1000 unit size, is not necessarily composed of 1000 particles of 1 unit size, but rather 50 particles of 20 unit size or 20 particles of 50 unit size. The hierarchical model of soil aggregation has since become a predominant paradigm in soil science and its implications are integral in our understanding of soils. Hence, rather than report on the model in a direct manner, the evidence used to support the model and the body of literature that has developed out of the paradigm will be examined throughout this review.

Early evidence for the hierarchical nature of soil aggregation was provided by Currie (1966), who measured the porosity of soil aggregates and predicted increasing porosity with increasing aggregate size. Dexter (1988) presented this as the "porosity exclusion principle". The principle states that larger aggregates have greater porosity due to increasing amounts of inter-microaggregate or intra-macroaggregate pores.

Additional evidence for soil aggregate hierarchy is provided by studies of aggregate strength and failure. Because aggregate fracture occurs due to the elongation and separation of cracks within an aggregate (which creates new surfaces), and since the distribution of cracks within an aggregate is assumed to be random, one can expect

increasing aggregate strength with decreasing aggregate size. This is because the probability of engaging a crack decreases with decreasing aggregate volume (Hadas and Wolf 1984). It was also theorized that the aggregate strength would depend on the hierarchical level of aggregation (Hadas 1987). In aggregate failure studies, Hadas used a statistical theory developed by Braunack et al. (1979) to relate ped failure strength to aggregate composition. The statistical theory developed by Braunack et al. proposes that an aggregate of volume V has a critical stress σ, and is made up of n sub-units of volume V_o that each have an internal strength σ_0. The diameter of the basic cell unit D_o, and the internal strength σ_0, can be calculated from the measured mean critical stress and the variance using the following equations (Braunack et al. 1979):

$$\bar{\sigma} = \sigma_0 \cdot \left(\frac{V}{V_0}\right)^{-\frac{1}{m}} \cdot \Gamma\left(1+\frac{1}{m}\right) \tag{2}$$

$$\sigma_{var} = \sigma_0^2 \cdot \left(\frac{V}{V_0}\right)^{-\frac{1}{m}} \cdot \left[\Gamma\left(1+\frac{2}{m}\right) - \Gamma^2\left(1+\frac{1}{m}\right)\right] \tag{3}$$

where m is a parameter of the soil related to the spread of failure zones, and Γ is the gamma function. The parameter values are determined by linear regression of a log-log plot of mean tensile strength ($\bar{\sigma}$) versus mean volume ($\bar{V}$). The regressions performed by Hadas (1987), resulted in unit cell diameter (D_0) values smaller than the mid-point of each aggregate size fraction and larger than primary particle diameters. The author concluded that the results support the concept of aggregate hierarchy, and that the distribution of soil aggregate strength was a result of differing volume fractions of various smaller aggregates within a given macroaggregate fraction.

The concept of aggregation as a hierarchy is further supported by experiments examining the breakdown of aggregates of three soil types under different levels of applied energy (Oades and Waters 1991). The authors hypothesized that if an aggregate hierarchy exists, then the aggregates would break down in a step-wise fashion without the initial release of silt and clay sized particles. Conversely, if the aggregates break down to release silt and clay sized materials directly, then no hierarchy exists. The authors measured the

aggregate size distribution of materials released after slow-wetted sieving compared to fast-wetted sieving, end-over-end shaking, and sonication. In the case of Alfisol and Mollisol samples, the results indicated stepwise aggregate break-down since fast-wetting released few particles < 20 μm and shaking released only a fraction of the clay. Sonication resulted in a particle size distribution similar to that achieved after chemical treatments. After examining differences in the aggregate size distributions between treatments, the authors suggested that fast-wetting disrupted aggregates >250 μm, shaking disrupted aggregates about 100 μm, and sonication disrupted aggregates 2-20 μm in diameter. In the case of the Oxisol samples, aggregate hierarchy was not observed to the same extent as silt and clay particles were released immediately. The authors used this observation as further support for the hierarchical behaviour observed in Alfisols and Mollisols.

The results reported by Oades and Waters support and help explain earlier findings by Coughlan et al. (1973a,b). The authors suggested that large aggregates of lower hierarchical order (i.e. secondary or tertiary aggregates) would exist only if the water stability of the larger aggregate is greater than that of the smaller constituent aggregates. Initial experiments (1973a) showed that the water stability of aggregates 0.1 - 0.5 mm were at a maximum, and larger aggregates had decreasing water stability. Additional experiments (1973b) yielded interesting and significant results showing that the distribution of the unstable fraction retained by any sieve was independent of the dry aggregate size originally selected (Table 1-1). The authors used the data generated to produce a single probability function to describe the distribution of the unstable fraction of each aggregate size fraction. The authors did not discuss the physical significance of a single probability function. However, the results appear to indicate that aggregates are composed of fairly uniform proportions of smaller aggregates, suggesting that the formation of increasingly larger aggregates consists of the simple addition of larger units.

The results of the experiments performed by Oades and Waters, and Coughlan et al. suggest that the breakdown of aggregates may be a function of their hierarchical composition of smaller aggregates with increasing water stability. Hence aggregate

breakdown is largely a function of aggregate formation mechanisms (Coughlan et al. 1973b) and/or the nature of the binding materials that keep the individual component aggregates together in the larger aggregate (Oades and Waters 1991).

Perhaps the best evidence for soil aggregate hierarchy is that provided by the examination of the organic binding agents. The hierarchy theory suggests that macroaggregates are enriched in organic matter compared to microaggregates, due to increased amounts of materials binding microaggregates into macroaggregates, and that the composition of the organic materials would differ between micro- and macroaggregates. Experimental evidence supporting these hypotheses has been reported (*e.g.* Elliott 1986) and will be discussed later.

2.4 Concentric model

Not necessarily contrary to the hierarchy theory, another model of aggregation has had some support. Researchers seeking organic matter, ion, or particle gradients through aggregates (*e.g.* Wilcke and Kaupenjohann 1997) have implied a concentric model of aggregation. Recent work by Santos et al. (1997) has described a method to remove concentric surface layers from soil aggregates. By removing layers using abrasion caused by cyclone air currents, the authors have proposed three concentric zones within aggregates 3-5 mm in diameter. The authors also sought organic carbon and exchangeable cation gradients across the zones. While some cation gradients were observed, organic carbon contents did not differ significantly among zones. Although not discussed in the literature as extensively as the hierarchy theory, the concentric model goes a step further than the hierarchy theory by describing how the particles and microaggregates may be spatially arranged in a macroaggregate.

2.5 Aggregate formation models

Each of the three major models reported above has sound evidence for its description of the nature of soil aggregation. However, a significant deficiency of all the models is that they are supported by *dis*-aggregation data alone. Processes of aggregate formation, or the state of intact aggregates in soil are not fully addressed.

In addition, the microaggregate theory and the hierarchical model based on disaggregation data suggest that aggregation is bi-directional or reversible, *i.e.* aggregates sequentially break down to release increasingly smaller components, and by inference, aggregates are formed by the sequential combination of increasingly larger components. However, some researchers (Oades 1984; Beare et al. 1994a; Golchin 1994) have proposed an alternate model of aggregate formation.

Oades (1984) suggests that macroaggregates are formed first by compaction or the actions of roots and hyphae, and microaggregates are subsequently formed through physical and chemical means. Beare et al. (1994a) expanded this conceptual model by suggesting that as the particulate organic matter (POM) occluded in macroaggregates decomposes, aggregates of decreasing size are released until fine microaggregates (< 53 μm) containing humified clay- and silt-bound organic matter are released. Golchin et al. (1994) furthered the model by proposing a similar process for microaggregates. Evidence for the model is provided by experiments examining organic matter and aggregate associations, and the dynamics of the organic matter in these associations. These studies will be further discussed in the section below.

The small number of studies reporting observations of the process of aggregate formation reveals that there is uncertainty and insufficient evidence to conclude whether aggregate formation necessarily occurs in a directional, hierarchical fashion similar to aggregate degradation (*i.e.* from the bottom up) or in the manner proposed by Oades (1984) and others (*i.e.* from the top down). In a given soil, both processes may indeed be occurring simultaneously.

3.0 Soil organic matter dynamics

The organic matter in soil represents a significant source and sink in the global cycling of carbon. Soil organic matter encompasses living and dead organisms, belowground phytomass, and plant and animal debris in various stages of decomposition and stabilization. The focus of this section is the introduction of the dynamic nature of organic matter in soil (principally during decomposition), and its quantification. The heterogeneous nature of soil organic matter poses problems in quantifying decomposition

dynamics, hence two approaches have developed: 1) dynamics based on the kinetics of individual chemical components, and 2) dynamics based on purely kinetic (abstract or statistical) compartments.

The need to characterize the nature of soil organic matter has led to studies examining the effect of the chemical nature of organic matter on its decomposition kinetics. In addition, the use of kinetic equations such as first-order, Michealis-Menten, or Monod kinetics, requires a defined chemical substance. Research in this area is summarized in a study reporting the decomposition of radio-labeled substrates in soil (Paul and van Veen 1978). The authors begin with the composition of soil organic matter in terms of chemical constituents (50% aromatics, 20% amino acids, 10-20% carbohydrates, 10% long-chain fatty acids) and state that the composition varies little between differing soils. Using cited data and first-order kinetics, the authors then developed a simple model to describe the decomposition of several compounds, yielding kinetic constants for each constituent (Table 1-2).

The value of results yielded from using chemical fractionation has proven limited because chemical composition is an important factor only in the short term (Oades 1988), and due to the incomplete description of soil organic matter dynamics that these results provide. Chemical fractionation does not account for functional or structural properties of organic materials, for example the encapsulation of labile cytoplasm substrates in a more recalcitrant cell wall or the encapsulation of cellulose in a lignin matrix. These functional properties often override chemical attributes as control on the decomposition of plant residues and other organic substrates, but chemical fractionation provides no information about them. Hence, much of the focus in examining organic matter dynamics has turned to the development of compartment models.

Kinetic models such as those developed by Jenkinson and Rayner (1977) and Parton et al. (1987) use conceptual pools to represent organic materials with a common rate of decomposition. The pools used in these models usually include an input pool, microbial biomass pool, and one or more pools representing soil organic matter. Each pool is identified "based on qualitative concepts rather than measurable entities" (Christensen

1996), which are used to explain the measured data selected to calibrate the models. The turnover of each pool and transfer between pools is most often described using first-order kinetic equations, and the calibration and application of the models requires determining the initial pool sizes and kinetic decay constants. One such compartment model, CENTURY as developed by Parton et al. (1987), has been used successfully in describing soil organic matter dynamics in arable and grassland soils over the short term, *i.e.* 5 growing seasons (Voroney and Angers 1995) and at long-term steady state, *i.e.* (Parton et al. 1987). The model parameters determined by these authors in their respective studies are summarized in Table 1-3. Parameterization of the model shows a small active fraction of organic matter with a half life of 5-9 wk, a slow pool with a half-life of 3.5-14 y, and a highly stabilized/humified (passive) pool with a half-life of 102-533 y. Although these pools were never measured directly, except where Voroney and Angers replaced active SOM with microbial biomass, they correspond well with the generally understood notions of soil organic matter dynamics.

The conceptual nature of compartment models has led several researchers to question their ultimate value, and some researchers have recently attempted to extend their value by suggesting more measurable soil organic matter pools or fractions (*e.g.* Balesdent 1996).

Although the description of organic matter dynamics by chemical or kinetic characterization is well developed, examination of the organic matter associated with aggregates, by either method does not provide a satisfactory description of the decomposition dynamics and fate of organic materials. New concepts, methods, and compartments, such as physical fractionation and the differences in the natural abundance of radioisotopes, have been developed to address the issue that, as some organic materials become aggregate binding agents, their dynamics in soil change. Hence an examination of the role of organic matter as a binding agent in soil aggregates is the first step in understanding the interactions between organic matter dynamics and soil aggregation.

4.0 Soil organic materials as aggregate binding agents

According to several researchers there are four principle mechanisms that act to form soil aggregates, each related to a size fraction. At the smallest scale, clay domains interact mainly through electrostatic mechanisms to form organo-mineral complexes and microaggregates (Murray and Quirk 1990). Larger aggregates are formed through particle re-arrangement due to environmental-physical processes such as freeze/thaw and wet/dry cycles (Dexter 1988), and still larger aggregates are formed through the binding actions of roots and fungal hyphae (Tisdall and Oades 1982). The largest aggregates are formed through compaction by pressing aggregates together (Coughlan et al. 1973a,b).

Several studies have shown that in many soils, aggregation is consistently associated with the presence of active organic matter (citings in Tisdall and Oades 1982). The various factors affecting the formation and stabilization of aggregates by organic binding agents has previously been reviewed (see Fig. 1 in Degens (1997)).

The most significant component of the hierarchical model of soil aggregation as presented by Tisdall and Oades (1982) is the description of various types of organic materials involved in binding together aggregates. The authors describe three broad groups of organic binding agents: transient, temporary, and persistent; each acting at different temporal and size scales. Transient binding agents are described as materials that decompose rapidly and thus have a transient effect on aggregation. The most significant component of transient binding agents are polysaccharides. These compounds have been found to bind aggregates < 50 μm and to have a decreased ability to bind larger aggregates. In addition, soils high in organic matter content show less aggregate binding due to transient agents (Tisdall and Oades 1982). Temporary binding agents include plant roots and fungal hyphae of mycorrhizal associations. Temporary binding agents act mostly on macroaggregates by entangling particles into aggregates and by supplying labile organic materials. Stabilized or humified organic materials that form the organo-mineral complexes of soil and thus act to create stable microaggregates are termed persistent binding agents.

In addition to the use of broad kinetic descriptions of organic binding materials, researchers have attempted to characterize the chemical composition of aggregate binding materials. Aside from humic materials, several chemical classes of compounds have been identified as aggregate binding agents. The class of compounds that has received the greatest attention are polysaccharides. The role of polysaccharides, particularly those of bacterial origin, has been studied for over 50 years (*e.g.* Martin 1946). In addition to microbial polysaccharides, increases in carbohydrates associated with growing crops have also been demonstrated (Angers and Mehuys 1989). Two main lines of evidence demonstrate the role of polysaccharides in aggregation. First, the addition of polysaccharides to soil promotes stable soil aggregation. Second, the use of periodate treatments, which are specific in cleaving C-C bonds in carbohydrate molecules, destroy soil aggregates (Cheshire et al. 1983). However, the easily decomposable nature of soil polysaccharides leaves some doubt about their longevity as binding agents and some researchers have demonstrated a lack of correlation between aggregation and soil polysaccharides (Degens and Sparling 1996).

Lipidic materials have also received some limited attention as aggregate binding organic materials. Capriel et al. (1990) demonstrated a significant correlation between supercritical *n*-hexane extracted aliphatic materials and aggregate stability. Dinel et al. (1992) suggested that as organic matter is decomposed increasing proportions of long-chain aliphatic compounds are produced, and they demonstrated that these materials were highly correlated with soil aggregate stability.

A more comprehensive study to characterize the chemical composition of organic aggregate binding agents using pyrolysis field ionization mass spectrometry (Py-FIMS) was undertaken by Monreal et al. (1995). The authors concluded that the most abundant classes of compounds in both micro- and macroaggregates were carbohydrates, lignin monomers, nitrogenous compounds, and alkylaromatics. They also found that macroaggregate stability was best correlated with lignin dimers, sterols, lipids and alkylaromatics; which aside from the alkylaromatics, were the least abundant compounds.

Our understanding of the role of various organic compounds in aggregation is based on attempts to identify potential binding agents by adding them to soils and observing changes in aggregation. The limited usefulness of this type of amendment experiment was recognized early on. Griffiths and Jones (1965) suggested that "organic materials themselves have no immediate effect but during and following their decomposition by microorganisms changes occur which lead to increased aggregation". Hence, aggregate binding agents are more likely to be microbial products of metabolism, rather than the original substrates themselves. This concept of increased longevity of stable aggregation versus that of the organic amendment was demonstrated in experiments using waste food oil amendments to soil (Plante 1996). Field studies showed that when oily food wastes were added to soil, microbial biomass C peaked after 3 weeks and subsequently returned to near baseline levels, while significantly increased aggregate water stability was maintained over the 3 month sampling period.

A more common approach of determining the role of organic compounds as aggregate binding agents is the use of statistical relationships (Dinel et al. 1992). The usual method is to correlate aggregate stability or mean aggregate size with a measured labile carbon fraction. However, Degens (1997) provides an excellent critique of these correlative methods and concludes that this approach has little value. Degens proposes a greater emphasis on binding and bonding mechanisms. Aside from the entanglement of fine roots and hyphae, it would appear that the physical-chemical mechanisms of many binding agents are not fully understood by those studying soil aggregation at the macro-scale. Yet contributions from soil chemistry and biochemistry have made the mechanisms by which some organic materials bind together soil mineral particles reasonably clear. Degens (1997) describes two mechanisms by which soil aggregates are held together; physical binding by roots and hyphae, and bonding by labile organic compounds. The bonding mechanisms used by organic compounds differ with the type of compound in question. In general, aggregates bound by polysaccharides and humic materials are held together in a strong, tensile configuration provided by the polyvalent metal cation bridging of most organo-mineral complexes, while aggregates bound by more hydrophobic compounds such as long-chain aliphatics or polyphenols are held together in a weaker, compressive

configuration due to encapsulation and an associated increase in resistance to wetting. The specific chemical bonding mechanisms involved in each of these configurations may include ion exchange, dipole interactions, H-bonding, London – van der Waals forces, and/or hydrophobic bonding (Mortland 1970). The lack of confidence in extrapolating the bonding mechanisms acting at the microscale to aggregate macroscale behaviour likely causes the apparent insecurity about aggregate bonding mechanisms.

Although significant advances have been made to describe the importance of various classes of organic compounds in soil aggregation and the mechanisms by which they act, few advances have been made to evaluate the relative contribution of individual compounds within the consortium of biochemical agents that bind and stabilize aggregates. This problem is analogous to that outlined above of describing the decomposition of various organic materials in soil. The use of individual chemical fractions to describe the dynamics of soil organic matter, and the use of individual chemical fractions to describe aggregate binding agents have proven to be similarly inadequate. Hence, researchers have turned to physical, rather than chemical methods to describe the associations between organic matter and soil aggregates.

5.0 Soil aggregate dynamics: formation and degradation

If the presence and disposition of organic materials in soil are transient and organic materials are the principle aggregate binding agents, then it follows that soil aggregates are themselves transient and thus form and degrade with some frequency. Similar to the experimental evidence for aggregate hierarchy, our understanding of the dynamics of soil aggregation is skewed toward aggregate degradation, and although many studies have observed changes in soil aggregate state over time, few have attempted to quantify them. Much of the difficulty in quantifying aggregate dynamics can be attributed to the fact that any measured result is the net difference between aggregate formation and degradation processes, and does not necessarily reflect the turnover rate of aggregates.

Early developments in the study of soil aggregation dynamics began as conceptual notions and subsequently examined large-scale changes over long time periods. Kay et al. (1988) developed a conceptual model of aggregate dynamics that described the rate of

change of a characteristic of structural form over time. The function is linked to a physical-chemical function consisting of a relative stability factor (R), the force per unit area (F/A), and a biological function (B) in the following form:

$$\frac{\partial \frac{S}{S_0}}{\partial t} = f\left[\left(\frac{R}{R_0}\right)_{SF}, \frac{F}{A}\right] + f\left[\frac{B}{B_0}\right] \tag{4}$$

where the zero subscript denotes initial conditions. In a subsequent study, Perfect et al. (1990) used regression analysis of wet aggregate stability (WAS) data to develop an exponential form of the conceptual model in the form:

$$WAS = WAS_{max} - M \cdot \exp(bt) \tag{5}$$

The model was used to describe changes in aggregate stability under different cropping management systems. Using three years of data, Perfect et al. (1990) calculated rates of increase in aggregate stability for soils under different cropping systems. The calculated half-lives reported ranged between 4.5 and 5.6 y when under various forages. In a similar study, Angers (1992) used the same model to correlate various cropping schemes with changes in soil aggregation and found a rate of improvement in alfalfa cultivation equivalent to a half-life of 0.91 y.

As discussed previously, physical processes such as freeze/thaw and wet/dry cycles, as well as organic binding agents are traditionally associated with changes in soil aggregation. In laboratory incubation studies, Chaney and Swift (1986) examined the effects of both physical processes and microbial activity on the re-formation of macroaggregates from soil previously crushed to < 0.5 mm. The authors applied several treatments to the crushed soil: wet/dry cycles, freeze/thaw cycles, a combination of both, incubation with glucose, and incubation with microbial polysaccharides (xanthate and alginate). The stability of reformed 2.0-2.8 mm aggregates was measured periodically and showed that the treatments involving physical processes did not produce stable aggregates, while incubation with organic substrates produced aggregates with short-term stability. Re-formed aggregates from samples incubated with glucose had increasing mean weight diameters through the first 21 days of incubation, followed by a steady

decline over the next 11 weeks. Samples incubated with microbial polysaccharides showed immediate (within 1 day) increases in mean weight diameter and a rapid decline over the next 21 days. The authors used the evidence to propose that the dynamics of aggregate formation and stabilization follow the dynamics of the transformation of added substrates. As the glucose is metabolized, microbial polysaccharides are produced which bind aggregates, as these substrates are subsequently attacked, the stability of aggregates decreases. Chaney and Smith's study clearly demonstrates that aggregates can form and degrade rapidly in conjunction with the addition of a labile substrate.

The studies cited above have attempted to quantify the dynamic nature of soil structure by using correlative methods and indicator parameters such as wet aggregate stability. This approach may be useful in examining long-term or large-scale management effects on soil structure, but provides limited insight into the small-scale turnover rates, or longevity of soil aggregates as they form and degrade. Only a small number of studies have specifically addressed the dynamics of soil aggregate formation and degradation, and still fewer studies have attempted to quantify the rates of change of these processes. Innovative research in this area of aggregate dynamics has examined formation and degradation processes by using labeling techniques or inert tracers.

Early work by Toth and Alderfer (1960a), proposed a method for labeling soil aggregates using a solution of radioactive Co^{60}. Tagged aggregates were created by isolating water stable aggregates 1-2 mm in diameter from a soil, soaking them in a solution of Co^{60}, and subsequently drying them. Breakdown of aggregates during soaking and further sieving created tagged aggregates of various sizes: 1.0-2.0, 0.5-1.0, 0.25-0.5, and < 0.25 mm.

In subsequent studies, Toth and Alderfer (1960b) applied the method to track the formation and degradation of Co^{60}-tagged aggregates. The tagged aggregate tracers were added to soil samples and incubated for 16 weeks. During the incubation, the authors observed the breakdown of tagged aggregates resulting in the redistribution of the radioactivity. The tagged aggregates >1.0 mm degraded rapidly in the first 4 weeks, degraded only slightly in weeks 5 to 12, and finally increased in the last 4 week period, while the smallest tagged aggregates showed a slow and steady decrease in activity. The

combination of these two results would indicate a trend toward the middle-sized aggregates of approximately 0.5 mm, as larger aggregates breakdown and smaller aggregates are incorporated into larger ones.

The most interesting observation in the study reported by Toth and Alderfer (1960b) is that the smallest aggregates comprise a lower proportion of mass in forming larger aggregates. As the authors noted, the tagged 0.5-1.0 mm aggregates contributed 11% to the formation of aggregates >1.0 mm, while the tagged aggregates <0.25 mm contributed only 6.8%, after 4 weeks. By the end of the 16 week incubation, the trend was clear: 15.8% contribution to the >1.0 mm fraction by the 0.5-1.0 mm tagged fraction, 13.4% by the 0.25-0.5 mm tagged fraction, and 12.8% by the <0.25 mm fraction. These results appear to support the hierarchical model and the results subsequently found by Coughlan et al. (1973b) that led them to propose that larger aggregates have a uniform composition of smaller components and are formed by the addition of increasingly larger components. The methods and results of the experiments by Toth and Alderfer are significant, and hence it is surprising that they remain ignored, and that this research approach was abandoned for nearly 30 years.

In later laboratory studies designed to simulate field conditions, Terpstra (1989, 1990) examined the formation and degradation of large aggregates (> 4 mm) using glass beads as tracers. The aims of the studies were to quantify aggregate formation (1989), and to examine the control of aggregate dynamics on weed seed germination (1990). The core of the studies was the examination of glass bead re-distribution after the application of various combinations of root growth, freeze/thaw, and compaction treatments. The method involved the incorporation 2.2 by 1.4 mm beads of different colours into different size fractions of artificially created aggregates. A sample initial distribution is recorded in Table 1-4a. The samples were then subjected to three 12-week cycles of the applied treatments to simulate three growing seasons, after which aggregate mean weight diameter and glass bead distribution were measured. Table 1-4b illustrates sample results of bead redistribution, however the author makes no indication of the treatment or time period associated with the data.

The measured re-distribution of beads was compared to the expected distribution if the beads were completely mixed across aggregate size fractions (Table 1-4b). Terpstra proposed that a measured number of beads lower than the expected value for complete mixing was consistent with the hypothesis of random mixing, while a measured value greater than expected was considered to be a deviation from the hypothesis. The percentage of beads in agreement with complete mixing ranged from approximately 75% after the first simulated season to approximately 95% after three seasons, suggesting rapid aggregate turnover. Two additional calculations were performed to elucidate aggregate formation and degradation processes.

Terpstra assumed that aggregates containing only beads of original colour were "probably undisturbed" after each simulated season. The percentages of undisturbed aggregates were subsequently determined for each size fraction after each 12-week cycle. In the second season, the percentage of undisturbed aggregates increased with increasing aggregate size from 7% for aggregates 4.0-4.8 mm to 24% for aggregates 8.0-10.0 mm. The percentages decreased across all aggregate sizes in the third season to a mean of 7%. The author suggested that the larger aggregates were more persistent than smaller ones, which contradicts the generally accepted notion put forth by the hierarchy model of aggregation, that larger macroaggregates are less stable and most susceptible to changes in management. Although the author made no reference to the implications of the results, the discrepancy may be due to the size scale examined by the authors, or laboratory conditions that did not properly represent field conditions.

A final calculation performed by Terpstra (1989) based on the glass bead re-distributions, has implications in the relative dynamics of aggregate formation versus aggregate degradation. After each simulated season, the beads in each aggregate size fraction were categorized as originating from larger or smaller fractions. Calculation of the percentages of beads originating from larger or smaller fractions were compared to the distribution which would result from complete mixing. The results showed differing rates of approach to complete mixing for beads from larger, compared to smaller, aggregate size fractions. This result led Terpstra (1989) to conclude that in the samples studied over three simulated field seasons, the process of aggregate breakdown was more rapid than that of

aggregate formation. In the subsequent study (Terpstra 1990), the implications of aggregate dynamics to weed seed germination were observed and discussed. Since weed seeds are more likely to remain dormant while occluded in aggregates, the increases in seed germination were supported by observations of rapid re-distribution of tracer beads due to aggregate breakdown and formation.

Several studies by Allmaras and colleagues have described the use of ceramic tracer spheres to examine the spatial fate of crop residues, fertilizer prill, and herbicide granules during tillage operations (Juzwick et al. 1997; Allmaras et al. 1996; Staricka et al. 1991, 1992). One study in particular (Staricka et al. 1992) sought to measure the longevity of aggregates by applying 1-3 mm ceramic spheres to field plots and measuring their association with large aggregates of various sizes (3 to 40 mm) over a four year period. The authors found that after initial application and tillage, the incorporated spheres were located on the surface of aggregates, and in subsequent years they were found in the interior of aggregates, suggesting that incorporation was initially due to compressive forces and subsequently due to aggregate breakdown and reformation.

The amount of incorporated spheres increased over the study period, leading the authors to suggest that at an infinite time a uniform distribution would occur. To estimate the turnover time of aggregates, a tracer-to-soil ratio (TSR) was calculated for the various aggregate size classes and sampling times. The TSR data was compared to an asymptotic model of the form:

$$TSR = 1 - \exp(k \cdot t) \qquad (6)$$

where k is a rate coefficient. The times required for TSR to reach 0.95 were calculated to be 3 y for > 40 mm aggregates, and 18 y for 3-5 mm aggregates, showing that larger aggregates turnover more rapidly than smaller ones confirming the hierarchy theory. Although the data fit the model well, in several instances TSR values peaked above a value of 1.0, then decreased to their equilibrium level.

The fraction of aggregates containing tracers (FAIT) was also calculated. The authors noted that, mathematically, if TSR > FAIT in a uniform aggregate size fraction, then some of the aggregates must contain more than their equilibrium number of tracers. In all

cases except one, FAIT was less than TSR. The authors concluded that the dynamics of tracer incorporation into aggregates is not a simple accumulation to an equilibrium value, but rather involves both the incorporation and release of tracers. This would suggest that aggregate longevity or turnover might be more rapid than that measured by the asymptotic model suggested above, and may also reflect the aggregate formation model proposed by Oades (1984). In their concluding statements, the authors also noted that the dynamics measured in their study may differ from those of the incorporation of smaller spheres, and that smaller spheres may better represent the incorporation of soil particles into aggregates.

Aside from inert tracers such as glass beads or ceramics spheres, some researchers have used organic matter itself as an indicator of aggregate dynamics. As outlined earlier, Besnard et al. (1996) examined the organic matter originating from a cultivation sequence of forest soil and soils under an increasing number of years under corn cultivation. In their examination of the hypothesis of whether organic matter is redistributed between aggregated and non-aggregated fractions, the authors interpreted their observations of organic matter dynamics in the context of the dynamics of aggregate formation and disruption necessary for their observations. They observed a decrease in microaggregates in the first 7 years of corn cultivation, after which equilibrium was reached between aggregate degradation and formation. The short time period required to reach equilibrium suggested to the authors that the lifetime of aggregates would be "a few years" (Besnard et al. 1996). They also concluded that aggregate formation and disruption produce an exchange or redistribution of organic matter between aggregated and non-aggregated fractions, which lead to the observed organic matter contents of particular aggregate size fractions.

In other experiments using organic matter as an indicator of aggregation dynamics, Jastrow (1996; Jastrow et al. 1996) examined carbon storage in a prairie restoration sequence. Changes in macroaggregation and total organic carbon across the sequence from currently cultivated to virgin grassland were modeled using the exponential equation proposed by Perfect et al. (1990). The results showed a much more rapid increase in macroaggregation ($t_{1/2}$ = 1.6 y) compared to organic carbon ($t_{1/2}$ = 58 y),

which led the author to support the Oades (1984) model that macroaggregation occurs before the formation of microaggregates. Jastrow also observed that the macroaggregate-associated C-to-N ratio increased over time from cultivated to virgin grassland, supporting Elliott's (1986) conclusion that organic matter associated with macroaggregates is "less highly processed". However, less than 20% of the organic inputs were in POM form, suggesting that the incoming organic matter is rapidly associated with the mineral fraction. This last observation led to a closer examination of the dynamics of aggregate-carbon interactions.

Jastrow et al. (1996) used $\delta^{13}C$ methods applied to the same restoration sequence outlined above, specifically examining the loss of C4 from crops and input of C3 from grasses, to investigate organic matter dynamics in macro- and microaggregates. The most significant observation in relation to aggregate dynamics was that the input rate of C3 carbon was the same in microaggregates (53-212 μm), as in small macroaggregates (212-500 μm). The authors hypothesized two causes for this observation: 1) the C3 associated with the microaggregates may be inter-microaggregate organic material found on the surface of the aggregates, which is consistent with the concept of inter-microaggregate binding agents or, 2) the microaggregates with which the organic matter is associated may form and degrade much more rapidly than suggested by the hierarchy model and the persistent binding agents of Tisdall and Oades (1982). Microaggregates are normally thought to be highly stable and bound by older, more recalcitrant organic materials. However, Jastrow et al. used the observed rapid inputs of C3 carbon into microaggregates to support the second hypothesis. Rapid incorporation of young, labile organic matter would form stable microaggregates in the manner proposed by Golchin et al. (1994). Jastrow et al. attributed the slow decomposition of old organic matter in the microaggregate fraction to "intimate association with mineral particles". Although discussed only indirectly, the authors appear to suggest that microaggregates may exist in two forms: one bound by old, recalcitrant organic materials, and the other bound by young, labile materials; each fraction having its own turnover rate.

Although the use of organic matter as an indicator of aggregate dynamics has proven useful, it does not allow the same degree of direct observation of aggregate formation and

degradation as the use of inert tracer spheres. In addition, Jastrow et al. (1996) recognized that the turnover rates of aggregate-associated organic matter may differ significantly from the actual turnover of the aggregates. Indeed, research has shown that the association of organic materials with aggregates and mineral particles alters their decomposition rates, yet a quantitative link between organic matter and aggregate association and organic matter decomposition has yet to be reported.

6.0 Soil organic matter and aggregate interactions

Independent research into the nature of soil organic matter on one hand, and into soil aggregation on the other, has revealed that these components are not independent: at the microscale, stabilized organic compounds are found associated with clay particles (Mortland 1970) and at the macroscale, organic materials are binding agents associated with micro- and macroaggregates (Tisdall and Oades 1982). Extensive research has been performed to describe the location of organic matter in the structural soil matrix in the aims of describing how aggregates are bound and how organic carbon is sequestered:

6.1 SOM and aggregate associations

The predominant tools used in describing organic matter and aggregate associations are size and density fractionations (Christensen 1992). Size fractionation is often followed by applying energy (usually via sonication) to disrupt aggregates within the size fractions yielding various particle size distributions and associated organic matter. Density fractionation involves dividing aggregate-associated soil organic matter into three pools: a light fraction (density < 1.6-2.0 g/cm^3) with little mineral association usually termed "the light fraction" or particulate organic matter (POM), a medium density fraction (2.0-2.4 g/cm^3) including the organo-mineral complexes, and a heavy fraction (> 2.4 g/cm^3) including mineral particles coated with organic matter (Shaymukhametov et al. 1985). Christensen (1992) states that the application of density fractions assumes that the organic matter in each pool differs in structure and function, however several of the studies cited below have used size and density fractionation and found some qualitative differences in organic matter across fractions, while others have found a range of organic matter qualities within fractions.

In experiments comparing native grassland soil to cultivated soil, Elliott (1986) found that the macroaggregates from both soils had significantly higher organic nutrient (C, N, P) contents than microaggregates, and that the macroaggregates from the native sod soil had higher nutrient contents than those from the cultivated soil. This result was previously suggested by the model of Tisdall and Oades (1982). However, Elliott notes that the loss of organic matter due to cultivation is much greater than the amount attributable to roots and fungal hyphae, which are the macroaggregate binding agents suggested by the model. Hence, Elliott proposed that the loss of organic matter came from clay associated organic materials, which suggests that this pool of organic matter is relatively labile. In additional experiments on the mineralization of the organic matter in macro- and microaggregates, Elliott found that mineralization of organic matter in macroaggregates was enhanced when the aggregates were crushed to microaggregate size. The total amount mineralized in macroaggregates (intact or crushed) was greater than in microaggregates. Crushing macroaggregates further enhanced mineralization, leading to higher amounts than in intact macroaggregates or microaggregates even when expressed as a percent of total C or N. These results led the author to conclude that the organic matter associated with macroaggregates is more labile than that associated with microaggregates. Although Waring and Bremner (1964) had previously observed this much earlier, the implications of such results gained acceptance only much later when Elliott renewed interest in organic matter and aggregate associations.

Elliott's research (1986; Elliott and Cambardella 1991; Cambardella and Elliott 1992) set the stage for a large body of experimental research occurring from the end of the 1980's to the present that uses size and densimetric fractionations to characterize aggregate-associated organic matter and the nature of POM. Christensen (1992) provides an extensive summary of the research performed in the area of organic matter contents of various size and densimetric separations. Although many studies have examined the absolute carbon content of aggregate fractions and mineralization therein, only a few recent studies have shed light on the nature of organic matter in different aggregate associations, and proposed significant hypotheses about the mechanisms at work and the fate of added organic materials in soil aggregates.

Golchin et al. (1994) used density fractionation before and after aggregate disruption to classify POM materials as free, occluded, or clay-associated. These fractions were used in experiments using NMR analysis to determine the chemical composition of the organic matter in each fraction. The results showed chemical differences between fractions: the free POM closely resembled plant and litter material, and the occluded POM showed decreasing O-alkyl C and increasing alkyl C contents with decreasing density (from 1.8-2.0 to <1.6 Mg/m^3). The results indicated that material associated with denser fractions was decomposed to a lesser degree, supporting previous findings by Elliott (1986). The authors also found that the clay-associated fraction contained a high carbohydrate content and low phenolic content. Results of the chemical composition of aggregates did not provide a clear trend across all density fractions. The authors suggested this was due to a shift from a predominantly organic complex comprised of a nucleus of POM encrusted by mineral particles in the fractions < 2.0 Mg/m^3, to a mineral dominated complex with adsorbed organic matter in the denser fractions. The chemical composition of the organic matter in the densest fraction indicated narrow C/N ratios, high carbohydrate content and low phenol content, which was attributed to a highly labile pool of materials.

Golchin et al. used the results of the study in the development of a model of microaggregation similar to that proposed by Beare et al. (1994a), focusing on the changes in organic matter and aggregate associations as incoming organic materials are decomposed (see Fig. 1 in Golchin et al. 1998). Golchin et al. (1994) outline that as POM enters the soil it is colonized by the soil microbial population and subsequently becomes encrusted with mineral particles, creating a stable aggregate. Although somewhat protected by the mineral particles, the labile fraction of the organic core of the aggregate decomposes, resulting in a less stable aggregate. The various degrees of decomposition of the organic core of aggregates are the cause of the release of particles into varying density fractions after applying dispersive energy. Stable aggregates with intact labile organic cores cannot be easily dispersed and are separated into the 1.8-2.0 Mg/m^3 fraction, while unstable aggregates will disperse to release recalcitrant POM (< 1.6 Mg/m^3) and mineral complexes with organic coatings (>2.0 Mg/m^3).

The model suggests that the fate of new, incoming organic materials in aggregates is an important factor in the formation of stable aggregates. A few studies have begun using differences in natural carbon isotope abundance, *i.e.* $\delta^{13}C$, to examine the relative age of organic matter in various aggregate fractions. The goal of these studies was to describe the physical location of soil organic matter as it is sequestered in aggregates, in an attempt to derive aggregate turnover rates.

Puget et al. (1995) proposed two mechanisms to explain the relative enrichment of organic matter in water-stable macroaggregates; lack of decomposition of organic matter in macroaggregates due to physical protection, and the direct link between carbon enrichment and water stability of macroaggregates. The authors suggested that both C_3- and C_4-derived organic matter should be equally protected in aggregates after 6 and 23 years of cultivation of forest soil with corn. However, they observed a relative enrichment of C_4 compared to C_3 in water-stable macroaggregates versus dry-sieved macroaggregates and microaggregates. It was concluded that the accumulation of young, labile organic matter (represented by C_4 enrichment) was responsible for the stability of aggregates, supporting the latter hypothesis. Similar results are reported by Angers and Giroux (1996) in experiments with continuous corn, a mixed C_3-C_4 rotation, and permanent pasture treatments. These results support the theory that young, active organic matter, rather than total soil organic matter, is responsible for water-stable aggregation as suggested by Tisdall and Oades (1982).

In additional experiments, Besnard et al. (1996) examined the fate of incoming POM in soil aggregates. A method adapted from Golchin et al. (1994) was used to fractionate free and occluded POM in soils from a sequence of native forest, and 7 and 35 years of corn cultivation. In addition, $\delta^{13}C$ data was used to trace forest- and corn-derived POM in various aggregate fractions. Based on observations of the forest- and corn-derived POM in both free and occluded pools, the authors hypothesized that there is redistribution or exchange of organic matter between the aggregated and non-aggregated fractions. Calculation of the rapid loss of free forest POM during the first 7 years after cultivation, coupled with the incorporation of corn-derived POM during this time led the authors to

support the hypothesis that exchange does occur, and hence organic matter and aggregate associations become dynamic.

Rather than examine organic matter and aggregate association dynamics in systems where macroaggregation and carbon storage is being depleted as a result of cultivating previously naturally vegetated soils, Jastrow (1996) studied the situation of grassland restoration. This approach allowed the examination of organic matter and aggregate associations during a period of net aggregate formation and organic carbon accumulation. The study examined the increases in macroaggregation, free and released POM, and mineral associated organic carbon in soils under corn cultivation, 4 and 10 growing seasons of restored prairie, and virgin prairie. Jastrow reported that the intra-macroaggregate POM pool, as a percentage of total soil carbon from whole soil samples, had a relatively narrow range: from 2.2% in the corn field to 4.1% in the virgin prairie. The results indicated that recent inputs of organic materials were quickly becoming associated with the mineral fraction rather than remaining in the POM pools, which the author attributed to the rapid decomposition of incoming POM and encrustation of residues by soil clays. The changes in the nature of the organic matter-aggregate associations were then used to support the Oades (1984) theory of microaggregate formation within macroaggregates.

In summary, the methods of size and density fractionation have yielded significant amounts of data about the associations between organic matter and soil aggregates. Free and occluded pools of POM have been used to indicate the physical fate of soil organic matter as it is lost by cultivation, or as it is accumulated due to increased organic inputs. However, the methods provide a static image of organic matter and aggregate associations. Even in the cases where these associations are examined in soils at varying stages of transition, there is no examination of the dynamic mechanisms and processes that result in the reported observations.

6.2 Soil aggregation controls on organic matter dynamics

The formation and degradation of soil aggregates change the associations between organic binding agents and aggregates, resulting in the protection of some organic

materials at certain times and the release of labile organic materials at other times. The protection and release of organic materials have a clear control over the decomposition kinetics of these materials as their availability to microorganisms changes. Physical protection has been recognized for some time and, in general, three methods have been used to investigate aggregation-related control over organic matter decomposition: addition of substrates to soil under varying degrees of aggregation, radiocarbon dating of various aggregate and organic matter associations, and measurement of mineralization in various aggregate and organic matter associations.

Initial studies on the correlation of aggregation with organic matter dynamics involved measuring the mineralization of substrates added under varying conditions of aggregation. Bartlett and Doner (1988) studied the effects of adsorption and aggregation on the decomposition of two radio-labeled amino acids. Four treatments were prepared: a non-aggregated (applied by surface spray) and non-adsorbed amino acid (leucine), a non-aggregated but adsorbed amino acid (lysine), an aggregated (incorporated by mixing) but non-adsorbed amino acid, and an aggregated and adsorbed amino acid. Samples of soil paste were used to create artificial aggregates of varying sizes to which the amino acids were either surface applied by spray, or incorporated into by mixing to create the aggregated and non-aggregated treatments. The results showed that the surface applied amino acids decomposed more rapidly than those mixed into aggregates, and that adsorption further decreased mineralization. The authors concluded that both adsorption and physical protection are important factors in the decomposition of organic substrates.

Previously, Adu and Oades (1978) examined the decomposition of labeled glucose and starch in aggregated and non-aggregated forms. To achieve this, the substrates were added to soil in the normal fashion to create non-aggregated samples, or mixed into soil slurries from which artificial aggregates of various sizes were created. The authors proposed that the substrates added to the slurry would be distributed in both micro- and macropores and would thus be less available than the substrates added to the bulk soil. The expected results were that mineralization would be higher in the non-aggregated treatments than in the aggregated treatments. The observed results were consistent with expectation in loam samples but not in clay samples. The study illustrates that many soil

environmental conditions can alter the expected results of a study that uses added substrates. For this reason, many studies have focused on the dynamics of *in-situ* organic matter contained in various physical fractions.

Anderson and Paul (1984) used radiocarbon dating to estimate the age of organic matter separated from various chemical and size fractions of cultivated grassland soils to investigate the turnover times of organic matter decomposition in the various fractions. The authors observed a large difference between the fine clay (< 0.2 μm) associated carbon, and the coarse clay (0.2-2 μm) and fine silt (2-5 μm) associated carbon, where the coarse clay and fine silt associated fraction was consistently the oldest and the fine clay fraction was much younger. The results defied a direct link between particle size and organic matter age/stability.

Although they examined primary particle size fractions, the authors discussed implications of the results in the context of microaggregation. Aggregates containing a combination of fine silt, and coarse and fine clay would presumably contain organic matter of similar age. They suggested that the observed younger age of organic matter associated with fine clay is due to its occurrence as individual particles, on aggregate surfaces, or in aggregate micropores that are easily released, and that more effective disruption of stable microaggregates would decrease the observed differences. The authors concluded that the radiocarbon dates obtained illustrated that protection by aggregation effectively lengthened decomposition turnover times from days to years or decades.

In a study designed to examine the decomposability of organic matter within aggregates, increasing intensities of ultrasonic dispersion ranging from 100 J/mL to 1500 J/mL were applied to soil aggregates to yield various aggregate and particle size fractions (Gregorich et al. 1989). Subsequently, mineralization rates in the size fractions were measured during 20-day incubations. In all size fractions, a large increase in carbon mineralization was observed between the application of 300 and 500 J/mL, which corresponds to the energy at which microaggregates are disrupted, indicating that a large portion of soil organic matter is protected in microaggregates.

The degree to which aggregate protection affects carbon mineralization is reflected in the amounts of organic matter mineralized in the sand- and clay-size fractions before and after microaggregate disruption. For the sand-size fraction, an over-all increase in mineralization after disruption indicated that the organic matter was more labile and likely consisted of protected microaggregate binding materials. The calculated half-lives of the organic matter mineralized before and after microaggregate disruption were 5.8-6.9 d and 5.0-5.3 d, respectively. In the case of the clay-size fraction, microaggregate disruption resulted in large differences in mineralization rates and patterns. The calculated half-lives of the organic matter before and after disruption were 9.2-11.6 d and 2.2-2.4 d, respectively. Microaggregate disruption resulted in an initial increase in mineralization (0-5 days) followed by a decrease in the organic matter mineralization rate, suggesting that two pools of organic matter were present within the microaggregates. This observation is consistent with the Tisdall and Oades (1982) model and hypotheses presented by Jastrow et al. (1996) that suggest that both labile polysaccharides and recalcitrant (persistent) organic materials are protected within, and act to bind microaggregates. Gregorich et al. concluded by suggesting that, overall, the mineralization of organic matter is reduced due to protection in micropores and by a stabilizing association with primary particles, rather than by sequestration within clay lattices because the energies used in the experiments were lower than those required to disrupt clay structures.

Further supporting studies in comparing the mineralization rates of aggregate protected and unprotected organic matter were performed by Beare et al. (1994b). The authors examined mineralization of organic matter in intact and crushed macroaggregates (> 2 mm and 250-2000 μm) and intact microaggregates (106-250 μm and 53-106 μm). Their results demonstrated that the protected pool (crushed minus intact) of organic matter was more labile than the unprotected pool, which was attributed to increased access to the unprotected pool resulting in the decomposition of the most labile fractions.

The approach used in the studies cited above have confirmed the generally accepted model of physical protection of organic matter within aggregate resulting in decreased rates and extents of decomposition. However, quantification of the impact of physical

protection on substrate decomposition or on the large-scale cycling of organic matter has yet to be achieved.

As discussed previously, several compartment models have been developed to study the dynamics of organic matter decomposition and cycling in soils. Several of these have recognized the importance of physical protection as a control on decomposition rates, but few have properly integrated the concept into the model. Some models have described physical protection in a mechanistic manner by introducing the concept of a protective capacity (Hassink and Whitmore 1997), or have attempted to use soil texture as a surrogate for aggregation protection (*e.g.* Parton et al. 1987). However, the former strategy is simply kinetic data fitting which may have a limited foundation in reality, and the latter strategy, as Elliott et al. (1996) point out, is inadequate since "at a given site, soil texture will presumably not be affected by soil disturbance…, but soil structure may be highly affected". In the search to better account for the protecting effects of aggregation, and for more concrete soil organic matter fractions, many researchers (*e.g.* Buyanovsky et al. 1994; Hassink 1995) have attempted to replace the traditional model compartments with physical and/or density fractions and their associated carbon mineralization rates.

Although the approach of "modeling the measurable" (Elliott et al. 1996) soundly addresses the conceptual problems of organic matter associations with aggregates and their impacts on kinetic rates, there is no accounting for the composition of the organic matter in the associations, which becomes important when the nature of the association changes. Hence, many problems remain in resolving the quantitative links between soil aggregation and organic matter dynamics.

7.0 Conclusions

Traditionally, research into soil structure and aggregation has focused on two aspects, the search for a single parameter to characterize the structural state of a soil (Hartge, 1995), or studies on the functionality of soil structure (Letey 1991). Research into how soil structure is linked to crop emergence, water and solute movement, and soil erosion and compaction has dominated the soil structure literature. Until recently, only occasional

studies were performed to study soil structure and aggregation themselves. However, the current trend in research concerning organic matter sequestration by soils has led to increased research interest in organic matter and aggregate associations, and the control of aggregation over organic matter dynamics. As Hartge (1995) points out, we have reached a point where soil aggregation and structure are no longer viewed in a broad sense similar to the historic view of "fertility".

This chapter has provided an extensive review of the scientific literature concerning organic matter and aggregate dynamics, and has demonstrated that our knowledge of the interactions between the two is limited. As stated previously, a better understanding of the dynamics of soil aggregate formation and degradation is essential to better understand how aggregation controls soil organic matter dynamics. The doctoral research reported in this thesis consists of the following components:

1. the development of a tracer particle quantifiable by neutron activation analysis, and the characterization of the selected tracers (Chapter 2),
2. experiments to observe the behaviour of the tracer spheres during the wet sieving procedure (Chapter 3),
3. a field study examining soil aggregate dynamics and organic matter dynamics in two contrasting soils (Chapters 4 and 6)
4. the development of a quantitative compartmental model to describe soil macroaggregation (Chapter 5), and
5. a laboratory study to examine soil aggregate dynamics and organic matter dynamics under differing frequencies of simulated tillage (Chapter 7).

The overall objective of the research is to quantify soil aggregate dynamics in order to better understand the role that aggregation plays in the physical protection of soil organic matter.

Table 1-1. Aggregate distribution (% retained) after wet sieving an aggregated clay soil. (*from:* Coughlan et al. 1973b)

Dry aggregate fraction (mm)	Water-stable aggregate fraction (mm)							
	>19.0	19.0 - 9.5	9.5 - 5.0	5.0 - 2.0	2.0 - 1.0	1.0 - 0.5	0.5 - 0.2	<0.2
>19.0	0*	0	7	36	24	15	11	7
19.0 - 9.5	-	0*	5	29	25	17	15	9
9.5 - 5.0	-	-	11*	35	22	13	12	7
5.0 - 2.0	-	-	-	51*	22	11	10	6
2.0 - 1.0	-	-	-	-	75*	9	8	8
1.0 - 0.5	-	-	-	-	-	75*	14	11
Expected	0	0	6	33	23	13	12	8

* Water-stable aggregate fraction.

Table 1-2. Kinetic parameters of decomposition of some organic compounds in soil. (*from:* Paul and van Veen 1978)

Substrate	Decay constant (y^{-1})	Half-life (y)*	Cited reference
Glucose	40.1	0.0173	Simonart and Mayaudon (1958)
Hemicellulose	29.2	0.0237	Simonart and Mayaudon (1958)
Cellulose	7.29	0.0951	Simonart and Mayaudon (1958)
Lignin	0.365	1.90	Minderman (1968)
Waxes	0.219	3.16	Minderman (1968)
Phenols	0.073	9.49	Minderman (1968)
Glycine	72.2	0.0096	Verma et al. (1975)
Lysine	47.7	0.0145	Verma et al. (1975)

* Calculated in this review.

Table 1-3. CENTURY model parameters used to describe soil organic matter dynamics. (*from:* Voroney and Angers 1995)

Model Compartment	Initial pool size (% of total SOM)		First-order decay constant (y^{-1})	
	Parton et al. (1987)[a]	Voroney and Angers (1995)[b]	Parton et al. (1987)	Voroney and Angers (1995)
Active SOM	7	3	7.3	4
Slow SOM	50	65	0.2	0.05
Passive SOM	43	32	0.0068	0.0013

[a] Model describes grassland soil in Colorado at steady-state.
[b] Model describes arable soil in Québec over 5 growing seasons.

Table 1-4a. Initial glass bead distribution in aggregate size fractions. (*from:* Terpstra 1989)

Bead Colour	Aggregate size fraction (mm)					
	10.0 – 8.0	8.0 – 6.3	6.3 – 4.8	4.8 – 4.0	< 4.0	Total
Red	267 *					
Blue		302				
White			317			
Green				369		
Yellow					346	
All colours						1601

* Total number of beads in each aggregate size fraction.

Table 1-4b. Final measured (A) and expected (B)* glass bead distribution in aggregate size fractions. (*from:* Terpstra 1989)

Bead Colour	Aggregate size fraction (mm)										
	10.0 – 8.0		8.0 – 6.3		6.3 – 4.8		4.8 – 4.0		< 4.0		Total
	(A)	(B)*	(A)	(B)	(A)	(B)	(A)	(B)	(A)	(B)	(A)
Red	75	37	47	40	22	31	20	22	103	137	267
Blue	44	41	58	45	51	35	19	25	130	156	302
White	43	44	59	48	38	37	29	26	148	162	317
Green	39	43	33	56	51	44	32	29	214	189	369
Yellow	20	48	44	52	26	41	30	28	226	177	346
All colours	221		241		188		130		821		1601

* Expected number of beads if completely mixed; *i.e.* 37 = (267÷1601) × 221.

References

Adu J.K. and J.M. Oades. 1978. Physical factors influencing decomposition of organic materials in soil aggregates. Soil Biol. Biochem. 10:109-115.

Allison F.E. (1969). Soil aggregation - Some facts and fallacies as seen by a microbiologist. Soil Sci. 106:136

Allmaras R.R., Copeland S.M., Copeland P.J. and M. Oussible. 1996. Spatial relations between oat residue and ceramic spheres when incorporated sequentially by tillage. Soil Sci. Soc. Am. J. 56:1591-1597.

Anderson D.W. and E.A. Paul. 1984. Organo-mineral complexes and their study by radiocarbon dating. Soil Sci. Soc. Am. J. 48:298-301.

Angers D.A. 1992. Changes in soil aggregation and organic carbon under corn and alfalfa. Soil Sci. Soc. Am. J. 56:1244-1249.

Angers D.A. and M. Giroux. 1996. Recently deposited organic matter in soil water-stable aggregates. Soil Sci. Soc. Am. J. 60:1547-1551.

Angers D.A. and G.R. Mehuys. 1989. Effects of cropping on carbohydrate content and water-stable aggregation of a clay soil. Can. J. Soil Sci. 69:373-380.

Balesdent J. 1996. The significance of organic separates to carbon dynamics and its modelling in some cultivated soils. Eur. J. Soil Sci. 47:485-493.

Bartlett J.R. and H.E. Doner. 1988. Decomposition of lysine and leucine in soil aggregates: adsorption and compartmentalization. Soil Biol. Biochem. 20:755-759.

Beare M.H., Hendrix P.F. and D.C. Coleman. 1994a. Water-stable aggregates and organic matter fractions in conventional- and no-tillage soils. Soil Sci. Soc. Am. J. 58:777-786.

Beare M.H., Cabrera M.L., Hendrix P.F. and D.C. Coleman. 1994b. Aggregate-protected and unprotected organic matter pools in conventional- and no-tillage soils. Soil Sci. Soc. Am. J. 58:787-795.

Besnard E., Chenu C., Balesdent J., Puget P. and D. Arrouays. 1996. Fate of particulate organic matter in soil aggregates during cultivation. Eur. J. Soil Sci. 47:495-503.

Braunack M.V., Hewitt J.S. and A.R. Dexter. 1979. Brittle fracture of soil aggregates and the compaction of aggregate beds. J. Soil Sci. 30:653-667.

Brewer R. 1976. "Fabric and Mineral Analysis of Soils". R.E. Kreiger, New York.

Buyanovsky G.A., Aslam M. and G.H. Wagner. 1994. Carbon turnover in soil physical fractions. Soil Sci. Soc. Am. J. 58:1167-1173.

Cambardella C.A. and Elliott E.T. 1992. Particulate soil organic matter across a grassland cultivation sequence. Soil Sci. Soc. Am. J. 56:777-783.

Capriel P., Beck T., Borchert H. and P Härter. 1990. Relationship between soil aliphatic fraction extracted with supercritical hexane, soil microbial biomass, and soil aggregate stability. Soil Sci. Soc. Am. J. 54:415-420.

Chaney K. and R.S. Swift. 1986. Studies on aggregate stability: I. Re-formation of soil aggregates. J. Soil Sci. 37:329-335.

Cheshire M.V., Sparling G.P. and C.M. Mundie. 1983. Effect of periodate treatment of soil on carbohydrate constituents and soil aggregation. J. Soil Sci. 34:105-112

Christensen B.T. 1992. Physical fractionation of soil and organic matter in primary particle size and density separates. Adv. Soil Sci. 20:1-90.

Christensen B.T. 1996. Matching measurable soil organic matter fractions with conceptual pool in simulation model of carbon turnover: Revision of model structure. *In* Evaluation of soil organic matter models. D.S. Powlson *et al.* (Eds.) NATO ASI Series Vol. 138.

Coughlan K.J., Fox W.E. and J.D. Hughes. 1973a. A study of the mechanisms of aggregation in a krasnozem soil. Aust. J. Soil Res. 11:65-73.

Coughlan K.J., Fox W.E. and J.D. Hughes. 1973b. Aggregation in swelling clay soils. Aust. J. Soil Res. 11:133-141.

Currie J.A. 1966. The volume and porosity of soil crumbs. J. Soil Sci. 17:24-35.

Degens B.P. 1997. Macro-aggregation of soils by biological bonding and binding mechanisms and the factors affecting these: a review. Aust. J. Soil Res. 35:431-459.

Degens B.P. and G. Sparling. 1996. Changes in aggregation do not correspond with changes in labile organic C fractions in soil amended with ^{14}C-glucose. Soil Biol. Biochem. 28:453-462.

Dexter A.R. 1988. Advances in the characterization of soil structure. Soil and Tillage Res. 11:199-238.

Dinel H., Lévesque P.E.M., Jambu P. and D. Righi. 1992 Microbial activity and long-chain aliphatics in the formation of stable soil aggregates. Soil Sci. Soc. Am. J. 56:1455-1463.

Edwards A.P. and J.M. Bremner. 1967. Microaggregates in soils. J. Soil Sci. 18:64-73.

Elliott E.T. 1986. Aggregate structure and C, N, and P in native and cultivated soils. Soil Sci. Soc. Am. J. 50:627-633.

Elliott E.T. and C.A. Cambardella. 1991. Physical separation of soil organic matter. Agric. Ecosyst. Environ. 34:407-419.

Elliott E.T., Paustian, K and S.D. Frey. 1996. Modeling the measurable or measuring the modelable: A hierarchical approach to isolating meaningful soil organic matter fractionations. *In* Evaluation of soil organic matter models. D.S. Powlson *et al.* (Eds.) NATO ASI Series Vol. 138.

Golchin A., Oades J.M., Skjemstad J.O. and P. Clarke. 1994. Soil structure and carbon cycling. Aust. J. Soil Res. 32:1043-1068.

Golchin A., Baldock J.A. and J.M. Oades. 1998. A model linking organic matter decomposition, chemistry, and aggregate dynamics. *In* R. Lal *et al.* (ed.) Soil processes and the carbon cycle. CRC Press, Boca Raton, FL.

Gregorich E.G., Kachanoski R.G. and R.P. Voroney. 1989. Carbon mineralization in soil size fractions after various amounts of aggregate disruption. J. Soil Sci. 40:649-659.

Griffiths E. and D. Jones. 1965. Microbial aspects of soil structure: I. Relationships between organic amendments, microbial colonization and changes in aggregate stability. Plant and Soil 23:17-33.

Hadas A. 1987. Long-term tillage practice effects on soil aggregation modes and strength. Soil Sci. Soc. Am. J. 51:191-197.

Hadas A. and D. Wolf. 1984. Soil aggregates and clod strength dependence on size, cultivation and stress load rates. Soil Sci. Soc. Am. J. 48:1157-1165.

Hartge K.H. 1995. Soil structure: Its Development and Function. CRC Press, Boca Raton FL.

Hassink J. 1995. Decomposition rate constants of size and density fractions of soil organic matter. Soil Sci. Soc. Am. J. 59:1631-1635.

Hassink J. and A.P. Whitmore. 1997. A model of the physical protection of organic matter in soils. Soil Sci. Soc. Am. J. 61:131-139.

Jastrow J.D. 1996. Soil aggregate formation and the accrual of particulate and mineral-associated organic matter. Soil Biol. Biochem. 28:665-676.

Jastrow J.D., Boutton T.W. and R.M. Miller. 1996. Carbon dynamics of aggregate-associated organic matter estimated by carbon-13 natural abundance. Soil Sci. Soc. Am . J. 60:801-807.

Jenkinson D.S. and J.H. Rayner. 1977. The turnover of soil organic matter in some Rothamsted classical experiments. Soil Sci. 123:928-305.

Juzwik J., Stenlund D.L., Allmaras R.R., Copeland S.M. and R.E. McRoberts. 1997. Incorporation of tracers and dazomet by rotary tillers and a spading machine. Soil Tillage Res. 41:237-248.

Kay B.D. 1990. Rates of change of soil structure under different cropping systems. Adv. Soil Sci. 12:1-51.

Kay B.D., Angers D.A., Groenevelt P.H. and J.A. Baldock. 1988. Quantifying the influence of cropping history on soil structure. Can. J. Soil Sci. 68:359-368.

Kemper W.D., Roseneau R.C. and A.R. Dexter. 1987. Cohesion development in disrupted soils as affected by clay and organic matter content and temperature. Soil Sci. Soc. Am. J. 51:860-867.

Letey J. 1991. The study of soil structure: Science or art. Aust. J. Soil Res. 29:699-707.

Martin J.P. 1946. Microorganisms and soil aggregation: II. Influence of bacterial polysaccharides on soil structure. Soil Sci. 61:157-166.

Martin J.P., Martin W.P., Page J.B., Raney W.A. and J.D. De Ment. 1955. Soil aggregation. Adv. Agron. 7:1-37.

Monreal C.M., Schnitzer M., Schulten H.-R., Campbell C.A. and D.W. Anderson. 1995. Soil organic structures in macro and microaggregate of a cultivated Brown Chernozem. Soil Biol. Biochem. 27:845-853.

Mortland M.M. 1970. Clay-organic complexes and interactions. Adv. Agron. 22:75-117

Murray R.S. and J.P. Quirk. 1990. Interparticle forces in relation to the stability of soil aggregates. *In* Soil Colloids and their Associations in Aggregates. M.F. de Boodt *et al.* (Eds.) Plenum Press, New York NY.

Oades J.M. 1984. Soil organic matter and structural stability: Mechanisms and implications for management. Plant and Soil 76:319-337.

Oades J.M. 1988. The retention of organic matter in soils. Biogeochem. 5:35-70.

Oades J.M. and A.G. Waters. 1991. Aggregate hierarchy in soils. Aust. J. Soil Res. 29:815-828.

Parton W.J., Schimel D.S., Cole C.V. and D.S. Ojima. 1987. Analysis of factors controlling soil organic matter levels in Great Plains grasslands. Soil Sci. Soc. Am. J. 51:1173-1179.

Paul E.A. and H. van Veen. 1978. The use of tracers to determine the dynamic nature of organic matter. 11th Congress Int. Soc. Soil Sci., Edmonton. 3:61-102.

Perfect E., Kay B.D., van Loon W.K.P., Sheard R.W. and T. Pojasok. 1990. Rates of change in soil structural stability under forages and corn. Soil Sci. Soc. Am. J. 54:179-186.

Plante A.F. 1996. Biodegradation of land applied oily food waste and associated changes in soil structural properties. M.Sc. Thesis. University of Guelph, Guelph ON.

Puget P., Chenu C. and J. Balesdent. 1995. Total and young organic matter distributions in aggregates of silty cultivated soils. Eur. J. Soil Sci. 46:449-459.

Santos D., Murphy S.L.S., Taubner H., Smucker A.J.M. and R. Horn. 1997. Uniform separation of concentric surface layers from soil aggregates. Soil Sci. Soc. Am. J. 61:720-724.

Shaymukhametov M.S., Titova N.A., Travnikova L.S. and Y.M. Labenets. 1985. Use of physical fractionation methods to characterize soil organic matter. Soviet Soil Sci. 16:117-128.

Staricka J.A., Allmaras R.R. and W.W. Nelson. 1991. Spatial variation of crop residue incorporated by tillage. Soil Sci. Soc. Am. J. 55:1668-1674.

Staricka J.A., Allmaras R.R., Nelson W.W. and W.E. Larson. 1992. Soil aggregate longevity as determined by the incorporation of ceramic spheres. Soil Sci. Soc. Am. J. 56:1591-1597.

Terpstra R. 1989. Formation of new aggregates under laboratory-simulated field conditions. Soil Tillage Res. 13:13-21.

Terpstra R. 1990. Formation of new aggregates and weed seed behaviour in a coarse- and in a fine-textured loam soil. A laboratory experiment. Soil Tillage Res. 15:285-296.

Tisdall J.M and J.M. Oades 1982. Organic matter and water-stable aggregates in soils. J. Soil Sci. 33:141-163.

Toth S.J. and R.B. Alderfer. 1960a. A procedure for tagging water stable soil aggregates with Co^{60}. Soil Sci. 89:36-37.

Toth S.J. and R.B. Alderfer. 1960b. Formation and breakdown of Co^{60}-tagged water-stable soil aggregates in a Norton silt loam soil. Soil Sci. 90:232-238.

Voroney R.P. and D.A. Angers. 1995. Analysis of the short-term effects of management on soil organic matter using the CENTURY model. *In* Soil Management and Greenhouse Effect. R. Lal *et al.* (Eds.) CRC Press, Boca Raton FL.

Waring S.A. and J.M. Bremner. 1964. Effect of soil mesh-size on the estimation of mineralizable nitrogen in soils. Nature 202:1141.

Wilcke W. and M. Kaupenjohann. 1997. Differences in concentrations and fractions of aluminum and heavy metals between aggregate interior and exterior. Soil Sci. 162:323-332.

Williams B.G., Greenland D.J. and J.P. Quirk. 1967. The effect of polyvinyl alcohol on the nitrogen surface area and pore structure of soils. Aust. J. Soil Res. 5:77-83.

Chapter 2:

Development of an inert tracer particle method for the study of soil aggregate dynamics[1]

1.0 Introduction

The use of an inert physical (or particle) tracer to study soil aggregation dynamics seems natural. Examining the behaviour of a particle tracer that would be an analogue for the constituents of soil aggregates would provide valuable information about aggregate formation and breakdown in a dynamic context, and may provide a means for determining soil aggregate turnover rates. While particle tracers have had some application in studies examining soil translocation due to erosion or tillage (e.g. Govers et al. 1994), their use in aggregation studies has been limited.

Toth and Alderfer (1960a) created soil aggregate tracers using tagged intact aggregates. Water-stable aggregates were soaked in a solution of radiocobalt (^{60}Co) and leached of excess cobalt to create tagged aggregates of various sizes. Using these tracers in incubation studies, Toth and Alderfer (1960b) found that the composition of soil aggregates is continuously changing and that the redistribution of aggregate fragments was widespread across all size fractions observed.

In several laboratory experiments, Terpstra (1989, 1990) used 2-mm glass beads to simulate soil particles and aggregates and observe aggregate formation and destruction. After applying several treatments, and observing the redistribution of glass beads towards a random distribution in various aggregate size fractions, the author concluded that the rate of aggregate destruction was greater than the rate of formation. In addition, almost all

---

[1] Versions of this chapter have been published.

Duke, M.J.M., Plante, A.F. and W.B. McGill. 2000. Application of INAA in the characterisation and quantification of Dy-labeled ceramic spheres and their use as inert tracers in soil studies. J. Radioanal. Chem. 244:165-171.

Plante A.F., M.J.M. Duke and W.B. McGill. 1999. A tracer sphere detectable by neutron activation analysis for soil aggregation and translocation studies. Soil Sci. Am. J. 63:1284-1290.

of the aggregates observed had been "reshaped" after two laboratory-simulated field seasons.

Field experiments using 1-3 mm ceramic spheres showed that the turnover of large macroaggregates was far less rapid (Staricka et al. 1992) than observed by Terpstra. The authors found that the tracer particles were incorporated into larger aggregates more rapidly than in smaller aggregates, and suggested that the larger aggregates breakdown and reform more frequently. Using a first-order model, the time required for 95% of the tracers to be incorporated, and hence the time required before reaching equilibrium, ranged from 3 to 23 years.

1.1 Objectives

The rates at which soil macroaggregates form, breakdown and turnover are not currently well known. To this end, the objective of the current study was to develop an improved particle tracer approach that could be used to directly observe the incorporation of soil particles and microaggregates into macroaggregates. The end goal is to be able to measure the rate at which soil macroaggregates form and breakdown.

The new tracer particle approach includes:

1) the manufacture of the tracer particle as a representative surrogate for soil macro- and microaggregates,
2) an analytical procedure for the detection and quantification of the tracer by instrumental neutron activation analysis, with the aim of devising an optimum procedure for routine analysis which would lend itself to automation, and
3) the characterization of the tracer particles for relevant properties.

2.0 Materials and Methods

2.1 Tracer sphere development

2.1.1 Tracer particle selection

Guiresse and Revel (1995) outlined several criteria for the selection of an appropriate tracer in soil translocation studies that can be applied to a soil aggregation application:

1) must be introduced homogeneously at a known concentration,

2) must not be transported in suspension or in solution, and

3) subsequent extraction and determination should be easy.

However, the primary deficiency of many previous studies using particle tracers is the lack of similarity between the selected tracer and soil. An effective particle tracer for soil aggregation studies must behave similarly to, or mimic, soil. This means the tracer must:

1) be of an appropriate size: if too large, the tracer may be avoided by soil fauna and can only be incorporated into large macroaggregates or soil clods.

2) be of an appropriate density: if too light, the tracer may float, and if too heavy, its movement down into the soil profile may be exaggerated.

3) have surface properties that allow normal interactions with soil particles and aggregates: aggregation is greatly affected by surface reactions and if the tracer does not have an appropriate surface the necessary interactions will not occur.

As outlined above, several different particles have been used as tracers in soil translocation and aggregation studies. However, the ceramic spheres used by Staricka et al. (1990, 1991, 1992) and Allamaras et al. (1996) hold the greatest potential for use in aggregation dynamics studies. The spheres are available commercially under the trade name Macrolite® and are manufactured by Kinetico Inc. (Nashwauk, MN). They are made of ground nepheline syenite, aluminium oxide, bentonite, and calcium carbonate. The ingredients are mixed with water to form a paste which is prilled to form spheres of various sizes which are first dried and then kiln fired at ~1500°C. The firing produces hardened spheres with a sealed rough outer surface and honeycombed interior (Figure 2-1). Variations in firing conditions give some control over the final density of the spheres, to between 0.3 g cm^{-3} to 3.0 g cm^{-3}. The final product is then sieved into various size fractions and ready for use.

The ceramic spheres were considered the best analogue to soil particles and aggregates because they are:

1) available in various size fractions ranging from 0.2 mm to over 6 mm,

2) rough surfaced and impermeable to water entry,

3) anionic,

4) hydrophilic,

5) slightly alkaline, and

6) of modifiable density by kiln firing to between 0.3 to 3.0 g cm^{-3}.

To this end, Macrolite® ceramic spheres were selected as our particle tracer, and by working closely with Kinetico, several batches of spheres were manufactured to meet our needs.

2.1.2 Tracer detection

Staricka et al. (1992) successfully used ceramic spheres (1-3 mm diameter) to estimate the longevity of large (>12 mm) soil aggregates. The ceramic spheres were painted with fluorescent paint and manually detected and quantified by visual inspection. Our interest in the sequestration of carbon in soils required us to examine much smaller soil aggregates (<8 mm) and hence the need for much smaller tracer particles. We concluded that the methods used to detect and quantify 1-3 mm diameter ceramic spheres would be inadequate for measuring the <1 mm diameter spheres required for our purposes. It was therefore considered worthwhile to investigate the application of neutron activation analysis as a potential means of detecting and quantifying the sub-millimetre diameter ceramic spheres.

The principles of neutron activation analysis are well summarized in DeSoete et al. (1972). Essentially, neutron activation analysis (NAA) involves the detection and quantification of gamma-rays (γ-rays) produced from the decay of radionuclides generated by the neutron irradiation of stable isotopes. These γ-rays are characteristic of the radionuclides producing them and the photopeak intensity is related to the element mass by the activation analysis equation (Duke, 1983):

$$A = \frac{m \cdot N \cdot \theta \cdot \delta \cdot \varphi \cdot I \cdot \varepsilon}{M \cdot \lambda} \left(1 - e^{-\lambda \cdot t_1}\right) \cdot e^{-\lambda \cdot t_2} \cdot \left(1 - e^{-\lambda \cdot t_3}\right) \qquad (7)$$

where:

A	=	photopeak area
m	=	mass of element
N	=	Avogadro's number
θ	=	fractional isotopic abundance of isotope
δ	=	effective cross section
φ	=	neutron flux (n cm^{-2} s^{-1})
I	=	fractional gamma yield
ε	=	fractional detector efficiency
M	=	molecular mass of target element
λ	=	decay constant ($\ln 2 / T_{1/2}$)
t_i	=	irradiation time (s)
t_d	=	decay time (s)
t_c	=	count time (s)

The source of neutrons for the irradiations in the current study was the University of Alberta SLOWPOKE II Nuclear Reactor Facility. A pneumatic "rabbit" system, with transit times into or out of the reactor of approximately 1.5 s and an automatic irradiation time controller, makes the analysis of short-lived radionuclides straightforward. From the equation above, it is apparent that the principle operational parameters for NAA are the irradiation time, decay time, count time, and the neutron flux.

The stability and reproducibility of the neutron flux is important when determining elements via their short-lived radionuclides. Variability of the neutron flux in SLOWPOKE reactors operating at normal flux levels (0.1 to 1 $\times 10^{12}$ n cm^{-2} s^{-1}) was found to be $< \pm 2\%$ (2σ) (Ryan et al. 1978; Bergerioux et al. 1979). The current work required a much lower neutron flux (2×10^{10} n cm^{-2} s^{-1}) due to large sample sizes. Stability and reproducibility at this decreased flux was recently found to be $\pm 1.35\%$ (1σ) (Duke et al. 2000). For this reason, it was unnecessary to constantly include flux monitors and elemental standards with samples, thereby greatly simplifying the analytical procedure.

The process of sample analysis by *instrumental* neutron activation analysis (INAA, which indicates no initial sample concentration or extraction) is to: irradiate the sample for an appropriate period of time (t_i), allow the sample to stand for a period of time (t_d) to allow the decay of interfering radionuclides, followed by placing the sample at a γ-ray detector and counting for a period of time (t_c).

2.1.3 Tracer labelling

The use of INAA in tracer studies requires a significant elemental difference between the tracer and matrix. Three possible approaches using ceramic spheres and INAA were considered for studying soil aggregate formation and breakdown:

1) the application of non-labelled ceramic spheres to soil and their later determination by INAA, thus requiring that the non-labelled spheres fortuitously contain some element(s) of sufficient concentration, in comparison to the soil, to be used as a tracer,
2) radiolabelling of the spheres by neutron activation before their use as a radiotracer, requiring that the spheres contain, again fortuitously, some element(s) suitable as long-lived radiotracer, or
3) doping the spheres at the time of manufacture with an inert, but readily activated element, that was absent (or in low concentration) in the soil matrix, with subsequent determination in the soil/sphere mixture by INAA.

Initial INAA of spheres, as supplied by the manufacturer, and of Malmo soil sampled from the Ellerslie research farm indicated that while lanthanum (La) and samarium (Sm) where much more abundant in the spheres than in the soil, it would be difficult to accurately quantify < 5% spheres in a soil/sphere mixture. This equated to hundreds or thousands of spheres and was much greater than the goal of quantifying ten or fewer spheres in a ~5 g soil sample. Furthermore, the analyses showed that the non-labelled spheres did not contain sufficient concentrations of those elements capable of producing the necessary quantities of long-lived radioactivity for use of the spheres as radiotracers. In addition, the use of radiotracers in field-scale experiments requires licensing and poses a radiological risk to both researcher and the environment. Consequently, the third option, that of labelling the spheres during manufacture with a readily activated element and subsequent detection and quantification by INAA, was pursued.

Several criteria guide the selection of an element with which to label the tracer spheres. The labelling element must:

1) be absent, or present in very low quantities in the background soil matrix,
2) have a high sensitivity by INAA, *i.e.,* activate readily due to a high neutron cross-section,
3) produce a short-lived radionuclide for the rapid analysis of large numbers of samples,
4) be non-volatile at the high temperatures (~1500°C) experienced during kiln firing of the spheres,
5) be commercially available and of high purity,
6) be relatively inexpensive,
7) be non-toxic, and
8) be chemically fixed in the ceramic spheres.

Various metals (*e.g.* Cr, Co, Ag, In, Ir, Au) and most of the rare earth elements (*e.g.* La, Sm, Eu, Tb, Dy, Ho) readily activate and have been employed as inert tracers determined by neutron activation analysis (e.g. Behrens et al. (1977), Kennelly et al. (1980, 1982), Reibe (1995)). For a short irradiation, decay, and count scheme, In (as ^{116m}In) and Dy (as $^{165m, 165}$Dy) demonstrate the greatest sensitivity by NAA. While indium naturally occurs at the sub-μg g^{-1} level in most soils, its high volatility at the temperatures required to fire the ceramic spheres rules out its choice as an ideal labelling element. While europium (as Eu_2O_3) and dysprosium (as Dy_2O_3) are both refractory, Dy is more sensitive to NAA (cross-section of 2000 barns versus 320 barns, respectively) and is significantly less costly. Dysprosium invariably occurs at less than 10 μg g^{-1} in most soil types and, in the oxide form, is readily available in a high purity form (i.e. ≥ 99%). An additional benefit of using Dy as the labelling element is the presence of both long- and short-lived radioisotopes after neutron activation. This property was used to our advantage when performing preliminary characterization experiments.

To achieve a reasonably low detection limit in soils, a nominal tracer sphere Dy content of 15 wt % Dy_2O_3 (99% pure, Stanford Materials Inc., Stanford CA) was prepared during the manufacture of the spheres by Kinetico.

2.2 Tracer sphere characterization

Prior to the full-scale implementation of the tracer particle approach, a small pilot batch of spheres was manufactured. Several characterization analyses were performed on the pilot batch to verify their effectiveness in planned experiments. Larger batches of spheres were subsequently manufactured for use in the field experiments. In all, three batches of spheres were produced:

1) the small pilot batch, for proof of principle characterizations,
2) a full-scale batch, which was subsequently used in the field experiments of 1998, and
3) a second full-scale batch, which was used in the field experiments of 1999.

Physical characterizations were performed on each batch used due to the variability created during the manufacture of different batch of spheres at different times.

In addition, each batch of spheres was subdivided into three size fractions of principle concern. To be consistent with how Kinetico classifies their prills, the size fractions considered during the course of the experiments will be referred to according to the mesh size attributed to them by Kinetico, although this labelling may not reflect the actual sizes of the spheres within the fraction. The size fractions are thus: Large (14 to 30 mesh), Medium (30 to 50 mesh), and Small (50 to 70 mesh).

2.2.1 Surface characteristics

The manufacturing process of Macrolite includes a kiln firing of the prill at 1500°C. This caused some concern about the integrity of the mineral and surface characteristics of the prill. Consequently, X-ray diffraction (XRD) analyses were performed on both non-fired and fired samples of prill from the pilot-scale batch to determine if the spheres maintained their mineral structure after kiln firing. Samples were analysed at 0% relative humidity using a Philips diffractometer (Model 1710, Philips Electronics Ltd., Scarborough ON) equipped with a LiF curved crystal monochromator using CoKα radiation generated at 50 kV and 25 mA. Step sizes of 0.05° 2θ and an accumulation time of 2 second step^{-1} were used for data acquisition.

2.2.2 Mass and size variability

Before using each batch, the mass and size variability within each of the size fractions was characterized to assess any potential problems in quantifying the sphere once added to soil samples.

Initially, the mean sphere mass in each size range of the pilot batch was determined in a composite sample by weighing and counting spheres collected on a previously weighed piece of adhesive tape. Subsequently, masses of randomly selected single spheres (n=30 for the pilot-scale batch and n=15 for full-scale batches) were recorded for the Dy concentration analysis. Mean sphere masses of each size fraction from each of the full-scale batches were determined by the latter approach only.

Sphere diameters were determined using image analysis using custom-developed software on a Macintosh personal computer after samples of spheres from each sieve size were mounted on microscope slides and digitally photographed. Cross-sectional area, and maximum X and Y length data were collected using image analysis software. Mean effective sphere diameters and their distributions were calculated from the cross-sectional area data, and a surrogate measurement for tracer particle "sphericity" was obtained by dividing the maximum X and Y lengths.

Mean single sphere masses and mean effective diameters were used to estimate sphere densities. In addition, actual sphere densities were measured using the pycnometer method (Blake 1965) for each size fraction from each of the pilot-scale and full-scale batches (replicated 4 times).

2.2.3 Dysprosium concentration

While the targeted Dy content of the tracer spheres was 13.7% Dy (by addition of 15% Dy_2O_3), measurements were made to determine the accuracy and variability of this value in each of the size fractions and batches produced. Randomly selected single spheres (those referred to above in single sphere mass tests) were analysed for Dy by INAA.

The individual spheres were sealed in narrow, ~250 µL polyethylene micro-centrifuge tubes. The micro-centrifuge tubes were then enclosed in a second larger (7 mL)

polyethylene rabbit vial for irradiation. Dysprosium standards were prepared from commercial atomic adsorption standard solutions (Sigma) that were dried in micro-centrifuge tubes. The single spheres and standards were irradiated for 30 s at a nominal neutron flux of 1×10^{11} n cm^{-2} s^{-1}. Following a decay time of 30 s (during which time the micro-centrifuge tubes were removed from their 7 mL irradiation rabbits and placed in the counting position) each sample was counted for 30 s live-time. Counting of the single spheres was performed using an ORTEC GEM series hyperpure GE detector, coupled to an APTEC 6300 spectroscopy amplifier and APTEC V4.3 PC-based MCArd (Aptec Instruments Ltd., Concord ON). The detector specifications include a relative efficiency of 22.1%, and a measured FWHM of 1.71 keV and peak-to-Compton ratio of 59.9:1, for the 1332 keV photopeak of ^{60}Co. Signals were assigned to one of 256 channels and stored for subsequent analysis.

The Dy content of the spheres was quantified by measuring the 108 keV γ-ray emission of the short-lived radionuclide ^{165m}Dy ($T_{1/2}$ = 75.48 s). Given the increasing Dy content with increasing size of labelled sphere the small, medium and large size fractions were counted at a sample-to-detector geometry of 1 cm, 3 cm, and 10 cm, respectively. The conical bottom of the micro-centrifuge tubes combined with a specific micro-tube sample holder provided a highly reproducible counting position for the tracer spheres. The dysprosium content of the spheres was determined via the semi-absolute method of NAA (Bergerioux et al., 1979) using two reference soil standards, SO-1 (4.5 ± 0.4 mg kg^{-1} Dy) and SO-2 (8.8 ± 1.4 mg kg^{-1} Dy) (Gladney and Roelandts 1989).

2.2.4 Label leaching and tracer integrity

To assess whether the Dy-label would readily leach from the tracer spheres and/or if the tracer spheres were sufficiently robust for experimental work, leaching and disintegration trials were performed. In leaching experiments, 200 mg of the large spheres from the pilot-scale batch were added to 100 mL of deionized water in a 125 mL Nalgene bottle and allowed to stand for 48 hrs. The disintegration experiments were similar, where three 6-mm diameter glass beads were added to the 200 mg of labelled spheres, again in 100 mL of deionized water in a Nalgene bottle and placed on a reciprocal shaking table for 48

hrs. Dy-label released due to leaching or sphere disintegration was determined by INAA, by analysing 2 mL aliquots of the respective solutions taken after a short shaking to re-suspend any fine particles. Samples and blanks were irradiated for 30 s at a nominal neutron flux of 5×10^{11} n cm^{-2} s^{-1} and following a decay period of 45 s were counted for 30 s live-time using a 6 cm horizontal geometry. The 22% Ge detector and spectroscopy system outlined above were used for data collection. The Dy content of the samples was quantified using the short-lived isotope, ^{165m}Dy, and given the high aluminum content of the spheres, Al as indicated by ^{28}Al was also measured to assess tracer sphere disintegration.

When compared to the original pilot-scale batch of sphere, the full-scale batches contained a large amount of dust and fine particles. To determine the composition of the fine materials and to assess their effect on detecting and quantifying the spheres, 4 replicates of 1 g of large spheres from the 1999 batch were manually shaken with 100 mL of deionized water for 1 minute in a 125 mL Nalgene bottle. After a period of standing sufficient to allow the settling of spheres but not suspended particles, 2 mL aliquots were taken for INAA for Dy. The remaining spheres were further washed on a 125 μm sieve and dried overnight at 105°C. Samples of approximately 20 mg of washed and unwashed spheres were analyzed by INAA to determine any differences in Dy-content.

2.2.5 Detection limit

Estimates of the detection limit number of spheres were calculated based on an estimated soil background Dy content of 4 μg g^{-1}, an assumed 13.7% Dy content of the spheres, and the measured mean sphere mass. These values were used as a basis for the spiking of 5 g soil samples (Malmo series, Orthic Black Chernozem, sampled from Ellerslie Research Station, Edmonton AB) with known numbers of spheres from the pilot-scale batch and subsequent INAA for Dy, and hence sphere content. The number of spheres added to each soil sample represented approximately 0.5×, 1×, and 2× the estimated detection limit. Samples of each number of added spheres were replicated 8 times in the Large fraction, and 6 times in the other fractions.

The soil-sphere mixtures, in 7 mL polyethylene irradiation vials, were irradiated in the SLOWPOKE reactor for 240 s at a nominal neutron flux of 0.2×10^{11} n cm^{-2} s^{-1} using an auto-irradiation stack loader. Activation of the soil matrix released an initially high level of short-lived radioactivity (e.g., ^{28}Al - $T_{1/2}$ = 2.24 min, ^{52}V - $T_{1/2}$ = 3.75 min and ^{51}Ti - $T_{1/2}$ = 5.75 min). Consequently, Dy in the spheres contained in the soil sample was detected following a decay period of ~30 minutes to reduce the interfering signal from high levels of ^{28}Al activity, during which time samples were transferred to an automatic counter. The samples were counted for 300 s live-time. Counting was performed using an ORTEC GEM series hyperpure Ge detector, coupled to an APTEC 6300 spectroscopy amplifier and APTEC V2.1 PC-based MCArd (Aptec Instruments Ltd., Concord ON). The detector specifications include a relative efficiency of 19.8%, and a measured FWHM of 1.68 keV and peak-to-Compton ratio of 58.4:1, for the 1332 keV photopeak of ^{60}Co. Signals were assigned to one of 4096 channels and stored for subsequent analysis.

The Dy content of each sample was determined by measuring the 94.7 keV γ-ray emission of the longer-lived Dy radionuclide, ^{165}Dy ($T_{1/2}$ = 2.334 hrs). Samples were counted at a sample-to-detector geometry of 3 cm. The dysprosium content of each sample was again determined *via* the semi-absolute method of NAA (Bergerioux et al., 1979). The CANMET soils SO-1 and SO-3, and NIST (formerly NBS) 1633a coal flyash were prepared and analysed with the samples as standards.

2.3 Quantification of tracer spheres by INAA

INAA permits an accurate quantification of tracers in soil samples by quantifying the gamma-rays emitted from the activated Dy. However, the data produced by the procedure requires several corrections for decay time and instrumental errors. These corrections are illustrated in Figure 2-2.

Decay time corrections are required to normalize the data for the variable time that a sample is allowed to decay. Deadtime losses occur during pulse height analysis and storage and are accounted for by extending the count time. A deadtime correction factor is necessary because more counts are lost at the beginning of the count time than are recovered at the end due to decay during the count time. The correction is particularly

important when counting isotopes with short half-lives. Therefore, corrections for counting short-live radionuclides in the presence of longer-lived radionuclides such as ^{56}Mn and ^{24}Na (Desoete et al. 1972) were applied to samples for single sphere Dy analysis. No deadtime correction factor was used in soil-sphere mixtures since the longer-lived isotope of Dy was measured.

A pulse pile-up correction factor (PPCF) is determined and applied for random summing effects, *e.g.* the arrival of multiple counts at once, using a pulser. For samples run with the pulser, the PPCF is calculated as shown in Figure 2-2. However, some soil-sphere samples were inadvertently run without a pulser. A "calibration curve" relating the dead time (as expressed by % Busy) to the PPCF was developed using samples run with a pulser and applied to those run without. The calibration data is illustrated in Figure 2-3, and shows a quadratic best-fit relationship between % busy and the PPCF.

Each of the appropriate correction factors were applied to the mass of Dy determined by INAA, and finally the mass of sphere-associated dysprosium measured in a sample is determined by subtracting the background soil-associated Dy (as determined by soil mass multiplied by mean soil Dy concentration) from the total measured sample Dy.

3.0 Results

3.1 Surface characteristics

The results of the XRD analyses of the kiln fired and non-fired sphere samples indicate that the mineral structure of the spheres is maintained during firing. Strong reflections associated with feldspathoid minerals (D-spacing of 3.30 to 3.18 Å) were generated by both the fired and non-fired samples, although the fired sample showed decreased intensity. The decreased intensity indicates a minor loss of crystalinity during firing of the spheres.

3.2 Mass and size variability

Variability of sphere masses in the pilot-scale batch samples mounted on adhesive tape was a function of sphere size, wherein variability generally decreased with decreasing sphere size (Table 2-1). When compared to the much smaller data set of the single sphere

masses collected for INAA (Table 2-2), sample size shows a significant effect on the variability in mass data.

Particle size distribution analyses by image analysis are reported as calculated mean effective sphere diameters (Table 2-3) and cumulative distribution functions of these diameters within size fractions (Figure 2-4). Variability in the size of spheres in each of the size fractions generally decreased with decreasing sphere size, which is consistent with mass variability. In addition, the sphericity of the tracer particles showed a trend to greater sphericity (X/Y approaching 1) in larger size fractions. This is due to the fact that the small size fraction contains irregularly shaped fragments rather than entire prills.

Sphere densities calculated using mean mass and diameter, and measured using pycnometers are summarized in Table 2-4. Any discrepancies between the calculated and measured densities are likely due to errors in the calculated values from a lack of sphericity, or due to the differential expansion of the spheres during kiln firing.

3.3 Dysprosium concentration

Mean single sphere Dy concentrations by mass for each batch are summarized in Table 2-5. The variable sample size in the pilot-scale batch was due to the escape of the smaller spheres through cracks that had formed in the micro-centrifuge tubes. Within sphere size fractions, the respective coefficients of variation ranged from 6.0% to 14.6%. No general trend between Dy concentration and size fraction, or tracer mass was observed (Figure 2-5).

3.4 Label leaching and tracer integrity

The results of the label leaching and tracer integrity tests are summarized in Table 2-6. Dysprosium was not detected in the 2 mL water aliquots taken after soaking in 100 mL of water for 48 hrs. This demonstrates that the Dy label is well fixed in the ceramic matrix and will not readily leach out in water. However, some Dy and Al were measured in 2 mL water aliquots taken from the samples that had been shaken with glass beads for 48 hrs. At first sight these results would indicate that there is some minor disintegration when abrading forces are applied. However, the amount of Al detected by INAA in the aliquots was not significantly higher than the blank water samples and the Bio-Rad

cryogenic sample containers that were used for irradiation and counting. One would expect that if the spheres were disintegrating and releasing fine ceramic material, that in addition to detecting Dy one would also detect a significant Al signal. Consequently, it is suspected that the Dy released during shaking was residual particulate Dy_2O_3 located on the surface of the tracer particles, which was released when shaking the samples. In any case, the Dy signal measured in samples after 48 h of shaking represented significantly less than 1% of the Dy content in the particles. These results indicate that tracer and label integrity are sufficient for practical experimental use.

In tests to examine the composition of dust associated with the full-scale batches of tracer spheres, the results were similar to those from the pilot-scale. INAA of water aliquots after manual shaking with 1999 full-scale batch spheres showed less than 1% of Dy was recovered in the solution. In addition, INAA of approximately 20 mg of washed and unwashed spheres resulted in 953.0 ± 20 and 928.8 ± 15 counts mg^{-1} of spheres, respectively. While a t-test found the difference to be statistically significant ($p = 0.105$), if one expected the dust and fine particles in the full-scale batches to contain a significant amount of Dy, the results would be reversed. Hence, we do not expect that the dust found in the full-scale batches will affect the results of subsequent analyses.

3.5 Detection limit

Analysis of 5 g soil samples spiked with known numbers of tracer spheres revealed that the detection limit of the method was more sensitive than anticipated from preliminary calculations (Table 2-7). INAA of soil samples containing no spheres showed a background dysprosium concentration of approximately 3.1 $\mu g\ g^{-1}$ soil. In addition to determining the threshold numbers of spheres, the INAA data were used to determine a calculated number of spheres present based on mean sphere mass and measured single sphere Dy content. The calculated number was then compared to the actual number using a paired t-test. Actual and calculated numbers of spheres did not differ significantly at $p = 0.05$ within size fractions (Table 2-7).

4.0 Discussion

For a tracer particle to be useful as a surrogate for soil aggregates and particles, it must have similar physical and chemical properties to soil particles. Unlike plastic or glass beads, the ceramic spheres selected have surface properties similar to soils, which allows for normal interactions between tracer and soil. The XRD results indicate that the kiln firing of Macrolite® spheres does not fuse the material to create a physico-chemically amorphous surface. This is an important result as it supports the decision to use the ceramic spheres as an appropriate surrogate for soil particles and aggregates.

An important property of particle tracers is their density. Tracer density determines how a tracer may behave within the soil matrix or on the surface of a hillslope. An advantage of using Macrolite® as a tracer material is that the density of the spheres may be customized to some degree by altering the kiln firing process to produce heavier or lighter spheres. The density of the ceramic spheres previously used by Staricka et al. (1990, 1991, 1992) and Allmaras et al. (1996) was approximately 0.35 g cm^{-3}. The measured densities of several sizes and batches of tracers used in this study ranged from 1.4 to 2.6 g cm^{-3} (Table 2-4). Lighter spheres such as those used previously can be useful as they are easily extracted by floatation when soil samples are washed. However, the use of INAA precludes the need for tracer sphere extraction, and hence tracers can more closely simulate soil particle or aggregate densities.

Effective use of the tracer spheres in ongoing experiments requires a reliance on the manufacturing process to produce consistent sphere characteristics in multiple batches. Several statistical tests were performed using SAS (SAS Institute Inc.) to compare the means and the variability around the means of various tracer sphere characteristics between and within batches (Table 2-8 and 2-9). Results of these tests show some significant differences in both the mean and variability of key tracer sphere characteristics between batch productions. The most significant differences in sphere characteristics occur in the large size fractions. This is likely due to the differential expansion of the spheres during kiln firing, which does not occur to the same extent in the smaller fractions. While statistical tests comparing Dy concentration between size

fractions within each batch showed some significant differences, these differences are usually quite small and no general trends between Dy-concentration and sphere mass were observed (Figure 2-5).

The reported significant differences do not necessarily impose barriers to the application of the developed method, but serve to clearly illustrate the need to characterize each batch of tracer sphere produced. In addition, it should be noted that significant differences in sphere properties between size fractions are not necessarily a concern, as a given experiment will use only one size fraction. To simultaneously study the behaviour of various sized particles would, at the least, require the use of a different elemental label for each size range. While this approach may be practical, it was not the goal of the current study.

More important than variability between batches or between size fractions, variability in size, mass and Dy concentration within particular size fractions of a given batch of tracer spheres is a significant concern since the detection and quantification of the tracers is based on the measured Dy content of a mixed sphere and soil sample. The variability affects the ability of INAA to detect and determine a given number of spheres in a soil sample. Coefficients of variance for the various sphere characteristics measured range from 5% up to 54%. Such high variability causes some concern that the tracer spheres would not be sufficiently homogeneous for experimental use. However, results of detection limit trials indicate that this source of error may not be as significant as originally suspected. The paired t-tests performed to compare the actual and calculated sphere numbers showed no significant differences within sphere size fractions (Table 2-7). This is an important result as it relieves some of the concern caused by variability in tracer sphere size, mass, and Dy concentration. The over-all variability present appears to be insufficient to affect the counting of spheres even at a level where few spheres are present.

INAA provides a detection method that is not only highly sensitive, but also independent of many soil and environmental variables. Figure 2-6 illustrates typical gamma-ray spectra of tracer spheres, soil, and a mixture of the two. Detection and quantification of

tracer spheres depends only on the Dy-label concentration of the spheres, sample mass, and the soil background concentration. This allows its application in varying water contents, bulk densities, and soil and vegetation types. Without the requirement for tracer extraction, concentration or visual enumeration, the INAA approach provides a rapid throughput of sample analyses. A throughput of 9 samples h^{-1} was achieved using the protocol established for ~5 g soil/sphere mixtures. In addition, the INAA of an inert tracer is superior to the use of radiochemical tracers as the latter requires licensing of field sites, and suffers from loss of tracer precision due to plant uptake (e.g. ^{32}P), leaching and/or due to decay of short-lived radionuclides over longer experimental periods. It should be noted that while specialized, neutron irradiation facilities are not uncommon (e.g.: 6 SLOWPOKE reactors in Canada, 40+ TRIGA and other research reactors in the U.S., and other reactor facilities around the world) and the cost of analyses is moderate ($6-10 per sample).

5.0 Conclusion

The objective of the current study, to develop an inert tracer particle and a routine analytical procedure for the INAA detection of the tracers for soil aggregation dynamics studies, has been met.

The study has shown that Macrolite® ceramic spheres (≤ 1 mm in diameter) enriched with a Dy label (~10-15% Dy) function as readily detected analogues for soil particles and aggregates. The use of the ceramic spheres is preferred over other potential tracers since the tracer closely simulates soil aggregate properties. The addition of Dy as a labelling element allows for the use of a rapid, routine, and non-destructive INAA detection technique. The dual short-lived radionuclides of Dy have been used to advantage; rapid characterisation of the Dy content of spheres is performed using ^{165m}Dy ($T_{1/2}$ = 2.24 min), while the Dy content of soil/sphere mixtures is best determined using ^{165}Dy ($T_{1/2}$ = 2.334 hr).

The inert tracer approach, with detection and measurement by INAA, offers the specificity of a radiotracer approach but without the potential health or environmental risks, or the need for tracer extraction or visual inspection and identification.

Table 2-1. Tracer sphere mass and variability in composite samples from pilot-scale batch †.

Mass characteristic	Size fraction		
	Large	Medium	Small
Mean (μg sphere^{-1})	978	109	20.8
CV (%)	16.6	8.3	5.3
Mean spheres per sample	56	179	72

† as collected on adhesive tape, n = 8 composite samples

Table 2-2. Tracer sphere mass (μg sphere^{-1}) and variability in single sphere samples †.

Batch	Size fraction		
	Large	Medium	Small
Pilot-scale (n = 30)	936 ± 503 (54%)	105 ± 55 (52%)	21.6 ± 6.5 (30%)
Full-scale 1998 (n = 15)	963 ± 489 (51%)	105 ± 56 (53%)	25.5 ± 5.4 (21%)
Full-scale 1999 (n = 15)	526 ± 277 (53%)	89.8 ± 26 (29%)	21.1 ± 7.5 (36%)

† Mean ± SD (CV)

Table 2-3. Mean sphere sizes determined from image analysis data.

Batch	Size characteristic	Size fraction		
		Large	Medium	Small
Pilot-scale	Mean diameter ± SD (μm)	850 ± 192	406 ± 79	290 ± 35
	Diameter range (μm)	407 – 1414	291 - 630	210 – 393
	X / Y	1.11	1.23	1.33
	Number of determinations	187	109	137
Full-scale 1998	Mean diameter ± SD (μm)	749 ± 124	425 ± 92	270 ± 34
	Diameter range (μm)	593 – 1135	171 - 609	189 – 353
	X / Y	1.09	1.19	1.25
	Number of determinations	36	90	120
Full-scale 1999	Mean diameter ± SD (μm)	613 ± 78	380 ± 76	259 ± 31
	Diameter range (μm)	427 – 775	223 – 620	176 – 353
	X / Y	1.11	1.23	1.36
	Number of determinations	36	61	101

Table 2-4. Calculated † and measured ‡ sphere densities (in g cm^{-3}, n = 4, CV < 1%).

Batch	Large		Medium		Small	
	Calculated	Measured	Calculated	Measured	Calculated	Measured
Pilot-scale	2.91	2.22	2.99	2.44	1.69	2.63
Full-scale 1998	4.38	2.44	2.99	2.57	2.47	2.85
Full-scale 1999	4.36	1.40	3.13	1.77	2.32	2.38

† using mean single sphere mass and diameter
‡ using pycnometer

Table 2-5. Concentration of Dy label in single spheres (% wt) †.

Batch	Size fraction		
	Large	Medium	Small
Pilot-scale (n = 30, 19, 18)	11.4 ± 0.7	11.8 ± 1.1	11.0 ± 1.2
Full-scale 1998 (n = 15)	14.5 ± 1.3	15.8 ± 1.1	14.3 ± 2.1
Full-scale 1999 (n = 15)	14.2 ± 0.5	13.3 ± 0.6	10.8 ± 1.6

† Mean ± SD

Table 2-6. INAA counts from 2 mL water aliquots taken from sphere integrity tests †.

	Al (counts)	Dy (counts)	% of initial
Blank (water and vial only)	1907 ± 32	n/d‡	-
Spheres soaking in water for 48 h	1909 ± 43	n/d	-
Spheres shaken in water with glass beads for 48 h	1874 ± 100	1213 ± 850	0.12

† Mean ± SD, n = 4 replicates
‡ not detected

Table 2-7. Dy content of soil samples with and without spheres from pilot-scale batch and associated calculated numbers of spheres [†].

Soil/sphere mixture	Sample Dy content ($\mu g\ g^{-1}$)	Number of spheres		Actual equal to Calculated? [‡]
		Actual	Calculated	
Blank soil	3.1 ± 0.2	0	—	—
with Large spheres	103.1 ± 25.3	5	4 ± 1	H_0
	46.7 ± 20.6	2	2 ± 1	
	22.9 ± 7.9	1	1 ± 0	
with Medium spheres	60.3 ± 16.0	15	23 ± 6	H_0
	23.4 ± 4.3	6	8 ± 2	
	10.6 ± 3.5	3	3 ± 1	
	6.0 ± 0.4	1	1 ± 0	
with Small spheres	19.7 ± 2.2	30	35 ± 5	H_0
	11.6 ± 1.5	15	18 ± 3	
	7.6 ± 1.2	8	9 ± 2	

[†] Mean ± S.D., n = 8 in Large and n = 6 in Medium and Small sphere size fractions for each number of added spheres.
[‡] by paired t-test at $p = 0.05$; H_0 = null hypothesis accepted

Table 2-8. Pair-wise comparisons of means and variances of sphere characteristics between manufactured batches [†].

		Batch comparison for size fraction								
		Large			Medium			Small		
		Pilot vs. F98[‡]	Pilot vs. F99	F98 vs. F99	Pilot vs. F98	Pilot vs. F99	F98 vs. F99	Pilot vs. F98	Pilot vs. F99	F98 vs. F99
Mass	$\bar{x}$	ns	***	***	ns	ns	ns	ns	ns	ns
	s^2	ns	*	*	ns	**	**	ns	ns	ns
Diameter	$\bar{x}$	***	***	***	ns	ns	*	ns	*	ns
	s^2	**	***	**	ns	ns	ns	ns	ns	ns
Dysprosium concentration	$\bar{x}$	***	***	ns	***	***	***	***	ns	***
	s^2	**	ns	***	ns	ns	ns	*	ns	ns

ns, *, **, *** Not significant, significant at the 0.05, 0.01, 0.001 probability levels, respectively.
[†] comparisons of means performed by LSMEANS in proc GLM and comparisons of variances by proc TTEST, in SAS.
[‡] Pilot is pilot-scale batch, F98 is full-scale batch from 1998, and F99 is full-scale batch from 1999.

Table 2-9. Pair-wise comparisons of mean and variance of Dy concentration between sphere size fractions within batches [†].

	Size fraction comparison for batch								
	Pilot-scale			Full-scale 1998			Full-scale 1999		
	Small vs. Medium	Medium vs. Large	Small vs. Large	Small vs. Medium	Medium vs. Large	Small vs. Large	Small vs. Medium	Medium vs. Large	Small vs. Large
Mean	*	ns	ns	***	**	ns	***	*	***
Variance	ns	ns	*	*	ns	ns	**	ns	***

ns, *, **, *** Not significant, significant at the 0.05, 0.01, 0.001 probability levels, respectively.
[†] comparisons of means performed by LSMEANS in proc GLM and comparisons of variances by proc TTEST, in SAS.

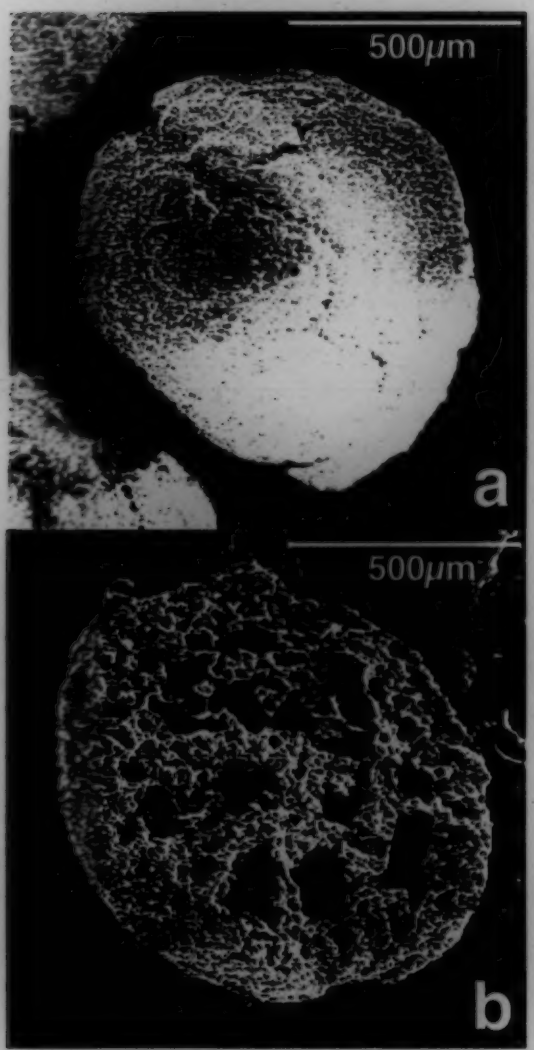

Figure 2-1. Scanning electron micrograph of tracer spheres showing (a) sealed exterior surface, and (b) honeycombed interior.

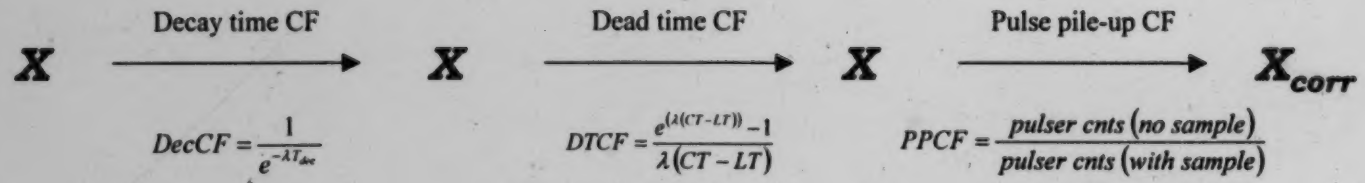

Where:

λ	=	$\ln 2 / T_{1/2}$
$T_{1/2}$	=	half-life of isotope in question (s)
T_{dec}	=	decay time (s)
CT	=	clock or true time (s)
LT	=	live time (s)

Figure 2-2. Correction calculations for determination of mass of tracer Dy.

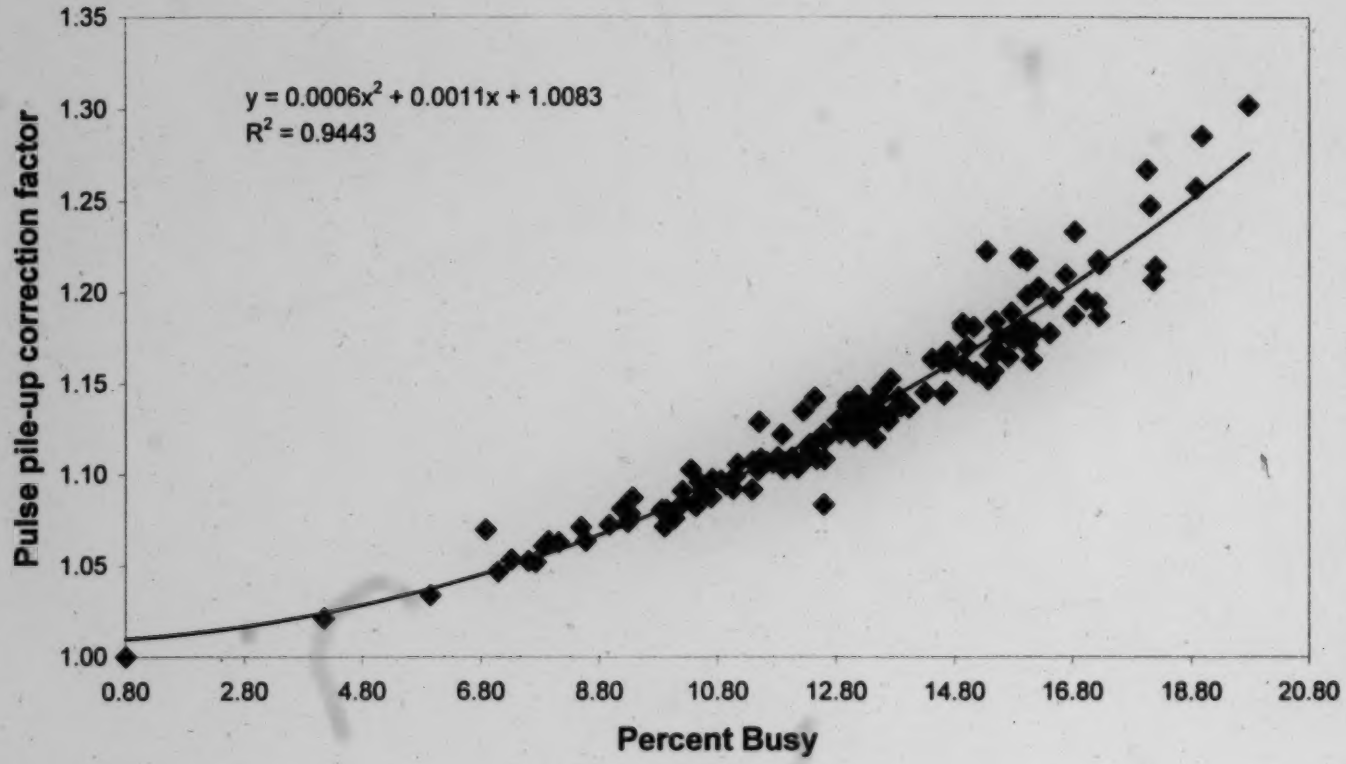

Figure 2-3. Calibration curve relating dead time to pulse pile-up correction factor.

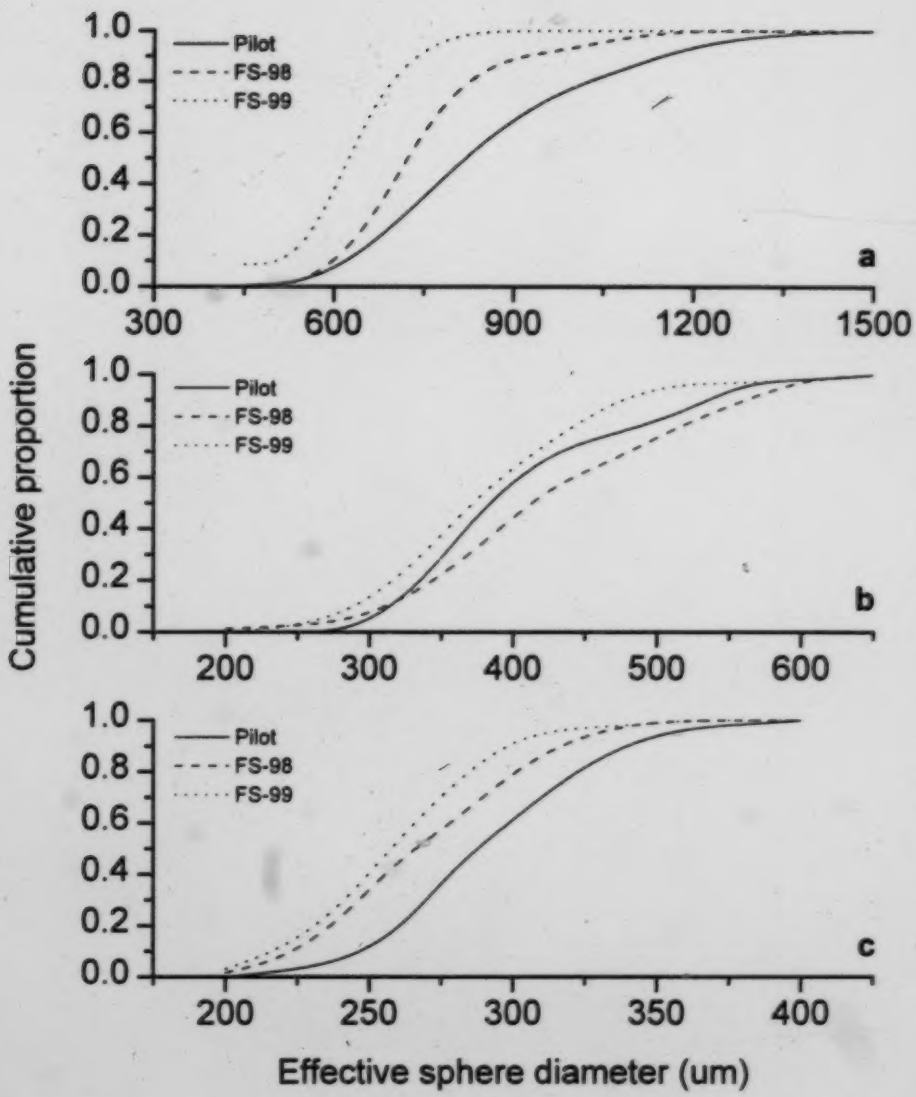

Figure 2-4. Cumulative particle size distributions of (a) large, (b) medium, and (c) small size fractions of Dy-labelled tracer spheres.

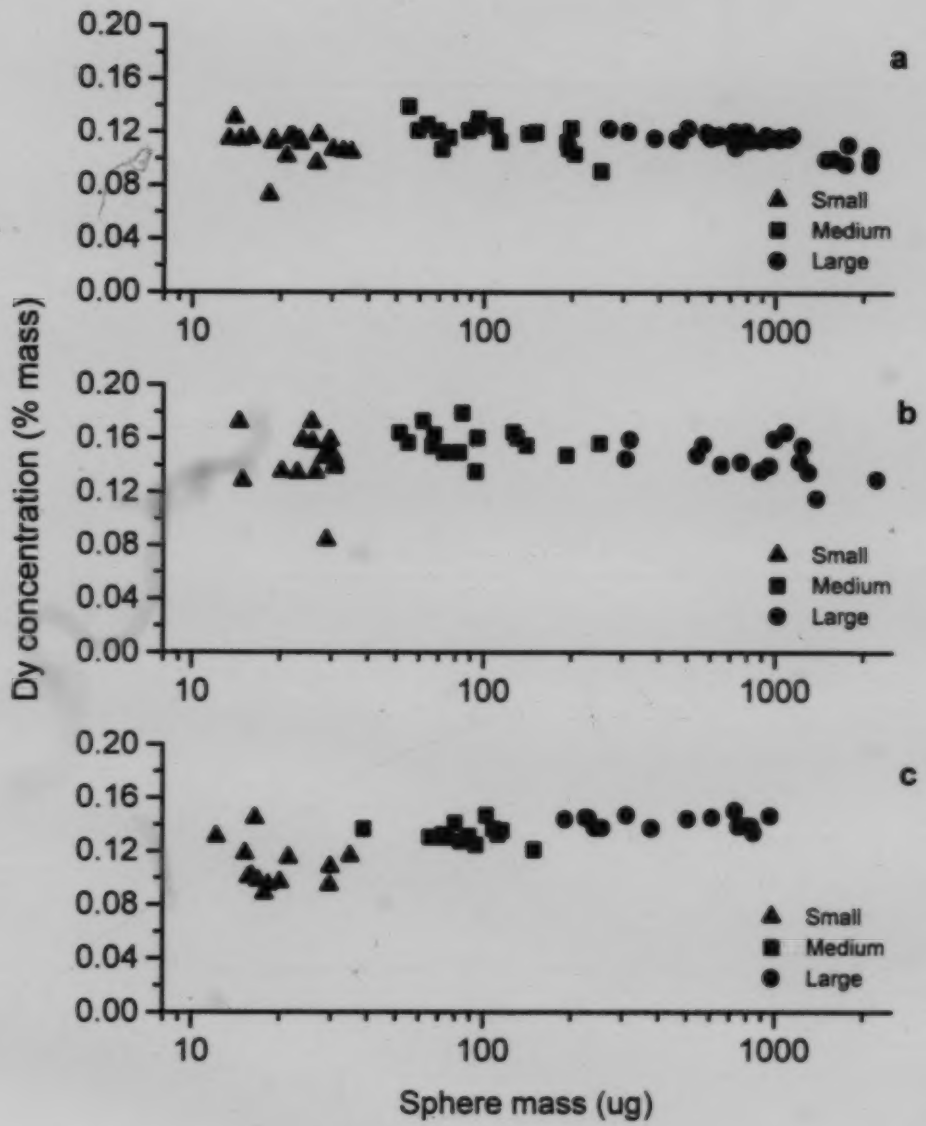

Figure 2-5. Tracer sphere Dy concentration as a function of sphere mass for the (a) pilot-, (b) 1998 field-, and (c) 1999 field-scale batches.

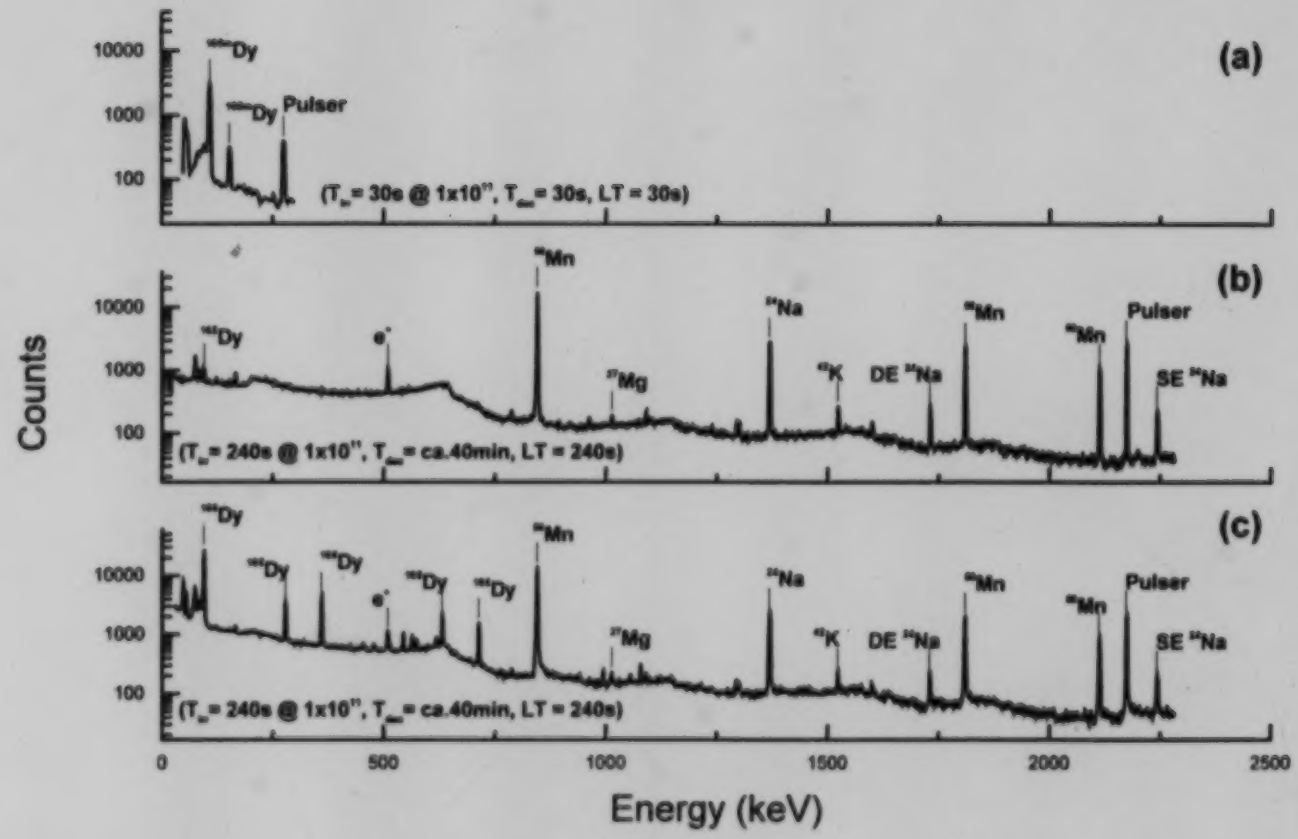

Figure 2-6. Typical gamma-ray spectra of (a) tracer spheres only, (b) soil only, and (c) a soil and sphere mixture.

References

Allmaras, R.R., Copeland, S.M., Copeland P.J. and M. Oussible. 1996. Spatial relations between oat residue and ceramic spheres when incorporated sequentially by tillage. Soil Sci. Soc. Amer. J. 60:1209-1216.

Behrens, H., Moser H. and E. Wildner. 1977. Investigation of groundwater flow with the aid of indium-EDTA-complex using neutron activation for the determination of the tracer. J. Radioanal. Chem. 38:491-498.

Bergerioux, C., Gijbels, R. and J. Hoste. 1979. Use of the semi-absolute method of neutron activation analysis. J. Radioanal. Chem. 50:229-234.

Besnard, E., Chenu, C., Balesdent, J., Puget, P. and D. Arrouays. 1996. Fate of particulate organic matter in soil aggregates during cultivation. Eur. J. Soil Sci. 47:495-503.

Blake, G.R. 1965. Particle density. In C.A. Black (ed.) *Methods of Soil Analysis: Part 1. Physical and Mineralogical Properties, including Statistics of Measurement and Sampling*. American Society of Agronomy, Madison WI.

DeSoete, D., Gijbels, R. and J. Hoste. 1972. Neutron Activation Analysis. P.J. Elving and I.M. Kolthoff (eds.) John Wiley & Sons Ltd., London UK.

Duke, M.J.M. 1983. Geochemistry of the Exshaw shale of Alberta – an application of neutron activation analysis and related techniques. Ph.D. Thesis. University of Alberta, Edmonton AB.

Duke, M.J.M., Plante, A.F. and W.B. McGill. 2000. Application of INAA in the characterisation and quantification of Dy-labeled ceramic spheres and their use as inert tracers in soil studies. J. Radioanal. Chem. 244:165-171.

Gladney E.S. and I. Roelandts. 1989. 1988 compilation of elemental concentration data for CCRMP Soil SO-1 to SO-4. Geostandards Newsletter. 13:217-268.

Govers, G., Vandaele, K., Desmet, P., Poesen, J. and K. Bunte. 1994. The role of tillage in soil redistribution on hillslopes. Eur. J. Soil Sci. 45:469-478.

Guiresse M. and J.C. Revel. 1995. Erosion due to cultivation of calcareous clay soils on hillslopes in southwest France. II. Effect of ploughing down the steepest slope. Soil Tillage Res. 35:157-166.

Kennelly, J.J., Apps, M.J., Turner, B.V. and F.X. Aherne. 1980. Dysprosium, cerium, and chromium marker determination by instrumental neutron activation analysis. Can. J. Anim. Sci. 60:749-761.

Kennelly, J.J., Turner, B.V. and M.J. Apps. 1982. Determination of non-radioactive liquid phase markers, Co-EDTA and Cr-EDTA, by neutron activation analysis. J. Sci. Food. Agric. 33:1235-1243.

Reibe, B. 1995. Monitoring the translocation of soil particles using a neutron activated tracer. In K.H. Hartge and B.A. Stewart (eds.) *Soil Structure: Its Development and Function*. CRC Press, Boca Raton FL.

Ryan, D.E., Stuart, D.C. and A. Chattopadhay. 1978. Rapid multielement neutron activation analysis with a SLOWPOKE reactor. Anal. Chim. Acta. 100:87-93.

Staricka J.A., Burford, P.M., Allmaras R.R. and W.W. Nelson. 1990. Tracing the vertical distribution of simulated shattered seeds as related to tillage. Agron. J. 82:1131-1134.

Staricka J.A., Allmaras R.R. and W.W. Nelson. 1991. Spatial variation of crop residue incorporated by tillage. Soil Sci. Soc. Am. J. 55:1668-1674.

Staricka J.A., Allmaras R.R., Nelson W.W. and W.E. Larson. 1992. Soil aggregate longevity as determined by the incorporation of ceramic spheres. Soil Sci. Soc. Am. J. 56:1591-1597.

Terpstra, R. 1989. Formation of new aggregates under laboratory-simulated field conditions. Soil Tillage res. 13:13-21.

Terpstra, R. 1990. Formation of new aggregates and weed seed behaviour in a coarse- and in a fine-textured loam soil. A laboratory experiment. Soil Tillage Res. 15:285-296.

Toth, S.J. and R.B. Alderfer. 1960a. A procedure for tagging water-stable soil aggregates with Co^{60}. Soil Sci. 89:36-37.

Toth, S.J. and R.B. Alderfer. 1960b. Formation and breakdown of Co^{60}-tagged water-stable soil aggregates in a Norton silt loam soil. Soil Sci. 90:232-238.

Chapter 3:

A particle tracer and wet sieving approach to the study of soil aggregate dynamics

1.0 Introduction

Since its original development (Yoder, 1936), the wet sieving procedure has been used extensively to determine the water-stability of soil aggregates, and the size distribution of water-stable aggregates. Subsequent to early developments, Kemper and colleagues (Kemper and Koch 1966; Kemper and Rosenau 1986) established a standardized method for using wet sieving in studies of aggregates and aggregate stability. However, a significant limitation of the wet sieving procedure is that the amount of energy applied to aggregates during sieving is unknown and cannot be easily quantified or standardized. For this reason, antecedent soil conditions and operational conditions can greatly affect the results obtained.

Several pre-treatment methods have been developed, each aiming to standardize or minimize the influence of initial water content on the results of wet sieving and to reduce variability in the results obtained (e.g. Dickson et al. 1990; Beare and Bruce 1993). While treatment comparisons using a standardized method may be of greater concern than the absolute value of the results obtained, a comparison of methods may provide information about the mechanisms of soil aggregation (Beare and Bruce 1993).

Previous studies have reported on the incorporation of tracer particles into aggregate size fractions separated by dry or wet sieving as a method of determining the dynamics of the soil matrix. In a laboratory study, Terpstra (1989) mixed 2 mm glass beads with soil and subjected the samples to several treatments. Tracers were recovered after "dry" sieving the soil at 15% moisture content to yield five aggregate size fractions ranging from less than four to ten millimetres. No further details concerning the method are provided. Staricka et al. (1992) used 1-3 mm ceramic spheres applied to field plots, which were subsequently recovered in six aggregate size fractions by rotary sieving air-dry samples. There are currently no reports on the behaviour of particle tracers during the wet sieving

procedure. This information is essential to studies on aggregate dynamics to ensure that results are relatively free of artefact.

1.1 Objectives

The objective of this portion of work is to demonstrate how the tracer spheres described in Chapter 2 behave in soil during the wet sieving process, and how antecedent and operational factors may affect their use in studying soil aggregate dynamics. The potential for tracer sphere incorporation during various stages of the wet-sieving procedure was determined using several pre-treatments.

2.0 Materials and Methods

2.1 Pre-treatments applied

To determine the behaviour of tracer spheres during various stages of the wet sieving procedure, including the potential for tracer sphere incorporation into soil aggregates, the soil-sphere mixtures were subjected to the following pre-treatment before wet sieving:

1. field-moist (T1): field-sampled soil was left at antecedent moisture content.
2. air-dried (T2): field-moist samples were air-dried for 72 h after layering with tracer spheres.
3. mixed, then incubated (T3): the tin containing the soil-sphere mixture was mixed with an electric mixer to simulate the mixing caused by rototillage, and then incubated in 2 L canning jars under moist conditions at room temperature for 7 days prior to wet-sieving.
4. mixed, incubated, then air-dried prior to wet-sieving (T4).

In addition to these pre-treatments, an additional run of double the amount of moist soil was performed to examine any potential impedance problems during the wet sieving procedure caused by increased sieve loadings. In all cases, the wet-sieving procedure was replicated eight times in two runs of four replicates each, and tracer sphere detection was limited to four of the eight replicates because of the cost of INAA.

2.2 Wet sieving procedure

Soils used were from the Malmo series (Black Chernozem) sampled from the Ellerslie research farm (53° 25'N, 113° 33'W), and the Breton series (Gray Luvisol) sampled from the Breton research farm (53° 07'N, 114° 28'W). Soils were stored cold (4 °C) and at field moisture until used. The tracer spheres used were from the medium size fraction of the 1999 full-scale batch, which previously characterized in Chapter 2 (mass = 90 μg sphere^{-1}, diameter = 380 μm, density = 1.77 g cm^{-3}, and Dy concentration = 13.3% by mass). The experiment consisted of several runs of the wet sieving procedure with varying pre-treatments. Samples were prepared by layering 20 g of field-moist soil, ~30 mg of tracer spheres, and another 20 g of field-moist soil in a drying tin. The drying tin was then subjected to the pre-treatments outlined below before wet sieving.

Wet sieving was performed using a standard method described by Angers and Mehuys (1993). The tin containing the pre-treated soil-sphere mixture was then poured onto the top of a sieve stack for ~2 min of rapid wetting and slaking, then wet sieved for 10 min. The wet-sieving apparatus subjected samples to a stroke length of 4 cm at 0.55 Hz (approximately 33 revolutions per minute). The sieve stack consisted of a geometric series of 4, 2, 1, 0.5, 0.25, and 0.125 mm sieves. After sieving, the soil retained on each sieve was oven dried at 105°C overnight and weighed. Corrections for the content of primary particles (*e.g.* gravel and sand) in each fraction were made by washing the material retained on each sieve to disrupt aggregates, followed by drying and weighing the retained primary particles. When reported, the < 0.125 mm fraction was determined by subtraction without primary particle correction.

2.3 Tracer content

The tracer content of each soil aggregate fraction was determined by instrumental neutron activation analysis (INAA) at the University of Alberta SLOWPOKE facility. The soil retained on each sieve was transferred to 7 mL polyethylene "rabbit" vials. Samples were subject to compaction during transport in the pneumatic transfer system of the reactor. Therefore, the headspace and pore space in the sample vials was filled with granular white sugar and mixed with a vortex shaker to prevent compaction and to maintain a

consistent counting geometry. Soil aggregate samples too large to fit one vial were split into several vials and the results were summed.

The aggregate-sphere mixtures were irradiated in the SLOWPOKE reactor for 240 s at a nominal neutron flux of 0.2×10^{11} n cm^{-2} s^{-1} using an automated stack loader. After irradiation, samples were allowed to decay for ~30 minutes to reduce the interfering signal from high levels of ^{28}Al activity. Samples were counted for 300 s live-time with a Ge detector connected to a MCA. Due to differing concentrations of interfering ^{56}Mn, Malmo soil samples were counted at a sample-to-detector geometry of 3 cm, while samples containing Breton soil were counted at 6 cm. The Dy content of each sample was determined by measuring the 94.7 keV γ-ray emission of the longer-lived Dy radionuclide, ^{165}Dy ($T_{1/2}$ = 2.334 hrs) with appropriate decay time and pulser corrections applied. Further details of the method are in Section 2.2.5.

Sphere-associated Dy was calculated by subtracting the soil-associated Dy (based on soil mass and previously measured soil Dy background concentration) from the total measured sample Dy. Hence, tracer sphere content is reported as μg Dy.

2.4 Mean Weight Diameter Calculations

The mean weight diameter (MWD) is calculated to express a size distribution as an index parameter. The MWD for either soil aggregates or tracer Dy can be determined using the following equation:

$$MWD = \sum_{i=1}^{n} x_i W_i \qquad (8)$$

where x_i is the mean diameter of the size fraction and W_i is the weight proportion of soil or Dy retained in the fraction. Resultant MWD values from each treatment were compared statistically using a protected least squared means procedure (LSMEANS) using SAS (SAS Institute, Cary NC).

3.0 Results

Air-drying of the soil prior to wet sieving changed the resulting water-stable aggregate size distribution compared to the field-moist samples (Figure 3-1), which is reflected in a

significant decrease in soil aggregate MWD (Table 3-1, 3-2). Soil aggregate MWD values decreased from 2.01 mm to 0.77 mm in the Malmo samples, and from 1.84 mm to 1.06 mm in the Breton samples. Similar results occurred when comparing the mixed-incubated (T3) samples with the mixed-incubated and dried (T4) samples. In this case soil aggregate MWD decreased from 1.43 mm to 0.56 mm in the Malmo soil, and from 0.88 mm to 0.48 mm in the Breton soil. The mixed-incubated pre-treatments were performed in an attempt to promote aggregation and tracer sphere incorporation in the samples. However, the result was to decrease the soil aggregate MWD in both soil types: from 2.01 mm to 1.43 mm in Malmo samples, and from 1.84 mm to 0.88 mm in samples from Breton. The decrease in the Malmo samples was not statistically significant at the 5% level while the decrease in Breton samples was, demonstrating the differences in aggregate stability between the two soil types (Table 3-2). An increased sieve loading (by doubling soil sample mass) slightly increased the apparent aggregation state of the soils. The increase in soil aggregate MWD values was statistically significant in Malmo samples, from 2.01 mm to 2.36 mm. Soil aggregate MWD also increased in samples from Breton, from 1.84 mm to 1.87 mm, but the change was not statistically significant (Table 3-2).

The expected distribution of tracer Dy in aggregate size fractions can be determined using the tracer sphere size distribution determined during the characterization reported in Chapter 2. Tracer sphere diameter data result in a Dy MWD of 0.39 mm. The wet-seiving results show that some tracer is impeded from reaching its proper size fraction during the procedure since the expected Dy MWD value is lower than any of the Dy MWD values determined in the wet-sieving trials.

While several pre-treatments resulted in significant changes in soil MWD, the distribution of tracer Dy remained consistent (Figure 3-2). Only the mixed-incubated pre-treatment (T3) was significantly different from the field-moist treatment (Table 3-3) where Dy MWD increased from 0.42 mm to 0.50 mm in Malmo samples, and from 0.42 to 0.46 mm in samples from Breton. This is likely due to the formation of new aggregates that incorporated tracer spheres. However, these new aggregates had limited stability as illustrated by the decreased soil MWD in mixed-incubated samples, and the re-release of

tracers in samples that were dried after mixing and incubation. Air-drying of samples had no effect on Dy MWD, except when it followed mixing and incubation. Increased sieve loadings (by doubling the sample mass) significantly increased Dy MWD in only the Malmo samples (from 0.42 mm to 0.46 mm). This increase may be due to tracer incorporation, but is more likely due to increased interception on higher sieves due to the increased amount of soil. The lack of differences due to doubling the soil sample in Breton soils is likely because of the lower stability, resulting in less soil retained on the higher sieves that can intercept tracer spheres.

4.0 Discussion

Perfect et al. (1990) demonstrated a significant relationship between water stable aggregation and soil moisture content at the time of sampling, where water-stable aggregation decreased with increasing soil moisture content. They found that up to 85% of the variability in wet aggregate stability within a growing season was accounted for by soil water content at the time of sampling. Both exponential (Perfect et al. 1990) and quadratic (Angers 1992) relationships have been demonstrated between water-stable aggregation and antecedent soil water content. Air-drying samples prior to wet-sieving was originally intended to minimize the effect of antecedent water content on the results of the wet sieving procedure, but the water content of soil samples at the time of wet-sieving has a much greater impact on the results (Dickson et al. 1991). Water-stable aggregate size distribution data collected by wet-sieving air-dried samples from field experiments performed in this study (see Chapter 4) do not show a strong relationship with antecedent water content (Figure 3-3). However, the air-drying of samples does appear to result in a greater dispersive energy being applied during the wet-sieving, which results in increased slaking and a reduced soil aggregate MWD. This response was much greater in the Breton soil than in the Malmo soil, reflecting differences its higher aggregate stability imparted by higher organic matter content in Malmo samples.

The potential for incorporating tracers into aggregates during the wet-sieving procedure was a significant concern in the design of the tracer spheres experiments because it would cause artefacts. The drying of moist aggregates is a primary means by which aggregates

are stabilized due to the tensile forces created by receding menisci. It was postulated that initially free tracer spheres might become associated with aggregates during the air-drying of field-collected samples, artificially inflating the degree of incorporation of tracers. Results from this experiment show that this was not the case. Air-dry samples had lower soil MWD, but did not show significantly different tracer sphere distributions.

The mixing of soil samples did, however, change the distribution of tracers in the aggregate fractions. The tracer associated Dy data show that some tracers were recovered in aggregate size fractions larger than their own size, indicating that some incorporation of tracer spheres into aggregates occurred. The mixing pre-treatment was designed to simulate soil tillage, where aggregates can be broken down or formed through contact. The incorporation of tracer spheres would suggest that new aggregates were formed during the mixing and incubation. However, the soil MWD data shows a marked decrease in the number of larger aggregates. Therefore, it is believed that a large number of aggregates were destroyed during the simulated tillage, but that in the subsequent incubation period a smaller number of aggregates were reformed.

5.0 Conclusions

The separation of water-stable aggregate size fractions by wet sieving is a standard method for determining the state of aggregation of a soil. When sieve sizes and sieving times are held constant, results of the procedure can be subject to variability caused by moisture content at time of sieving, sieve loading, and to a lesser degree antecedent soil moisture content. Overall, the wet-sieving procedure did not appear to significantly affect the distribution of tracer spheres in the aggregate size fractions. While some tracer impedance occurred in all cases, tracer incorporation occurred only in the pre-treatments involving mixing and incubation of soil samples. The pre-treatment appears to have created tracer Dy-containing aggregates even though many aggregates were destabilized resulting in a decreased soil MWD. Our assessment that the tracer spheres are appropriate analogs for studies of aggregate dynamics is further supported by these results.

Table 3-1. Mean soil aggregate and dysprosium mean weight diameters (mm)

	Malmo		Breton	
	Soil	Dy	Soil	Dy
Control, moist (T1)	2.01	0.42	1.84	0.42
Air-dry (T2)	0.77	0.43	1.06	0.44
Mixed-incubated (T3)	1.43	0.50	0.88	0.46
Mixed-incubated, air-dry (T4)	0.56	0.42	0.48	0.41
Double soil	2.36	0.46	1.87	0.44

Table 3-2. Statistical significance (*p*-values) of pre-treatment comparisons of soil MWD.

Malmo	Control (moist, T1)	Air-dry (T2)	Mixed (T3)	Mixed, air-dry (T4)
Air-dry (T2)	< 0.0001			
Mixed (T3)	0.0765	< 0.0001		
Mixed, air-dry (T4)	< 0.0001	0.3220	< 0.0001	
Double soil	0.0012	< 0.0001	0.0007	< 0.0001
Breton	**Control (moist, T1)**	**Air-dry (T2)**	**Mixed (T3)**	**Mixed, air-dry (T4)**
Air-dry (T2)	< 0.0001			
Mixed (T3)	0.0005	0.3599		
Mixed, air-dry (T4)	< 0.0001	0.0496	0.3880	
Double soil	0.7559	< 0.0001	0.0003	< 0.0001

Table 3-3. Statistical significance (*p*-values) of pre-treatment comparisons of Dy MWD.

Malmo	Control (moist, T1)	Air-dry (T2)	Mixed (T3)	Mixed, air-dry (T4)
Air-dry (T2)	0.5527			
Mixed (T3)	< 0.0001	0.0001		
Mixed, air-dry (T4)	1.0000	0.5527	< 0.0001	
Double soil	0.0118	0.0338	0.0059	0.0118
Breton	**Control (moist, T1)**	**Air-dry (T2)**	**Mixed (T3)**	**Mixed, air-dry (T4)**
Air-dry (T2)	0.2062			
Mixed (T3)	0.0479	0.3886		
Mixed, air-dry (T4)	0.6619	0.1016	0.0222	
Double soil	0.3178	0.7700	0.2572	0.1640

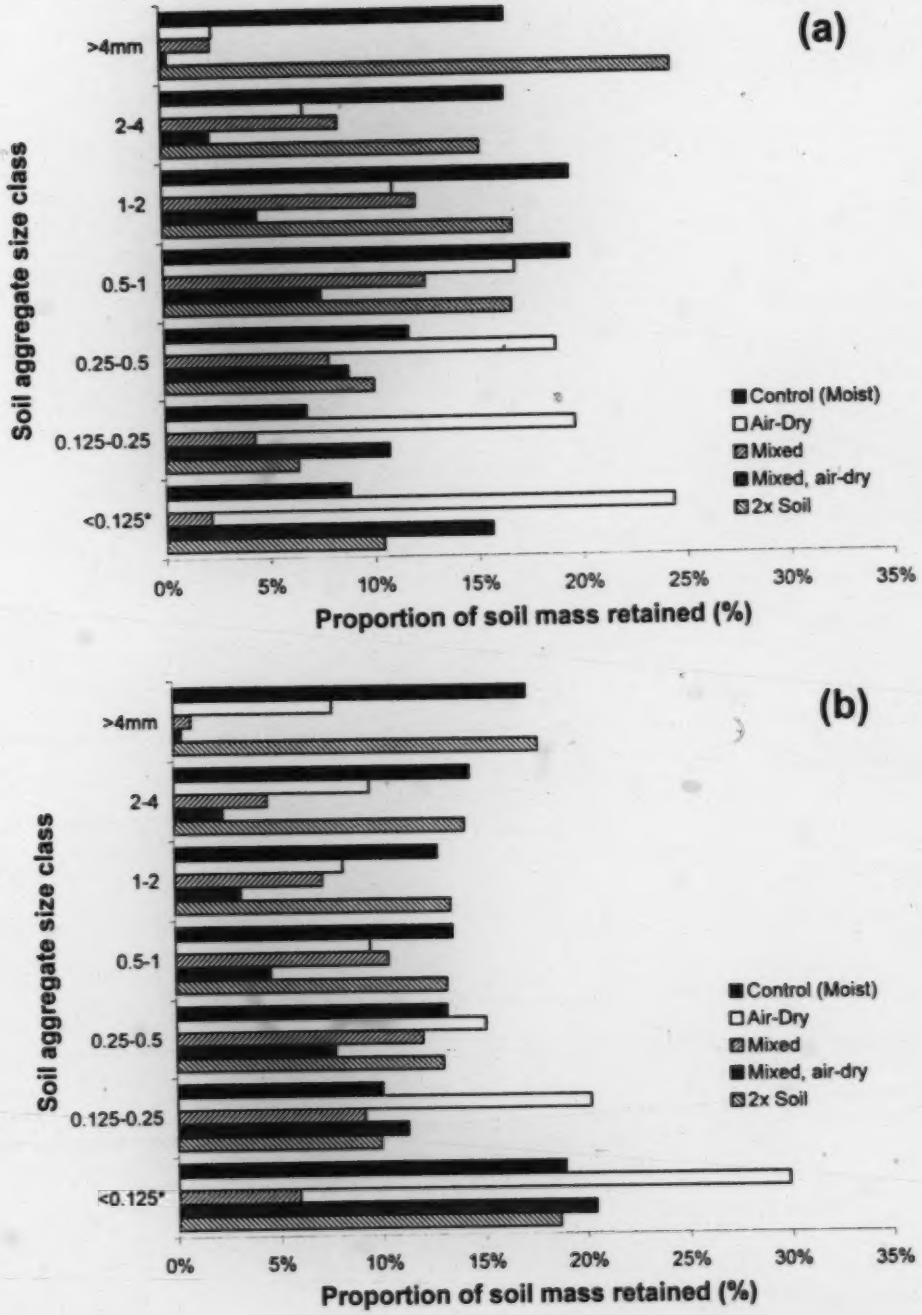

Figure 3-1. Water-stable aggregate size distribution of (a) Malmo, and (b) Breton samples.

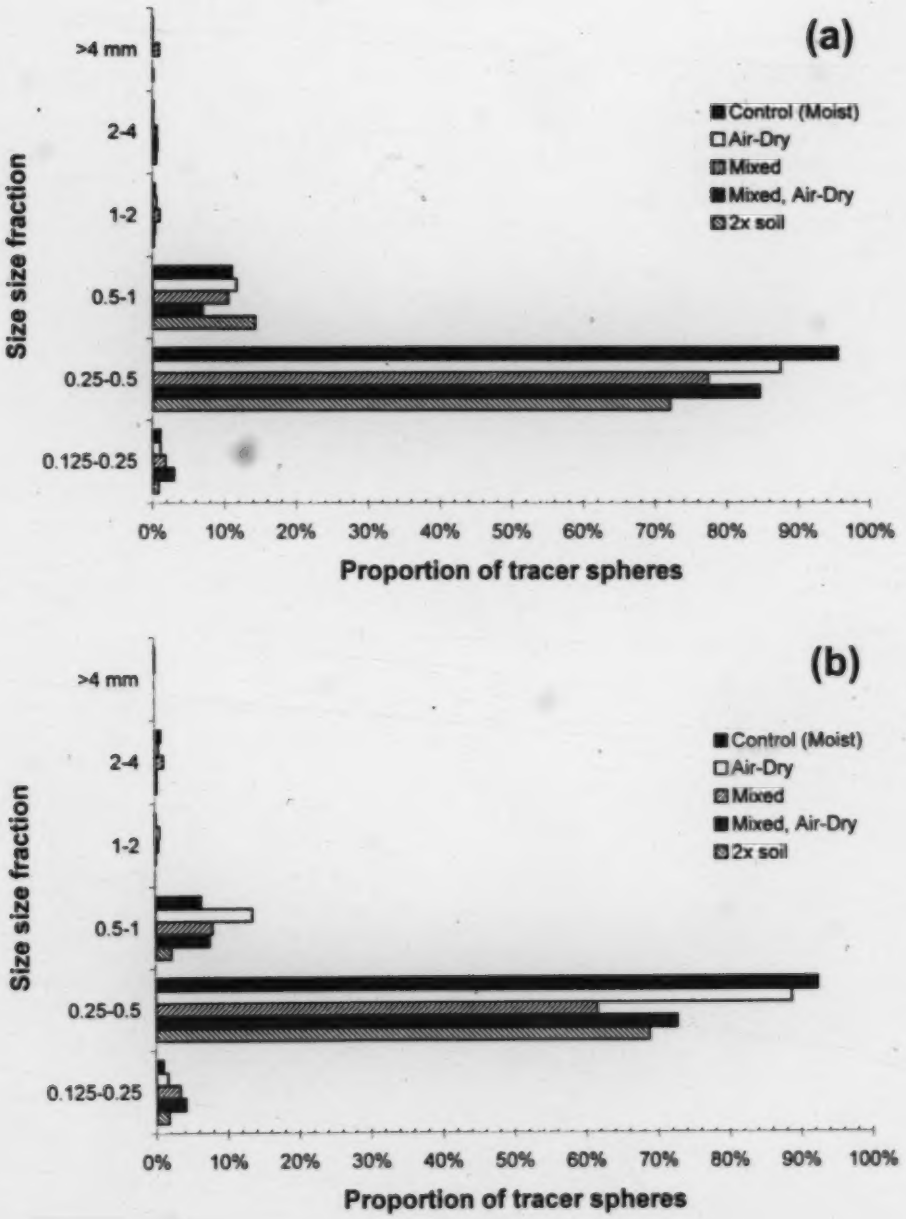

Figure 3-2. Distribution of tracer Dy in water-stable aggregate size fractions of (a) Malmo, and (b) Breton samples.

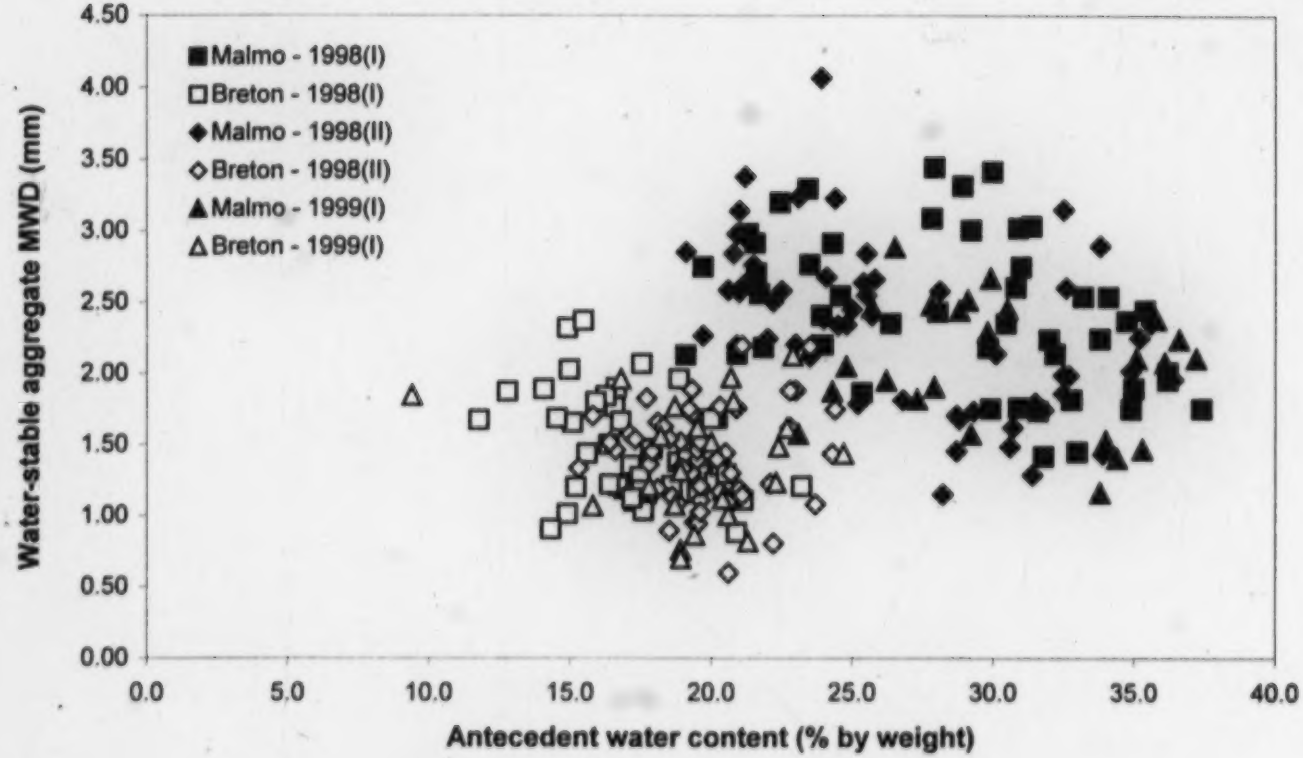

Figure 3-3. Water-stable soil aggregate mean weight diameter as a function of antecedent soil moisture content in air-dried samples from field study reported in Chapter 4.

References

Angers D.A. 1992. Changes in soil aggregation and organic carbon under corn and alfalfa. Soil Sci. Soc. Amer. J. 56:1244-1249.

Angers, D.A. and G.R. Mehuys. 1993. Aggregate stability to water. *In* M.R. Carter (ed.) Soil Sampling and methods of Analysis. Canadian Society of Soil Science, Lewis Publishers, Boca Raton FL.

Beare M.H. and R.R. Bruce. 1993. A comparison of methods for measuring water-stable aggregates: implications for determining environmental effects on soil structure. Geoderma 56:87-104.

Dickson E.L., Rasiah V. and P.H. Groenevelt. 1991. Comparison of four prewetting techniques in wet aggregate stability determination. Can. J. Soil Sci. 71:67-72.

Kemper W.D. and Koch E.J. 1966. Aggregate stability of soils from Western United States and Canada. Tech. Bull., 1355, Agricultural Research Service, U.S. Dept. of Agriculture, Washington, DC.

Kemper W.D. and Rosenau R.C. 1986. Aggregate stability and size distribution. *In* A. Klute (Ed.), Methods of Soil Analysis. Part 1. 2nd ed. Agron. Monogr., 9. ASA and SSSA, Madison, WI.

Perfect E., Kay B.D., van Loon W.K.P., Sheard R.W. and T. Pojasok. 1990. Factors influencing soil structural stability within a growing season. Soil Sci. Soc. Amer. J. 54:173-179.

Staricka J.A., Allmaras R.R., Nelson W.W. and W.E. Larson. 1992. Soil aggregate longevity as determined by the incorporation or ceramic spheres. Soil Sci. Soc. Amer. 56:1591-1597.

Terpstra R. 1989. Formation of new aggregates under laboratory-simulated field conditions. Soil Tillage Res. 13:13-21.

Yoder R.E. 1936. A direct method of aggregate analysis of soils and a study of the physical nature of erosion losses. J. Am. Soc. Agron. 28:337-351.

Chapter 4:

Intra-seasonal turnover of soil aggregates in two contrasting field soils using a labelled tracer particle

1.0 Introduction

The dynamics of soil aggregation has gained increasing attention because of its role in the sequestration of organic C in soils. The dynamics of soil aggregation have been expressed as changes in water-stable aggregate mean weight diameter (MWD) related to differences in management (e.g. Perfect et al. 1990a). Other studies have inferred aggregate dynamics from the accrual or loss of organic matter in aggregates over time. Jastrow et al. (1996) investigated the inputs and turnover of organic C in water-stable aggregates of different sizes. They used the change in natural abundance of ^{13}C following a vegetation change to measure the turnover of organic matter in the aggregates. Turnover times for micro- and macroaggregates were estimated from first order rate constants calculated from $\delta^{13}C$ data. In general, turnover time increased with decreasing aggregate size, suggesting that aggregate turnover was more rapid for larger aggregates. However, Jastrow (1996) showed that soil macroaggregate formation occurred 35 times faster than total soil organic C accumulation. Furthermore, macroaggregation was more rapid than accumulations of various forms of soil C: total, mineral-associated, and macroaggregate-associated C. This suggests that organic C accumulation or loss may not be a precise tracer for soil aggregate dynamics. The use of a dynamic tracer substance (e.g. decomposing organic materials) to study a second dynamic system (e.g. mainly inorganic soil macroaggregates) may yield confounded results.

Six et al. (1999) synthesized the differences in aggregation and organic matter in conventional- versus no-till soils into a conceptual model where OM losses under tillage are due to increased aggregate turnover in a rapid "cultivation loop" which is determined by tillage frequency, versus the slower "decomposition loop" which occurs under no-till where aggregate turnover is determined by the decomposition of the binding agents. Although several authors have concluded that soil aggregate turnover is a significant

control on organic C turnover and have proposed similar concepts, the direct evidence currently available to test this hypothesis is insufficient. Studies using rates of organic matter accumulation or loss, or the measurement of gross changes in aggregation over time provide only indirect evidence. Staricka et al. (1992) used a direct tracer approach to examine aggregate dynamics, but the tracers used and the aggregate sizes measured were too large. The study was pertinent to only a small fraction of the soil mass since the ceramic spheres in the study were 1-3 mm in diameter and the aggregates separated were 3-40 mm.

1.1 Objectives

It is our contention that determining how soil aggregate turnover controls organic matter turnover requires determining the turnover of the aggregates themselves. To this end, the objectives of the work reported here were:

1. to observe the incorporation of tracer spheres into soil aggregate fractions, and
2. to use incorporation of spheres into aggregate fractions to describe patterns in aggregation.

The observation of tracer sphere incorporation into soil aggregates will provide direct observations of soil aggregate formation and turnover and will provide insight into the patterns of aggregation, which can be subsequently quantified.

2.0 Materials and Methods

2.1 Experimental Field Sites

Experiments were conducted on long-term plots established in 1983 at the Ellerslie (53° 25'N, 113° 33'W) and Breton (53° 07'N, 114° 28'W) research stations near Edmonton, Alberta (Solberg et al. 1997). The plots are currently managed by the Agronomy Unit of Alberta Agriculture, Food and Rural Development, and are located on two contrasting soils, a Black Chernozem, Malmo series (Haplocryoll) at Ellerslie, and a Gray Luvisol, Breton series (Haplocryalf) at Breton. Soil properties reported in Table 4-1 show that the sampling locations and treatments permitted comparisons between soils with similar

climate, but with contrasting organic C contents and contrasting organic C dynamics (Solberg et al. 1997; Dinwoodie and Juma 1988).

At each site, only two of the established treatments consisting of annual N additions of 56 kg ha^{-1}, with (T8) or without (T10) straw addition were used. Original plots sizes were 2.75 m × 6.86 m, but were split into three to form plots of 2.75 m × 2.29 m. In addition to the existing four replicates, the subdivision of the field plots allowed us to repeat the experiments in consecutive years (1998 and 1999), maintain ongoing experiments over the same years, and reduce the amount of tracer spheres required for each application. Hence, each subplot will be referred to as follows: 1998(I), the first year of sampling on subplots where tracers were applied in 1998, 1998(II), the second year of sampling (1999) on subplots where tracers were applied in 1998, and 1999(I), the first year of sampling on subplots where tracers were applied in 1999.

The ceramic tracer spheres used in the field experiments are from batches produced in 1998 and 1999. The spheres were previously characterized and results are reported in detail in Chapter 2. Table 4-2 provides a summary of tracer sphere properties. The tracer application rate previously reported by Staricka et al. (1992) was 2 spheres (1-3 mm diam.) cm^{-2} of soil, which if incorporated to 15 cm depth in a soil with 1.0 g cm^{-3} bulk density would represent ~0.23 mg sphere g^{-1} soil. A significant increase in application rate was suggested to improve the power of the experiment, especially considering the use of smaller spheres[1]. Due to a limited supply of tracer spheres, the application rate in 1998 was operationally set to 0.65 kg spheres $plot^{-1}$. Based on plot size, this rate is approximately 0.63 and 0.49 mg spheres g^{-1} soil to a depth of 15 cm for the Ellerslie and Breton sites, respectively. Differences in the rates are due to differences in soil bulk density values used in the calculations, 1.1 g cm^{-3} for Malmo soil and 1.4 g cm^{-3} for Breton soil. This rate is 2-3 times that used by Staricka et al. (1992). The operational application rate was retained in 1999. However due to differences in the mean mass of individual spheres between batches, an increased number of spheres were applied.

---

[1] J.A. Staricka, 1997, personal communication.

Differences in tracer sphere Dy concentration between the 1998 and 1999 batches also resulted in differing application rates of Dy, which is important because the measurement of tracer content is in μg of Dy. Thus, the Dy application rates were 98.9 and 83.3 μg Dy g^{-1} soil in 1998 and 1999 at Ellerslie, and 77.6 and 65.3 μg Dy g^{-1} soil in 1998 and 1999 at Breton. (Details of the sphere and Dy application rate calculations are in Appendix A.)

In 1998, the ceramic tracers were hand broadcast to the plots on May 30 (at Ellerslie) and 31 (at Breton). Plots were tilled and seeded to wheat on June 2, 1998. In 1999, the tracers were applied on May 6 (at Ellerslie) and 12 (at Breton), and plots were tilled on May 7 and 12. Plots were seeded to glyphosate-resistant canola to control weed infestation. Personnel from Alberta Agriculture, Food and Rural Development performed all plot seeding and tillage. Soil samples were taken by core sampler to a depth of 15 cm every three weeks beginning approximately 7 days after tillage and returned to the laboratory for analyses. Gravimetric water content was determined by overnight oven drying of ~10 g samples at 105°C. Separate sub-samples were taken and used to determine water-stable aggregate size distribution, and tracer contents. Analyses were performed on the 1998(I), 1998(II) and 1999(I) subplots.

2.2 Water-stable aggregate size distribution

The water-stable aggregate size distribution was determined using a standard wet sieving method (Angers and Mehuys, 1993). Details of the method are reported in Chapter 3. Briefly, a 40 g air-dry sub-sample was placed on the top of a sieve stack for 2 min for rapid wetting and slaking, then wet sieved for 10 min. The sieve stack consisted of a geometric series of 4, 2, 1, 0.5, 0.25, 0.125 mm sieves. The soil retained on each sieve was oven dried at 105°C overnight, weighed, and corrected for primary particle content. When reported, the <0.125 mm fraction was determined by subtraction without correction.

The mean-weight diameter of the water stable aggregates (MWD) of soil was calculated as an integrated representation of the "degree of aggregation". The formula used to calculate the MWD is:

$$MWD = \sum_{i=1}^{n} x_i W_i \quad (9)$$

where x_i is the mean diameter of the size fraction and W_i is the weight proportion of soil retained in the fraction.

2.3 Tracer content

The tracer content of individual soil aggregate fractions was determined by instrumental neutron activation analysis (INAA) at the University of Alberta SLOWPOKE facility using the method described in Chapters 2 and 3 for soil-sphere mixtures.

In summary, the aggregate-sphere mixtures were irradiated in the SLOWPOKE reactor for 240 s at a nominal neutron flux of 0.2×10^{11} n cm^{-2} s^{-1}, allowed to decay for ~30 minutes and counted for 300 s live-time. Samples from Ellerslie were counted at a sample-to-detector geometry of 3 cm, while samples containing Breton soil were counted at 6 cm because of an increased concentration of interfering ^{56}Mn in the Breton soil. The Dy content of each sample was determined by measuring the 94.7 keV γ-ray emission of the longer-lived Dy radionuclide, ^{165}Dy ($T_{1/2}$ = 2.334 hrs), with appropriate decay time, pulser, and soil content corrections applied.

2.4 Statistical analyses

Several approaches were attempted for the statistical analysis of the measurements taken. The simplest approach is to use the univariate analysis of a split-plot design where the date of sampling is the split. This approach is valid only when the within-subject (observations on the same subject over time) variance-covariance matrix has compound symmetry (Thompson, 1990), or more generally is of Type H (Wolfinger and Chang, 1995). Observations were expected to be correlated because samples were taken periodically from the same subject (a soil plot), *i.e.* "repeated measures".

When the within-subject observations are correlated, two approaches can be used. The first is to adjust the univariate tests using degrees of freedom adjustment factors (ε) developed by Greenhouse and Geiser (G-G) or Huynh and Feldt (H-F). The H-F factor is preferred, because the G-G factor has been shown to be too conservative for small samples (Wolfinger and Chang, 1995). However, in most tests on the data the H-F

estimate of ε was greater than 1, which is then reset equal to 1 when multiplying the degrees of freedom. The result is no effect on the univariate tests. The second approach involves using multivariate tests. However, multivariate tests in either the repeated measures analysis in PROC GLM or by use of the MANOVA statement could not be performed due to insufficient error degrees of freedom. In addition, the repeated measures analysis in PROC GLM of SAS/STAT (SAS Institute, 1999) was unable to perform the sphericity test on a Type H matrix, and the repeated measures analysis in PROC MIXED provided results only when using the compound symmetry form of the covariance matrix.

In the end, the univariate analysis of the data as a split-plot design with sampling date as the split, and the selection of appropriate error and interaction terms, was selected. The condition of independence of within-subject observations was probably not violated because the samples were taken three weeks apart, when several physical and biological processes may occur to change the condition of the soil. Statistical analyses were performed using PROC GLM in SAS/STAT and a value of 5% was selected as the level of significance for all tests, unless otherwise noted.

3.0 Results and Discussion

3.1 Patterns of soil aggregation

The Malmo soil demonstrated a higher "degree of aggregation", with more soil retained in the upper sieve fractions, when compared to the Breton soil (Figure 4-1). This is also illustrated by the MWD values calculated for each soil at each sampling period (Figure 4-2). MWD values averaged over the duration of the experiment are 2.42 ± 0.54 mm for Malmo soil, and 1.46 ± 0.37 mm for Breton soil. Straw addition significantly increased values of MWD in both Malmo ($p = 0.013$) and Breton ($p = 0.014$) samples.

Previous studies report similar results for aggregate MWD for the same soils, but under slightly different wet sieving protocols. Singh et al. (1994) used a wet sieving time of 30 min compared to our 10 min. They reported values of 2.3 ± 0.4 mm for samples under tillage and straw addition, and 1.3 ± 0.3 mm for samples under tillage without straw addition. Toogood and Lynch (1959) reported an average aggregate MWD value of 0.86

mm for the rotation cropping system on the Breton Classic plots, which are adjacent to the plots used in this work. In their wet sieving procedure Toogood and Lynch forced the soil sample through the 4 mm sieve resulting in a lower value. Calculating aggregate MWD values from data in this work without the mass retained on the 4 mm sieve yields an average value of 0.83 mm. The close correlation between previously reported aggregate MWD values and those reported in the current study suggest that the soils appear to be at "steady-state" in reference to aggregation, and are not aggrading or degrading over the span of several years to several decades.

While the soils appear to be at steady-state over the medium- to long-term, they displayed short-term cyclical dynamics. Soil aggregation generally followed a "saw-toothed" pattern (Figure 4-2). This pattern is likely controlled by climate and plant growth changes over the growing season. The soil MWD data showed some correlation with antecedent soil water content (see Figure 3-3), similar to that reported by Perfect et al. (1990a; 1990b). Water content generally decreased during the growing season, which may help to increase soil aggregate stability. The growth of plants increased labile organic C inputs through root exudates, which could also stabilize aggregates leading to increases in aggregate MWD. The repetition of the saw-toothed pattern suggests that the over-winter period, when several freeze-thaw cycles occurred, along with spring tillage may "reset" the state of aggregation.

3.2 Tracer sphere incorporation

Recovery rates of applied tracer spheres were calculated using the rate of application and the total amount of sphere Dy detected in all sieve fractions of a sample. Recovery of Dy ranged from 22 to 264% (Table 4-3). We believe this reflects "hot spots" of localization due to uneven application and imperfect homogenisation during tillage. After the first tillage, the mean recovery rates (averaged over the whole season) were 81% for Malmo and 54% for Breton. Recovery improved after one year in the field and a second tillage in 1999 with mean values of 98% for Malmo and 66% for Breton and a narrowing of the range of values. The mean recovery rates of tracer spheres applied in 1999 were 77% for both Malmo and Breton. The general trend for less than 100% recovery suggests some

loss of the tracer during tillage. A significant amount of soil translocation occurred during tillage. We found elevated levels of Dy in random samples taken outside the border of the plots before tillage in the spring of 2000. We believe that tillage translocation removed some of the tracer spheres from the plots to which they were applied.

Due to the varying amounts of total spheres detected, all sphere contents of aggregate fractions are reported as values normalized to the total amount detected in all aggregate fractions of the sample ($\mu g\ Dy\ (\Sigma \mu g\ Dy)^{-1}$). Considering the size of the tracer spheres ($\bar{x}$ = 425 μm in 1998 and $\bar{x}$ = 380 μm in 1999 batches, respectively) and if no aggregation of the tracer was to occur, the largest proportion of the spheres would be expected to be found in the 0.25-0.5 mm sieve fraction. The next largest sieve fraction will also contain some free tracer spheres because approximately 15% of the spheres are > 500 μm in diameter (see Figure 2-2 and Figure 3-2). However, an estimation of the free versus incorporated amounts of tracer spheres in the 0.5-1 mm fraction is not possible without tracer extraction and inspection, and is not critical for our purposes. Instead, individual aggregate fractions can be combined to form a 1 - >4 mm fraction that would represent the incorporated, or aggregated, tracer sphere pool. No tracer Dy should be observed in this fraction unless it has been incorporated into larger aggregates.

Results of tracer analyses from field samples show a very rapid incorporation of the tracer spheres shortly after the initial tillage events in both 1998 and 1999, where approximately 25% of the tracers appear in the aggregated pool (Figure 4-3). This result is significantly greater than that reported by Staricka et al. (1992), who found that <5 % of tracers were incorporated after initial tillage. In part, the differences can be attributed to differences in experimental designs. Staricka et al. (1992) used much larger spheres (1-3 mm compared to our ~0.4 mm) and examined their incorporation into much larger aggregates (3-40 mm compared to our 1-4 mm). In addition, the field plots in the Staricka et al. (1992) experiments were tilled by mouldboard or chisel, whereas our plots were rototilled. We expect that the rototillage produced much greater soil mixing, thus increasing the likelihood of tracer sphere incorporation. While several researchers have suggested that tillage promotes losses of particulate organic matter and decreases in aggregate MWD (Elliott 1986; Beare 1994a, b; Six et al. 1998), others have suggested

that tillage may promote the physical protection of organic matter by increasing the occlusion of particulate organic matter within aggregates (Puget et al., 1996; Balesdent et al., 2000). The large amount of tracer detected in aggregates suggests that a large number of new aggregates are formed and stabilized during and shortly after tillage.

3.3 Spatial fate of incorporated tracer spheres

Having observed that a significant proportion of the tracer spheres are rapidly incorporated after an initial tillage event, it is interesting to note their spatial fate. The distribution of Dy in aggregate size fractions separated by wet sieving shows a large proportion of tracer spheres are incorporated in the largest aggregate fraction (> 4 mm) in Malmo samples, but less so for Breton (Figure 4-4).

An alternate method of expressing the tracer Dy distribution in aggregate size fractions is using the MWD calculation. "Dy MWD" can be calculated in a manner similar to soil aggregate MWD:

$$\text{Dy MWD} = \sum_{i=1}^{n} x_i W_i \qquad (10)$$

where x_i is the mean diameter of the aggregate size fraction and W_i is the weight proportion of tracer Dy retained in the size fraction rather that of soil. The Dy MWD data were calculated without the size fractions smaller than 250 μm because INAA detected no tracer-associated Dy in these fractions. The data for time zero are from wet sieving performed immediately after tracer sphere addition to soil without mixing. We found approximately 90% of the spheres in the 0.25 to 0.5 mm and none in any aggregate size fraction >1 mm (see Figure 3-2). Dy MWD values over the two field seasons for each soil and treatment are illustrated in Figure 4-5. The increasing Dy MWD data reflect the increasing amount of tracer incorporated in aggregates during the growing season.

For proper comparison with Dy MWD, the soil aggregate MWD data were recalculated excluding the size fractions < 250 μm. Figure 4-6 compares the soil versus Dy MWD over the two growing seasons. Comparing the Dy MWD with the soil MWD values provides a better representation of the spatial fate of the tracer spheres. A Dy MWD value larger than soil MWD indicates a preferential enrichment of the largest aggregate size

classes. The Dy MWD values were consistently higher than soil MWD values in the Breton samples, while in Malmo samples the Dy MWD values began lower then increased beyond the soil MWD values.

Two explanations are proposed for the preferential enrichment of the largest aggregates. The first is that due to the architecture of soil aggregates, the 400-μm tracer spheres can be incorporated in only the largest aggregate fraction, because aggregates less than 4 mm in diameter cannot accommodate structural units of ~400 μm. However, in studies using ^{60}Co-tagged aggregates of various sizes, Toth and Alderfer (1960) noted that "as the size of tagged water-table aggregates decreases, its contribution to the formation of larger aggregates [also] diminishes", suggesting that aggregates are made of few large constituents rather than many smaller ones.

Alternatively, the observations may be due to tracer spheres "skipping" the intermediate size fractions and becoming incorporated into large macroaggregates because these larger aggregates are formed first. Indeed, as the free tracer pool is depleted over the course of the growing season, increases are observed most clearly in the > 4 mm fraction. These results provide direct evidence to support a model of aggregate formation where macroaggregates are formed first and smaller aggregates are subsequently created when the larger become unstable and are disrupted (Oades 1984; Beare et al. 1994a; Golchin et al. 1994). Measurements of C accumulations in macro- versus microaggregate fractions have alluded to this phenomenon (Jastrow et al. 1996), however the use of organic C as a tracer for aggregate formation may be confounded by the dynamics of the C itself.

3.4 Dynamics of tracer sphere incorporation

The field plots used for the experiment were selected on the expectation that soil aggregation was at steady-state because the tillage and cropping treatments had been consistently applied for 15 years. This expectation was supported by the correlation of aggregate MWD reported in previous studies and those measured in the current study (see section 3.1). Therefore the incorporation of the tracer spheres was not simply due to net aggregate formation, but was mostly due to the internal cycling of aggregates within a short-term cyclical dynamic. The rise in 1998 and flattening in 1999 of normalized tracer

contents of the aggregated pool (Figure 4-3) and Dy MWD (Figure 4-5) data suggest that tracer incorporation was approaching equilibrium with aggregate turnover. The apparent rapid approach to steady-state indicates that the turnover time of aggregates in the tilled soils studied is short. Our results indicate that while a soil may not express significant changes in net aggregate formation or disruption from year to year, approximately 50% of the macroaggregates may turnover in a single growing season.

Several indicators suggest that the internal turnover of aggregates is more rapid in the Breton soil than in the Malmo soil. Figure 4-6a shows that, the Dy MWD began lower than the soil MWD then gradually climbed higher in the Malmo soil. In contrast, the Dy MWD values in Breton samples were consistently higher than the soil MWD from the earliest sampling period (Figure 4-6b). The quantification of aggregate turnover rates will be examined more closely in Chapter 5.

While the loss of organic matter has been attributed to the increased turnover of aggregates during conventional tillage (e.g. Six et al. 1999), the observations of rapid aggregate turnover in a tilled soil with high organic matter content suggests that aggregate turnover must also provide the opportunity for the occlusion of organic materials in aggregates leading to "physical protection" and eventually to stabilization. Without the rapid internal cycling of soil aggregates, there is little opportunity for the creation of new occlusion sites for the sequestration of organic C. However, the threshold between the exposure of organic C to microbial decomposition, and occlusion and physical protection during soil aggregate turnover remains unclear.

4.0 Conclusions

In general, soil aggregation followed a saw-toothed pattern dominated by season. The saw-toothed pattern is "reset" each year by the over-wintering period and tillage. Over the course of the field study, tracer spheres were detected in larger aggregate fractions than allowed by their size, thus providing a direct observation of aggregate formation. The observed tracer incorporation reflects the internal cycling or turnover of soil aggregates occurring within the growing season. During incorporation, the tracers moved directly into the largest aggregate fraction suggesting that macroaggregates are formed

first and subsequently degrade to form smaller aggregates. The incorporation of the tracers into aggregates appeared to approach equilibrium with soil aggregates within two growing seasons, reflecting a rapid turnover of aggregates in both soils studied. From the observations of aggregate dynamics in tilled soils with contrasting organic matter contents, we suggest that soil aggregate turnover may not always result in the loss of organic matter but may also provide the mechanism for physical protection.

Table 4-1. Selected site characteristics and surface layer (0-15 cm) properties of field soils used (from Solberg et al. 1997).

	Ellerslie	Breton
Mean annual air temperature (°C)	1.7	2.1
Mean annual precipitation (mm)	452	547
Classification	Black Chernozem (Malmo series) (Haplocryoll)	Gray Luvisol (Breton series) (Haplocryoalf)
Texture (clay content, g kg^{-1})	360	220
Total Organic C (g kg^{-1})	60.9	13.1
Bulk Density (g cm^{-3}) †	1.1	1.4
Water-stable Aggregate Mean Weight Diameter (mm) ‡	2.42 ± 0.54	1.46 ± 0.37

† from Dinwoodie and Juma (1988)
‡ Mean ± SD, from all measurements made in 1998 of the current study.

Table 4-2. Selected properties of tracer particles applied to field plots †.

Property	1998 application	1999 application
Mass (µg $sphere^{-1}$)	105 ± 56	90 ± 26
Diameter (µm)	425 ± 92	380 ± 76
Density (g cm^{-3}) ‡	2.57	1.77
Dy concentration (% wt)	15.8 ± 1.1	13.3 ± 0.6

† Mean ± SD
‡ measured using pycnometer method of Blake (1965)

Table 4-3. Mean[†] tracer sphere recovery based on applied rates and detected Dy[‡] for the 1998 subplots (%).

	Days after tracer addition												
	1998						1999						
	9	31	51	72	93	114	341	359	380	401	422	443	466
Malmo – with straw	63	57	67	81	148	69	145	76	128	106	89	82	79
Malmo – without straw	96	105	68	33	78	109	84	68	143	86	77	101	114
Breton – with straw	44	35	52	77	38	36	103	49	65	79	88	48	79
Breton – without straw	40	58	62	94	58	59	80	53	71	66	40	50	56

[†] n = 4

[‡] Sum of detected Dy in all aggregate fractions

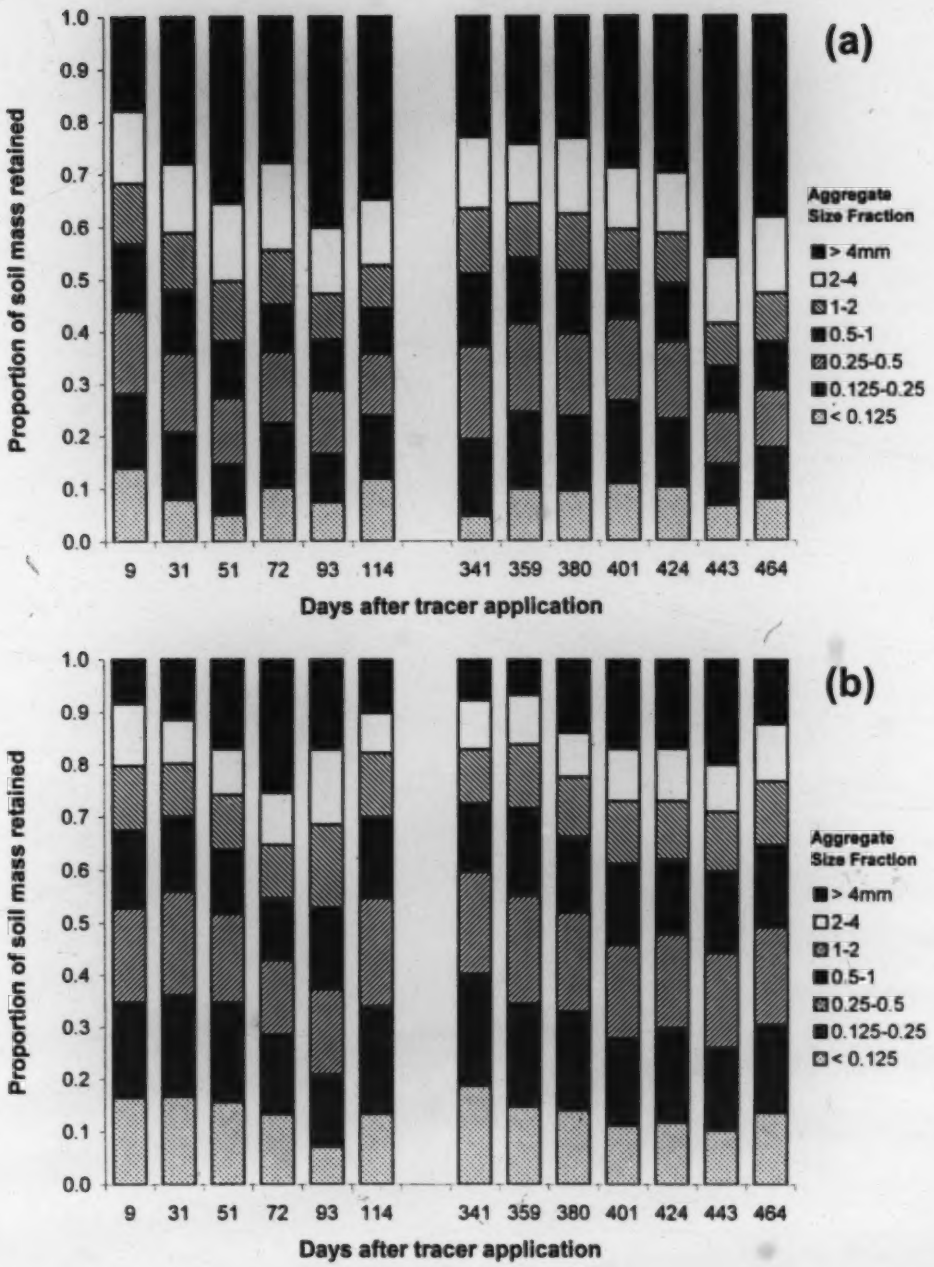

Figure 4-1. Water-stable soil aggregate size distribution in straw amended (T8) plots from (a) Malmo and (b) Breton soils.

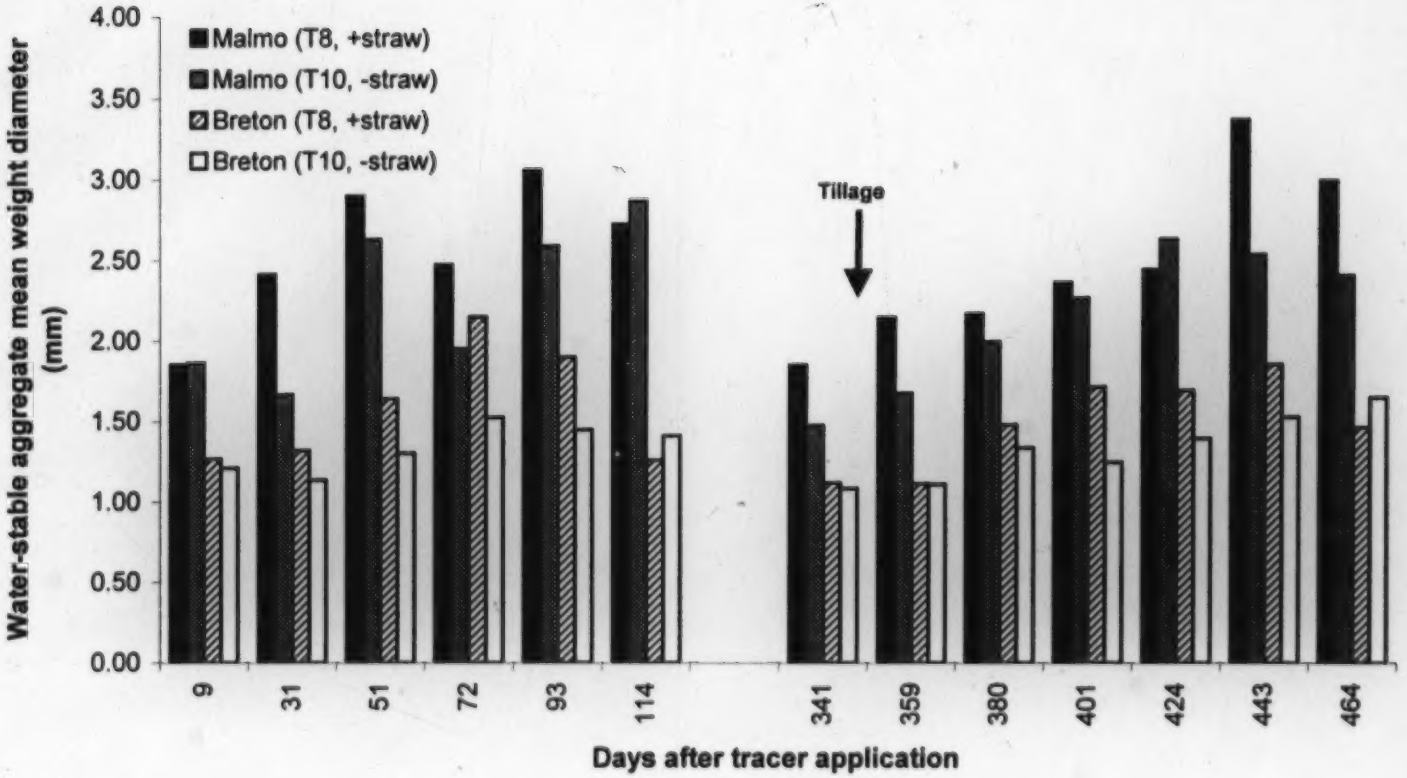

Figure 4-2. Water-stable soil aggregate mean diameter (MWD).

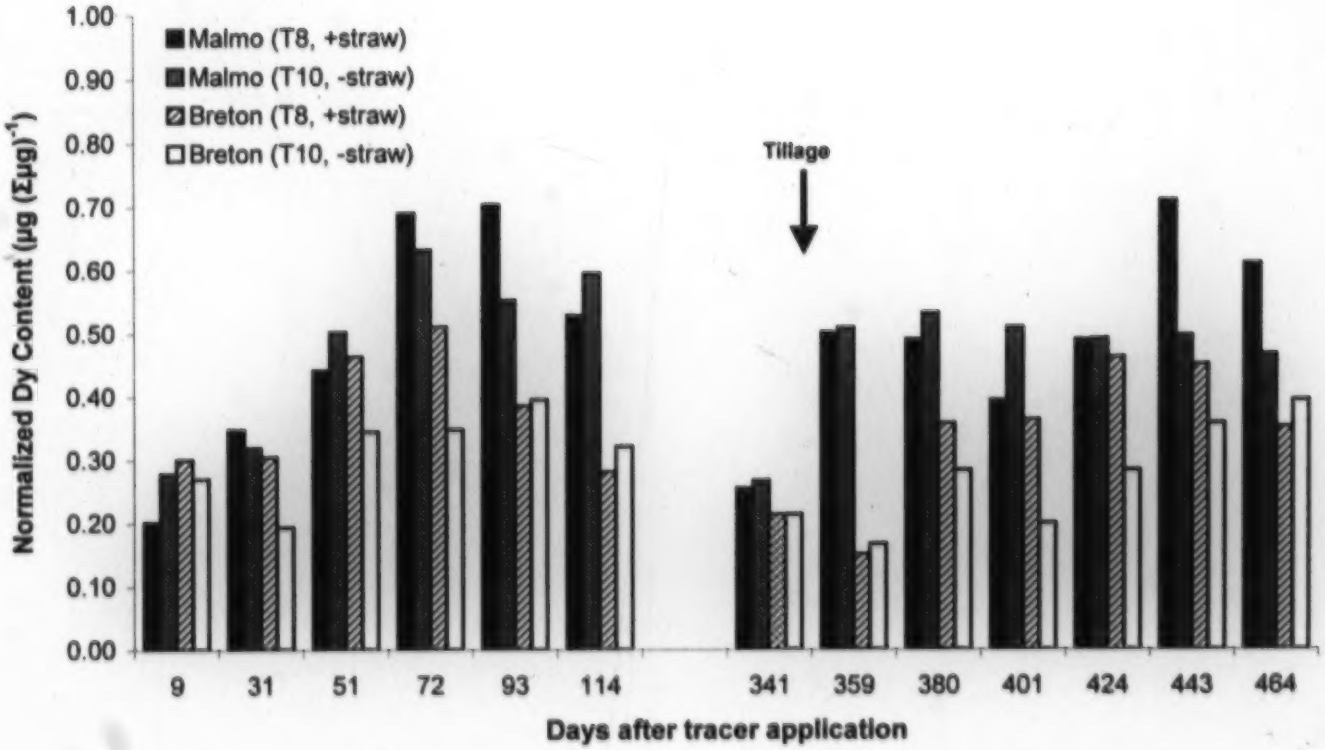

Figure 4-3. Normalized tracer sphere Dy content of the pooled "aggregated" fraction (1 to >4 mm).

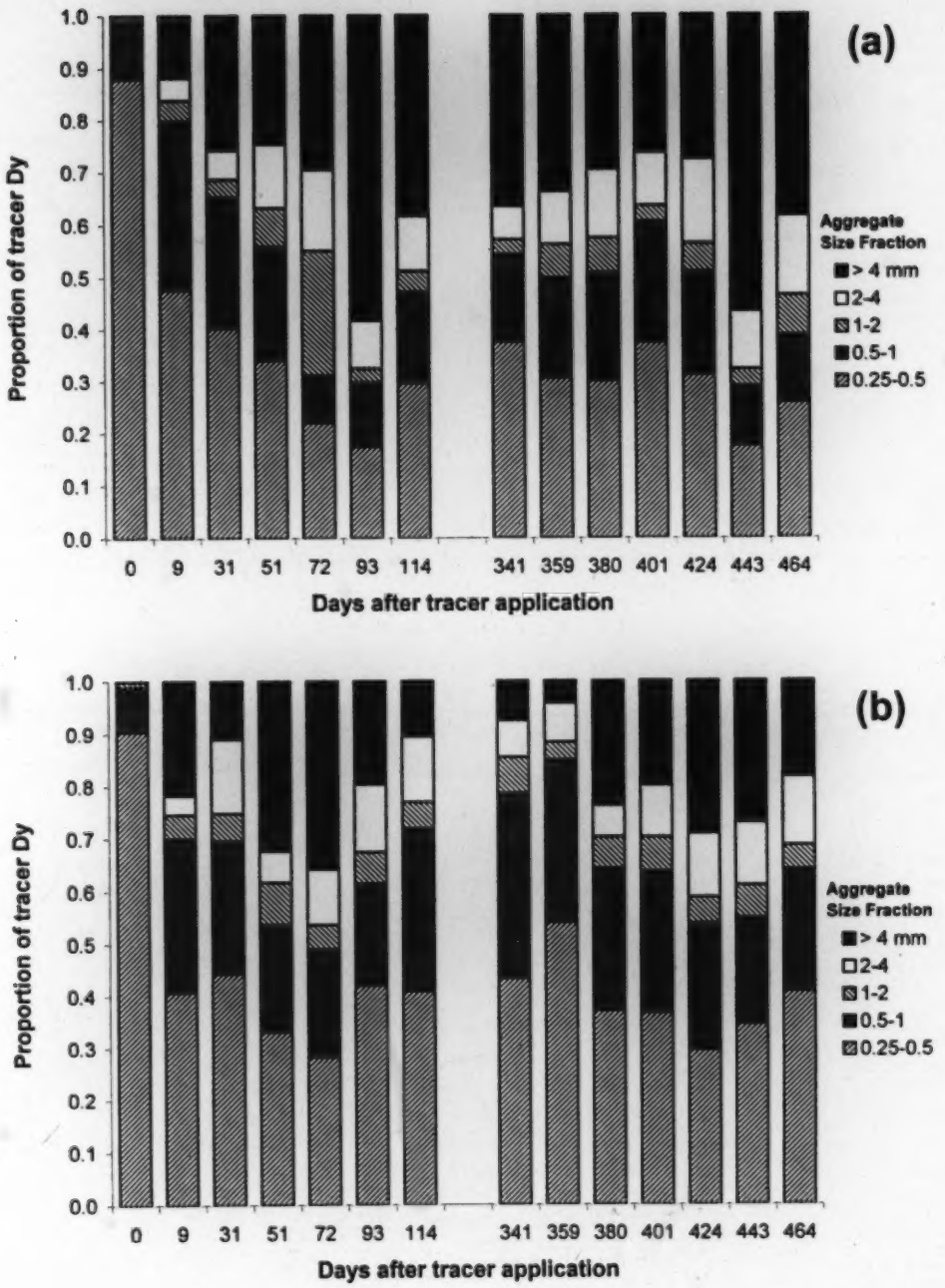

Figure 4-4. Tracer sphere Dy distribution in aggregate size fractions of straw amended (T8) plots from (a) Malmo and (b) Breton soils.

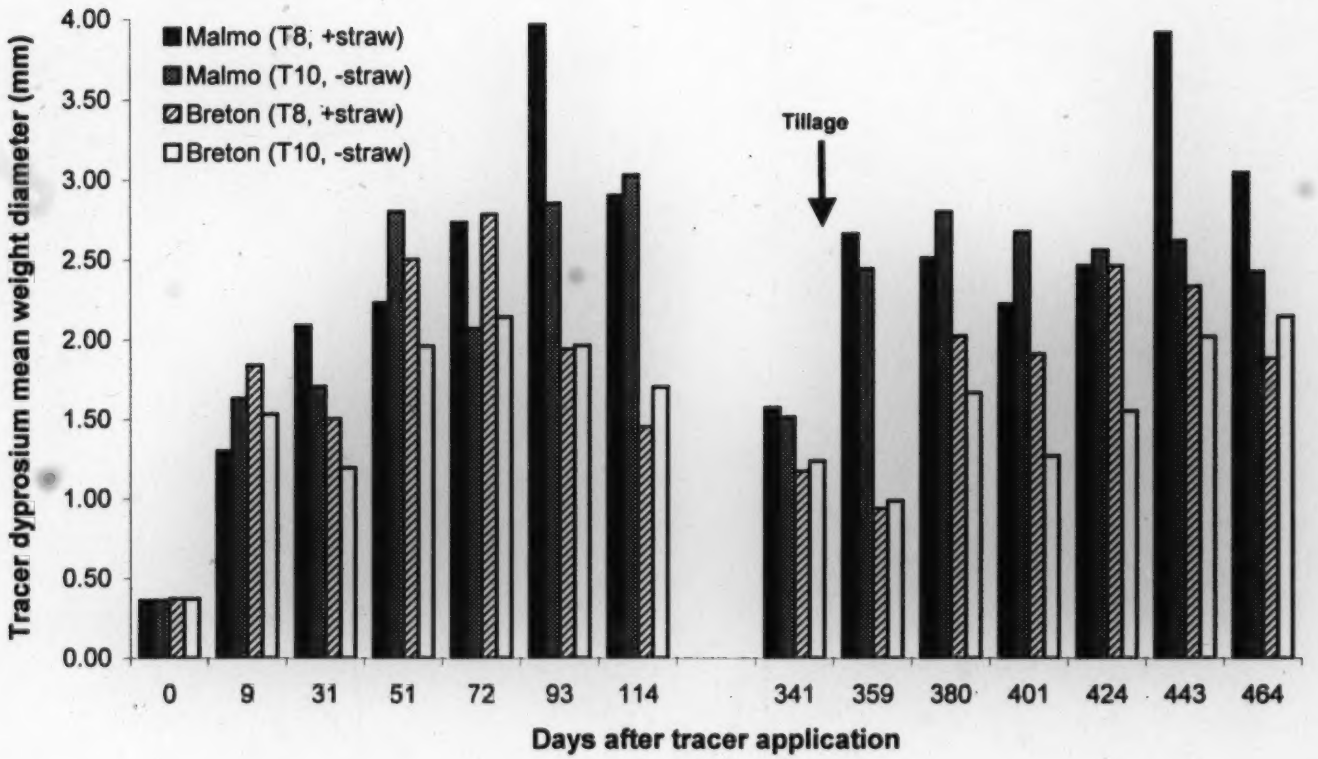

Figure 4-5. Tracer sphere Dy mean weight diameter (MWD).

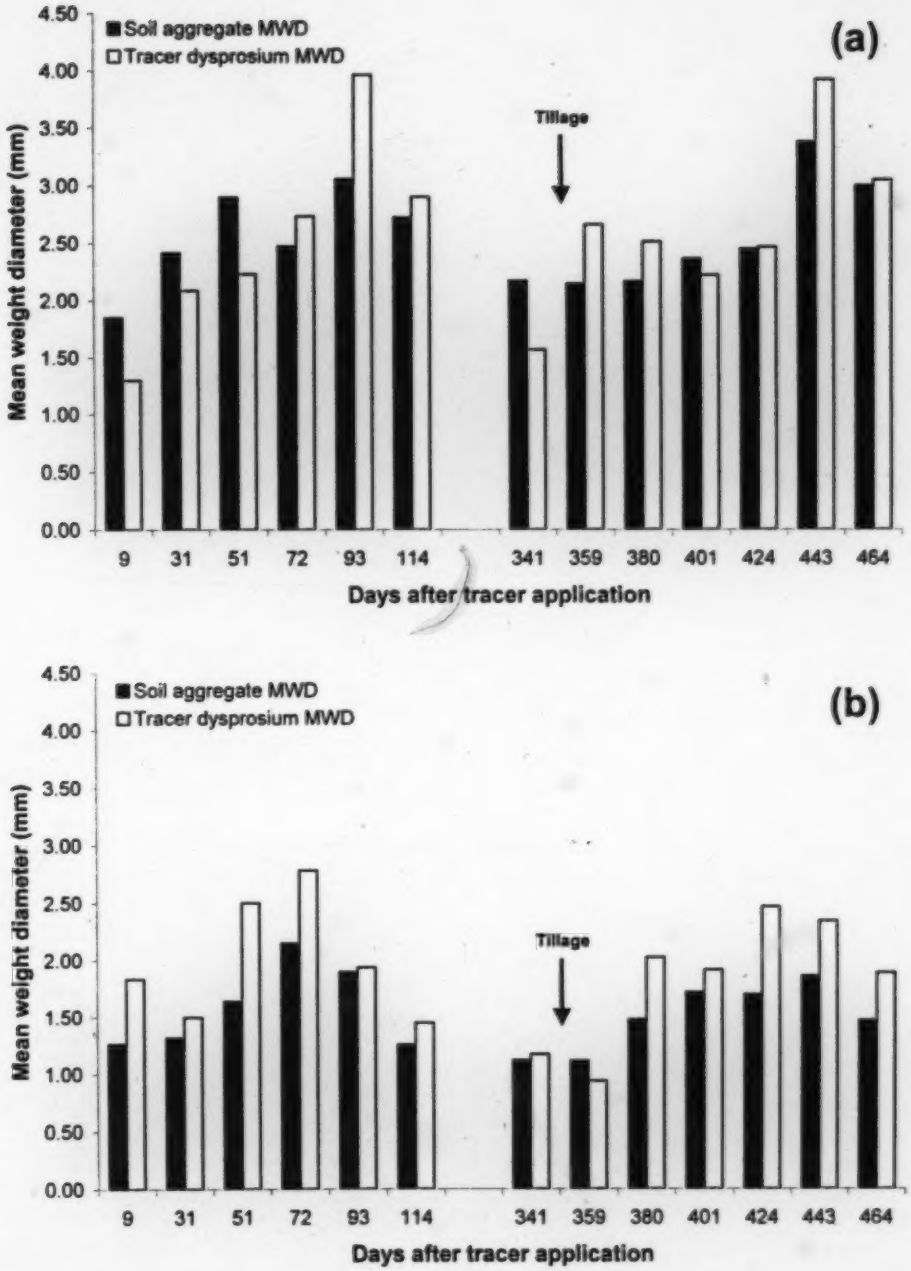

Figure 4-6. Comparison of soil aggregate versus Dy MWD in straw amended (T8) plots from (a) Malmo and (b) Breton soils.

References

Angers, D.A. and G.R. Mehuys. 1993. Aggregate stability to water. *In* M.R. Carter (ed.) Soil Sampling and methods of Analysis. Canadian Society of Soil Science, Lewis Publishers, Boca Raton FL.

Balesdent J. Chenu C. and M. Balabane. 2000. Relationship of soil organic matter to physical protection and tillage. Soil Till. Res. 53:215-230.

Beare M.H., Hendrix P.F. and D.C. Coleman. 1994a. Water-stable aggregates and organic matter fractions in conventional- and no-tillage soils. Soil Sci. Soc. Amer. J. 58:777-786.

Beare M.H., Cabrera M.L., Hendrix P.F. and D.C. Coleman. 1994b. Aggregate-protected and unprotected organic matter pools in conventional- and no-tillage soils. Soil Sci. Soc. Amer. J. 58:787-795.

Dinwoodie, G.D. and N.G. Juma. 1988. Allocation and microbial utilization of C in two soils cropped to barley. Can. J. Soil Sci. 68:495-505.

Elliott E.T. 1986. Aggregate structure and carbon, nitrogen, and phosphorous in native and cultivated soils. Soil Sci. Soc. Amer. J. 50:627-633.

Golchin A., Oades J.M., Skjemstad J.O. and P. Clarke. 1994. Soil structure and carbon cycling. Aust. J. Soil Res. 32:1043-1068.

Jastrow J.D. 1996. Soil aggregate formation and the accrual of particulate and mineral-associated organic matter. Soil Biol. Biochem. 28:665-676.

Jastrow J.D., Boutton T.W. and R.M. Miller. 1996. Carbon dynamics of aggregate-associated organic matter estimated by carbon-13 natural abundance. Soil Sci. Soc. Amer. J. 60:801-807.

Oades J.M. 1984. Soil organic matter and structural stability: Mechanisms and implications for management. Plant and Soil. 76:319-337.

Perfect E., Kay B.D., van Loon W.K.P., Sheard R.W. and T. Pojasok. 1990a. Factors influencing soil structural stability within a growing season. Soil Sci. Soc. Am. J. 54:173-179.

Perfect E., Kay B.D., van Loon W.K.P., Sheard R.W. and T. Pojasok. 1990b. Rates of change in soil structural stability under forages and corn. Soil Sci. Soc. Am. J. 54:179-186.

Puget P., Besnard E. and C. Chenu. 1996. Une méthode de fractionnement des matières organiques particulaires des sols en fonction de leur localization dans les agrégats. C.R. Acad. Sci. Paris. 322:965-972.

Singh B., Chanasyk D.S., McGill W.B. and M.P.K. Nyborg. 1994. Residue amd tillage management effects on soil properties of a typic cryoboroll under continuous barley. Soil Tillage Res. 32:117-133.

Six J., Elliott E.T. and K. Paustian. 1999. Aggregate and soil organic matter dynamics under conventional and no-tillage systems. Soil Sci. Soc. Am. J. 63:1350-1358.

Six J., Elliott E.T., Paustian K. and J.W. Doran. 1998. Aggregation and soil organic matter accumulation in cultivated and native grassland soils. Soil Sci. Soc. Am. J. 62:1367-1377.

Solberg E.D., Nyborg M., Izaurralde R.C., Malhi S.S., Janzen H.H. and M. Molina-Ayala. 1997. Carbon storage in soils under continuous cereal grain cropping: N fertilizer and straw. *In* R. Lal et al. (eds.) Management of Carbon Sequestration in Soil. CRC Press, Boca Raton FL.

Staricka J.A. 1997. (personal communication).

Staricka J.A., Allmaras R.R., Nelson W.W. and W.E. Larson. 1992. Soil aggregate longevity as determined by the incorporation of ceramic spheres. Soil Sci. Soc. Am. J. 56:1591-1597.

Thompson S. 1990. Performance of multiple comparisons in repeated measures designs under nonsphericity. SAS Institute Inc., *Proceedings of the Fifteenth SAS Users Group International Conference*, Cary NC.

Toogood J.A. and D.L. Lynch. 1959. Effect of cropping systems and fertilizers on mean weight-diameter of aggregates of Breton Plot soils. Can. J. Soil. Sci. 39:151-156.

Toth S.J. and R.B. Alderfer. 1960. Formation and breakdown of Co60-tagged water-stable aggregates in a Norton silt loam soil. Soil Sci. 90:232-238.

Wolfinger R. and M. Chang. 1995. Comparing the SAS GLM and MIXED procedures for repeated measures. SAS Institute Inc., *Proceedings of the Twentieth SAS Users Group International Conference*, Cary NC.

Chapter 5:

A quantitative compartmental model of soil macroaggregate dynamics

1.0 Introduction

The development of several conceptual models of soil aggregation has occurred as both the ability to observe aggregate components, and our understanding of the processes involved, have improved. Initially, soils were considered a random assemblage of primary particles separated by a random network of failure planes. However, the development of ultrasonic dispersion methods where the input energy could be quantified led Edwards and Bremner (1967) to suggest the microaggregate theory. The authors found that large aggregates were easily dispersed, while smaller microaggregates (< 250 μm) required much larger dispersing energies. The current paradigm for soil aggregation stems from a progression of work proposing a hierarchical model of soil aggregation (e.g. Dexter 1988; Tisdall and Oades 1982; Oades and Waters 1991). The hierarchical model was supported by experiments observing porosity exclusion (Currie 1966), aggregate strength (Hadas 1987), and aggregate breakdown with differing levels of applied energy (Oades and Waters 1991).

While previous models were supported largely by aggregation disruption data and made little reference to dynamics, new models focus on how soil aggregates may form and their associations with organic materials. Several researchers (Beare et al. 1994; Golchin et al. 1994; Six et al. 1999) have proposed conceptual models of soil aggregation that dynamically link the decomposition of organic materials in soil to the formation of aggregates. Generally, the models propose that large soil aggregates form around nuclei of particulate organic matter, and that smaller aggregates are subsequently released by the dispersion of the macroaggregates as the organic matter decomposes and is no longer able to stabilize the macroaggregate.

While the models of soil aggregation have evolved from static to dynamic representations, they remain largely conceptual and lack significant quantitative components. The demand for a quantitative, dynamic model of soil aggregation is

significant. While experiments have shown that aggregation plays a significant role in the stabilisation of organic matter by physically protecting it through occlusion within aggregates, Elliott et al. (1996) states our current understanding is weak. Most of the current models of soil organic matter turnover use an oversimplified approach based on soil texture (e.g. Parton et al. 1987) or land use (e.g. Van Veen and Paul 1981) to account for the processes of physical protection and tillage. Balesdent et al. (2000) suggest that modeling of SOM dynamics should ideally be more mechanistic and reproduce the processes of physical protection as described in the current conceptual models of soil aggregation. The first step in developing a mechanistic model of SOM dynamics that accounts for physical protection and physical disturbances such as tillage is the development of a quantitative model for the soil aggregates themselves. A quantitative model of soil aggregate formation and disruption may provide data concerning the rates of occlusion or release of labile organic materials and therefore their availability for mineralization or stabilisation.

1.1 Objectives

Studies in the literature have proposed that soil aggregate turnover may control the decomposition of organic matter. Quantification of soil aggregate turnover is therefore essential to testing any hypothesis regarding the relationship between aggregate turnover and organic matter decomposition. The goal of the current work is to develop a simple, quantitative model of soil macroaggregate dynamics. The objectives of the model development are:

1. to propose a model structure congruent with conceptual models developed in the literature and data from tracer spheres studies reported in previous chapters,
2. to estimate kinetic parameters for the compartmental model developed,
3. to compare predicted versus measured soil aggregation dynamics.

2.0 Theory

The foundation of a model for soil aggregate dynamics is data concerning "aggregate architecture". Knowing the composition of soil aggregates is essential for determining

what materials flow into and out of aggregates. Several studies have reported on the textural composition of soil aggregates. Christensen (1986) found macroaggregates were enriched in clay- and silt-sized particles, while Dormaar (1983) and Elliott (1986) found that microaggregates were enriched in sand. Christensen (1996) reviewed the findings and warned that observed primary particle enrichments might be artefacts of the sieving procedures used. He concluded that generally, the distribution of primary soil particles in wet- and dry-sieved aggregates is consistent across size fractions. While textural components may play a minor role in the formation of aggregates, most soil macroaggregates are composed of a combination of microaggregates. Determining the microaggregate distribution within macroaggregates is more difficult because of the difficulties in isolating component microaggregates, which depends largely on the energy applied to the macroaggregates. However, Coughlan et al. (1973) found that after wet-sieving macroaggregates of various sizes separated by dry sieving, the size distribution of the unstable portions was similar and independent of the dry aggregate size. In an earlier study, Toth and Alderfer (1960) traced the fate of labelled aggregates and found that as the size of the labelled aggregate decreased, its contribution to the formation of larger aggregates decreased. Together, these results suggest that the architecture of aggregates is not random, and may be defined and predicted.

The development of an aggregation model requires not only a description of aggregate architecture, but must also describe the patterns of aggregate formation and disruption that will lead to the turnover or cycling of aggregates. Initially, the hierarchical model implied the formation of microaggregates followed by the formation of macroaggregates by the combination of microaggregates. More recently, it is proposed that macroaggregates are formed first, followed by the release of microaggregates as the occluded organic materials are decomposed. Our tracer sphere data (see Chapter 4) provide evidence that small microaggregates contribute directly to the formation of the largest aggregates. Figure 5-1a illustrates a "fully developed" compartmental model of soil aggregate dynamics where A_i are a series of water-stable aggregate size classes as determined by wet-sieving. The "fully developed" model structure, where each compartment is connected to all others, implies a random model of soil aggregate

architecture and provides little information about the patterns of formation and disruption. This structure can be simplified using a small number of aggregate size compartments and some presumed patterns of aggregate dynamics. Figure 5-1b represents an oversimplified aggregation model structure consisting of four compartments and the flow of aggregates downward during disruption and the return of the smallest aggregates to the largest size compartment during formation.

3.0 Model development

Since there is limited data concerning the patterns of aggregate formation and disruption, the approach taken to develop our model was to begin with a fully developed model structure with a small number of compartments, then systematically eliminating inter-compartmental flows based on the fit of the model and the calculated values for fractional flow rates.

Considering the fully developed model, we can define first order equations for the flow of materials out of each aggregate size compartment, such that:

$$\frac{dA_i}{dt} = -k_{ii} \cdot A_i + \sum_{i \neq j} k_{ji} \cdot A_j \qquad (11)$$

Where $-k_{ii}A_i$ represents the outward flow of soil materials from size fraction i, and the sum of $f_{ij}A_j$ represents the inward flow of soil materials from all other size fractions. Equation 1 can be written in discrete form as:

$$A_i(t + \Delta t) = (1 - \delta_i) \cdot A_i + \sum_{i \neq j} f_{ji} \cdot A_j \qquad (12)$$

where $1 - \delta_i = e^{-k_{ii}\Delta t}$ and represents the fraction of soil material in compartment i which remains after time step Δt, and $f_{ji} = k_{ji}\, e^{-k_{ii}\Delta t}$ and represents the fraction of soil material moving out of compartment i and into compartment j. In matrix form, the model can be represented as:

$$\begin{bmatrix} A_1 \\ A_2 \\ A_3 \\ A_4 \end{bmatrix}_{t+\Delta t} = \begin{bmatrix} 1-\delta_1 & f_{21} & f_{31} & f_{41} \\ f_{12} & 1-\delta_2 & f_{32} & f_{42} \\ f_{13} & f_{23} & 1-\delta_3 & f_{43} \\ f_{14} & f_{24} & f_{34} & 1-\delta_4 \end{bmatrix} \begin{bmatrix} A_1 \\ A_2 \\ A_3 \\ A_4 \end{bmatrix}_t \quad (13)$$

The model is then constrained by:

$$(1-\delta_i) + \sum_{i \neq j} f_{ij} = 1 \quad (14)$$

because it is a closed system where the total mass of soil is constant and the model compartments are represented by proportions of the total mass.

3.1 Model calibration

The model was calibrated using the water-stable soil aggregate data collected from two contrasting field soils, as reported in Chapter 4. Soil samples were collected periodically from field plots established on a Black Chernozem, Malmo series (Haplocryoll) at the Ellerslie Research station (53° 25'N, 113° 33'W), and on a Gray Luvisol, Breton series (Haplocryalf) at the Breton Research station (53° 07', 114° 28'W) (Solberg et al. 1997). Only the straw amended treatment plots (T8) were sampled from three subplots over two growing seasons: the first year and subplot combination - 1998(I), a second year in the first subplot - 1998(II), and an alternate first year in a second set of subplots - 1999(I). Samples were brought to the lab, air-dried, then subjected to wet-sieving to produce water-stable aggregate size distribution data consisting of six size fractions. The soils at Ellerslie and Breton were found to be at steady-state with respect to water-stable aggregation, with no significant net aggradation or degradation over the span of several years (Chapter 4). Therefore, water-stable aggregate size distribution data for 1998(I), 1998(II) and 1999(I) were pooled into a single "mean" season using the number of days after spring tillage.

The model structure used consisted of four compartments: A_1 (> 4 mm), A_2 (2-4 mm), A_3 (1-2 mm), and A_4 (< 1 mm) (Figure 5-1). The A_4 compartment represents a pooling of the bottom three aggregate size fractions to form a "free tracer pool" based on the size of the

tracer spheres used in the field experiment, where any tracer Dy detected outside of A_4 is assumed to be due to incorporation into aggregates (Chapter 4).

The model was fit to the data by the method of least squares, using a 3-day time step and by minimizing SS where:

$$SS = \sum \left(\hat{A}_{iT} - A_{iT} \right)^2 \qquad (15)$$

where $\hat{A}$ is the predicted value and A is the measured value of soil mass contained in the aggregate size fraction, and T represents the discrete sampling date. Minimization was performed by adjusting parameters in the f_{ij} matrix. The procedure was performed iteratively such that f_{ij} values less than 0.01 where eliminated by setting them to zero, and repeating the fitting process with the remaining values.

The first-order rate constant (k_{ii}) and mean residence time ($1/k_{ii}$) of soil material in each aggregate size fraction were calculated using Equation 3, where the best-fit values for $1 - \delta_i = e^{-k_{ii}\Delta t}$ and $\Delta t = 3$ days. Distributions of outgoing soil materials were calculated as proportions of the total amount leaving the compartment, i.e. $f_{12} \div (f_{12} + f_{13} + f_{14})$.

3.2 Prediction of tracer sphere dynamics

The tracer spheres used throughout this research project were selected because they are expected to mimic soil particles and aggregates. The model of aggregate dynamics should therefore predict their incorporation into soil aggregates from an initially free state. After calibration, the best-fit models for Malmo and Breton soils were used to predict the distribution of tracer Dy within the compartments over two growing seasons. The initial distribution of tracer spheres was A_1, A_2, $A_3 = 0$ and $A_4 = 1$. No information about aggregation or the behaviour of the tracers was available for the over-winter period. Therefore the prediction of tracer distributions over the two growing seasons was performed sequentially. The distribution of tracers at the start of the second growing season was set to the measured distribution because the tracers were assumed not to be at equilibrium with soil aggregation, which is reset during the over-winter period. The predictions were compared with the actual tracer Dy distribution data determined using INAA of the aggregate fractions (Chapter 4).

4.0 Results and Discussion

4.1 Model structure

Soil aggregate data were used to calibrate the model, rather than using the tracer data, because the soil aggregation showed a cyclical pattern reset by the over-winter period and spring tillage (Chapter 4), while the pattern may appear to be at steady-state over the long-term, it was the intra-seasonal dynamics of aggregation that were of interest. Tracer Dy data did not appear to reach equilibrium with the soil within a season and therefore year-over-year replication was not possible, resulting in too few degrees of freedom for the model fitting process. In addition, modeling of the tracer spheres from their initial distribution would describe only their exit from the A_4 compartment, and therefore the simultaneous description of the dynamics all four compartments in the model could not be achieved with confidence until the tracer had reached each compartment. The use of the soil aggregate data to calibrate the model resulted in a stronger fit, but a weaker validation.

The method of least squares generated model regression coefficients (R^2) for the model calibration of 0.959 for the Malmo soil, and 0.982 for the Breton soil (Figures 5-2, 5-3). The model fitting process yielded different model structures for the Malmo and Breton soils (Figure 5-4). An unbiased fitting of data from each soil separately, without the imposition of constraints based on inferred notions of aggregate dynamics, resulted in differing model structures. The lack of apparent universality of the models reflects the impact of soil properties on the dynamics of the aggregate components. Properties such as organic matter content may alter the patterns and rates of aggregation dynamics, as suggested by the concept of "self-protection" proposed by Balesdent et al. (2000). However, we do not believe that sufficient data exist to impose physical constraints on the flow of soil materials through aggregate size fractions and therefore we allowed the model fitting process to yield the fractional flow values. Once the required data are generated, the model can be improved to include more empirical, observational, and physical constraints on aggregate flows.

While the literature (e.g. Beare et al. 1994) and our tracer data (Chapter 2) suggest that macroaggregates form first, such that microaggregates (or free tracer spheres) are incorporated into the largest size fraction with minimal incorporation into intermediate size fractions, the pattern of aggregate formation in the models for both Ellerslie and Breton suggest a sequential movement of soil materials upwards through the size fractions. However, given the short residence times of the intermediate fractions, it is possible that macroaggregate formation is sufficiently rapid that no observations of intermediate formation may be made without a fine temporal resolution. The patterns of aggregate disruption displayed by the models were also unexpected. Data from Coughlan et al. (1973) suggest that the size proportions of the products of aggregate disruption are independent of initial aggregate size. Conversely, our models display differing patterns of aggregate disruption for each size fraction.

The patterns of aggregate formation and disruption proposed in the models do not provide sufficient evidence to refute a random model of soil aggregation. In addition, the model of concentric aggregate formation proposed by Santos et al. (1999) does not appear to be supported by our model structures. The more rapid turnover of the largest macroaggregates modelled here supports the hierarchical models of aggregation previously proposed (e.g. Oades and Waters, 1991), but models that suggest macroaggregate are formed first and release microaggregates cannot be support or refuted by our model due to the lack of resolution in the smaller aggregate sized fractions.

4.2 Kinetic parameters

The resultant best fit of Equation 3 for the Malmo soil is:

$$\begin{bmatrix} A_1 \\ A_2 \\ A_3 \\ A_4 \end{bmatrix}_{t+\Delta t} = \begin{bmatrix} 0.91 & 0.24 & 0 & 0 \\ 0.09 & 0.57 & 0.31 & 0 \\ 0 & 0.11 & 0.69 & 0.03 \\ 0 & 0.07 & 0 & 0.97 \end{bmatrix} \begin{bmatrix} A_1 \\ A_2 \\ A_3 \\ A_4 \end{bmatrix}_t \quad (16)$$

The resultant best fit of Equation 3 for the Breton soil is:

$$\begin{bmatrix} A_1 \\ A_2 \\ A_3 \\ A_4 \end{bmatrix}_{t+\Delta t} = \begin{bmatrix} 0.86 & 0 & 0.22 & 0 \\ 0.08 & 0.81 & 0.05 & 0 \\ 0.06 & 0 & 0.50 & 0.07 \\ 0 & 0.19 & 0.23 & 0.93 \end{bmatrix} \begin{bmatrix} A_1 \\ A_2 \\ A_3 \\ A_4 \end{bmatrix}_t \quad (17)$$

The first-order constants and associated mean residence times for the aggregate size components suggest aggregate turnover in both soils is rapid, but generally 2-3 times more rapid in the Breton soil compared to the Malmo soil (Table 5-1). Soil differences in aggregate turnover are likely due to differences in soil properties such as organic matter contents and dynamics, and clay content (Chapter 6), which many researchers attribute as contributors to soil aggregate stability (e.g. Angers et al. 1993).

In general the aggregate turnover rates suggested by the models are much higher than those reported in the literature. Few studies have quantified rates of soil aggregate turnover and most are inferences based on measurements of carbon accumulation in aggregates. Besnard et al. (1996) suggest that the lifetime of aggregates in cultivated soils would be "a few years". In a prairie restoration experiment, Jastrow (1996) reported a first-order rate constant for macroaggregate formation of 0.438 yr^{-1} ($t_{½}$ = 1.6 yr). Jastrow et al. (1996) equated the loss of C4-C from aggregate size fraction to the turnover rate of the aggregates themselves and reported aggregate turnover times from 412 yr for 53-212 μm aggregates to 74 yr for aggregates > 4750 μm.

Turnover rates determined by the model are two orders of magnitude higher than those proposed in the literature because they reflect gross aggregate turnover rather than net rates of aggregate formation or disruption. The model developed here quantifies the inflows and outflows into each aggregate size fractions, which represent the sum of all formations and disruptions of that particular aggregate size fraction. The distinction between gross aggregate turnover and aggregation becomes important when observations of tracer incorporation (which signifies aggregate formation) are made when the net process occurring in the soil is aggregate disruption, i.e. decreasing soil aggregate MWD. Using a similar tracer particle approach, Staricka et al. (1992) reported first-order rate

constants for their "tracer-to-soil" ratios that yield turnover times of 0.4 to 5 yr. Differences between results of the model and the Staricka study are likely due to differences in the size of tracer sphere used (1-3 mm by Staricka et al. versus 400 μm in this study), and the aggregate size fractions separated from the soil (3 to >40 mm by Staricka et al. versus 125 μm to >4 mm in this study). As illustrated by the results of the model, soil particles or aggregates of differing sizes are expected to express differing dynamics during aggregate turnover.

Results of the model also suggest that the largest and smallest macroaggregate components turnover less rapidly than the intermediate size fractions (Table 5-1). The hierarchical model of soil aggregation suggests that macroaggregate turnover is more rapid than microaggregates (Tisdall and Oades, 1982). The differences observed are likely due to the size fractions used in the modeling exercise, which are mostly considered macro-sized. The selection of compartments used in the model was based a geometric series of sieves from 4 mm to 125 μm used in the tracer sphere field experiment, and A_4 represents the pooled soil aggregate size fraction less than 1mm in diameter which is the free pool of tracer spheres (Chapter 4). An increase in the number size fractions represented in the model requires more degrees of freedom to determine the f_{ij} parameters than are available from the dataset.

4.3 Prediction of tracer sphere dynamics

The field study reported in Chapter 4 contains data of not only the water-stable aggregate size distributions over the course of two growing seasons, but also the distributions of trace sphere Dy that were used to examine gross rates of aggregate formation and disruption. Model estimation of tracer contents in individual aggregate fractions was generally better for the Breton soil; the overall correlation coefficients (R^2) for the predictions were 0.732 for Malmo soil, and 0.902 for Breton. However, the results of goodness of fit F-tests showed a significant lack of fit for the Malmo model and a significant fit for the Breton model (Table 5-2). Generally, the model underestimated tracer incorporation in A_1, and therefore overestimated the tracer content in A_4 (Figures 5-5, 5-6). This may be due to limitations of using first-order kinetics to describe the flow

of soil materials. It may be that an alternate model should be used, such that the kinetic constant changes over time.

While the model did not appear to consistently predict tracer sphere content of individual aggregate fractions, the mean weight diameter of tracer-associated dysprosium (Dy MWD) was predicted reasonably well (Figure 5-7). From an initial state where all tracer sphere Dy was in A_4, which yields a Dy MWD value of 0.50 mm, the model predicted Dy MWD values at the end of two growing seasons of 3.09 mm versus the measured value of 3.06 mm for Malmo. The predicted Dy MWD at the end of two growing seasons for the Breton soil was 1.81 mm versus a measured value of 1.90 mm.

4.4 Limitations of the model

While the model developed here fits the soil aggregate data well and was able to predict tracer Dy MWD over the course of two growing seasons, it has some limitations.

1. The development of the model was a data-fitting exercise rather than a mechanistic, or process based on known physical phenomena. While this approach was necessary due to the lack of data concerning soil aggregate dynamics, it is difficult to be certain that particular model outcomes can be related to physical processes. In addition, fitting the model to the two soils separately yields an apparent lack of universality because the model cannot account for other soil properties that will alter aggregate dynamics in differing soils.
2. The use of only four model compartments reduced the number of kinetic parameters and thus the mathematical demands of model, but in doing so also reduced the resolution of aggregate size fractions. The model is not able to make any predictions of the dynamics of microaggregates in its current form.
3. The use of the soil aggregate data for model calibration and tracer Dy data for model verification does not provide a large degree of independence since both were measured simultaneously on the same samples. However, to our knowledge, no other datasets exist that could be used to test the model and make it more robust.

5.0 Conclusions

We developed a quantitative compartmental model of water-stable macroaggregate dynamics because the quantification of aggregate turnover is essential to testing any hypothesis concerning the relationship between aggregate turnover and organic matter decomposition. Aggregate dynamics were modelled using four compartments representing three macroaggregate fractions (> 4, 2-4, 1-2 mm) and a pooled fraction (< 1 mm). The flow of soil aggregate components into and out of macroaggregate size fractions was described using first order kinetics. The best fitting model structure revealed a non-random arrangement of aggregate components and soil-specific patterns of aggregation. Mean residence times of the model aggregate components ranged from 4 to 95 days, and were generally 2-3 times more rapid in the Breton soil than in the Malmo soil. Model prediction of the pattern of tracer sphere incorporation was poor for the Malmo soil and good for the Breton soil, however the model was able to predict tracer Dy MWD. While the model has limitations, it makes no assumptions about flows of soil materials, it fits temporal changes in measured soil aggregate size distributions, and we believe it is the first attempt to quantitatively describe soil aggregate dynamics reported in the literature.

Table 5-1. First-order constants and associated mean residence times of model aggregate size components.

		First-order rate constant, k (d^{-1})	Mean residence time, 1/k (d)
Malmo	A_1 (> 4 mm)	0.030	33.3
	A_2 (2-4 mm)	0.188	5.3
	A_3 (1-2 mm)	0.121	8.2
	A_4 (< 1 mm)	0.010	95.3
Breton	A_1 (> 4 mm)	0.052	19.3
	A_2 (2-4 mm)	0.070	14.2
	A_3 (1-2 mm)	0.231	4.3
	A_4 (< 1 mm)	0.026	38.5

Table 5-2. Statistical diagnostics of model predictions of tracer sphere dynamics.

	Correlation	Goodness of fit F-test			
	R^2	Degrees of freedom		F	*p*
		Model	Error		
Malmo	0.732	56	72	0.469	0.998
Breton	0.902			27.84	< 0.0001

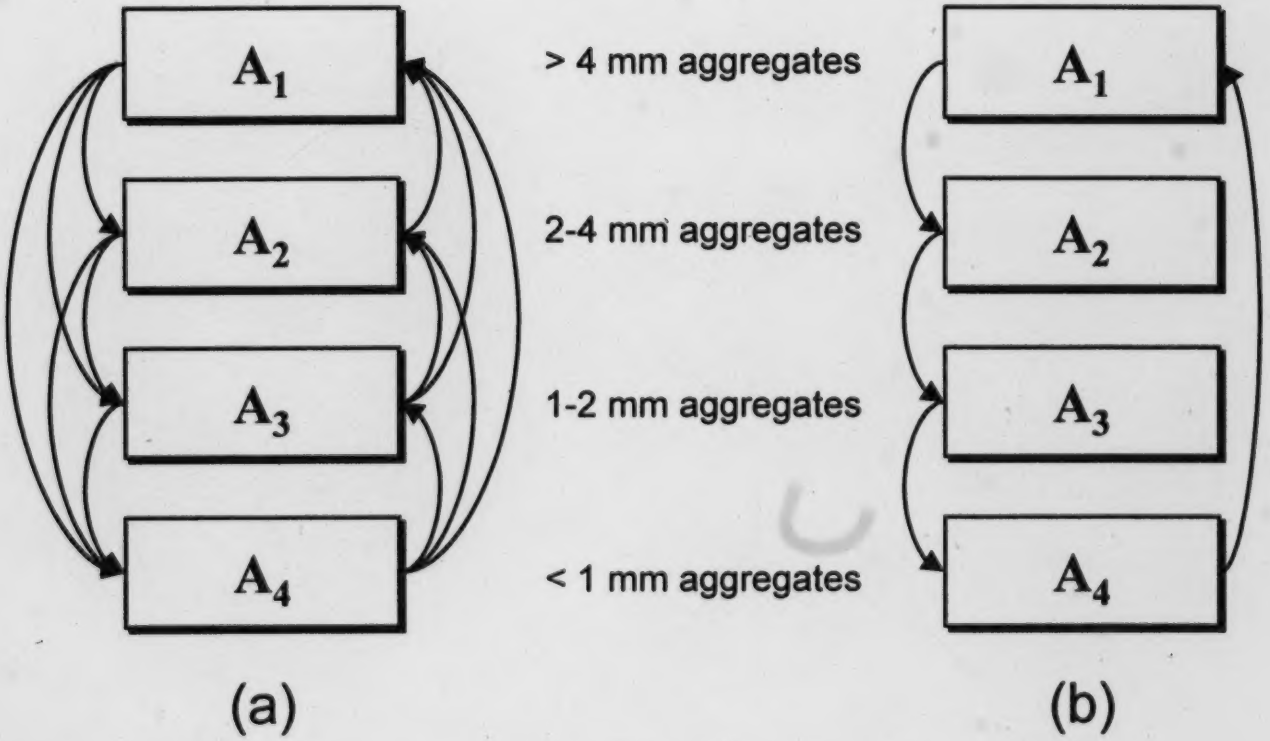

Figure 5-1: Schematic representation of (a) a fully developed model structure, and (b) an oversimplified model structure for aggregate dynamics.

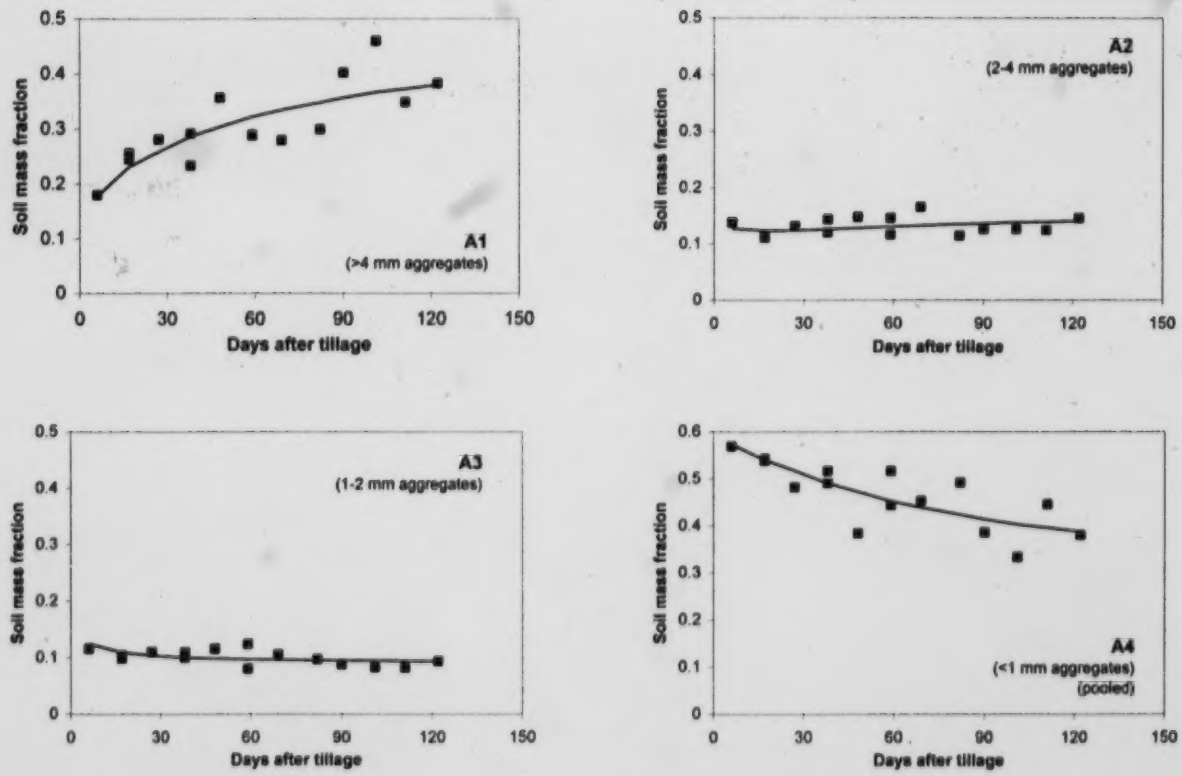

Figure 5-2: Compartmental water-stable macroaggregate dynamics model fit for the Malmo soil. (■, calibration data from field study; —, model output)

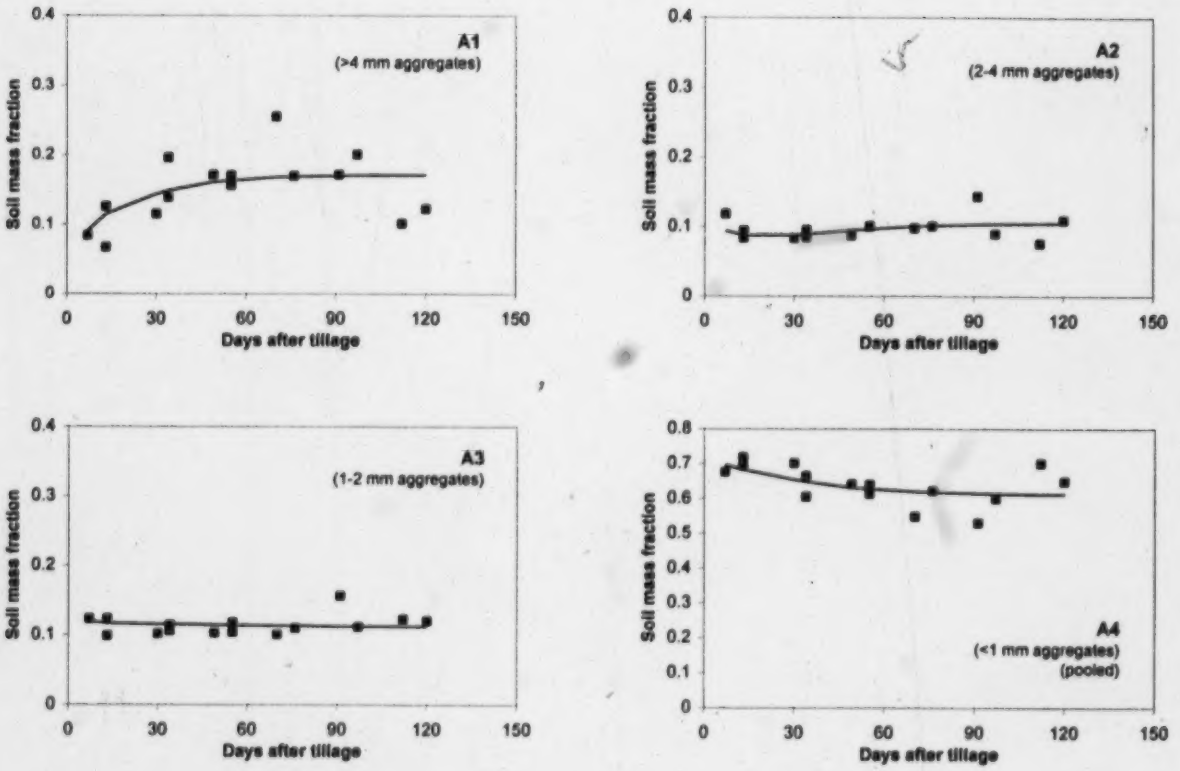

Figure 5-3: Compartmental water-stable macroaggregate dynamics model fit for the Breton soil. (■, calibration data from field study, –, model output)

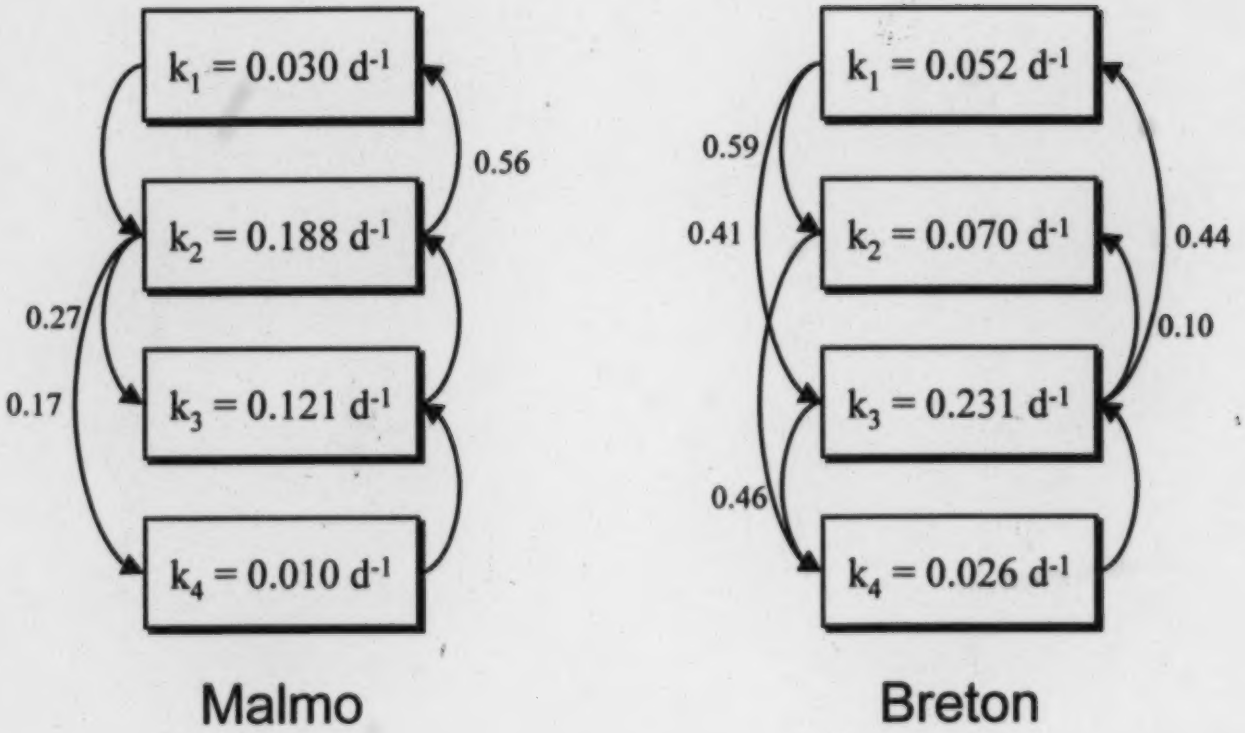

Figure 5-4: Model structures for Malmo and Breton soils. (Numbers next to flow arrows represent proportion of material leaving compartment, flow arrows without numbers represent all the material leaving.)

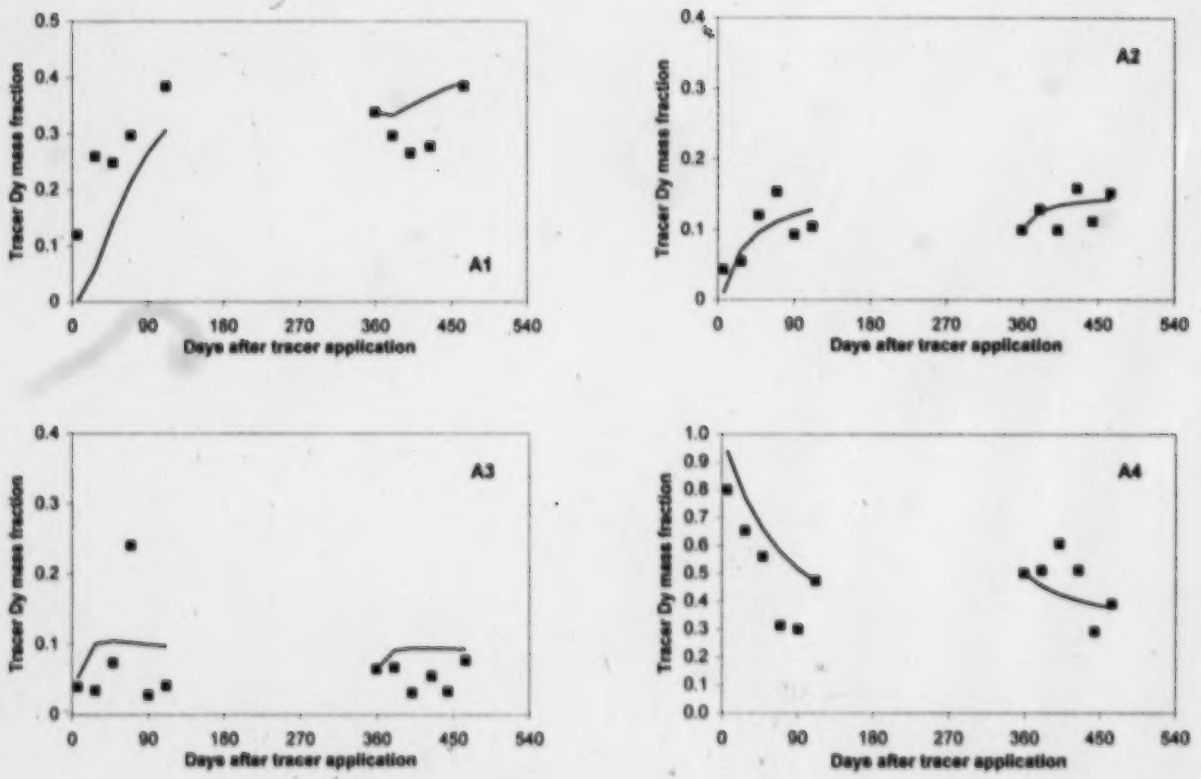

Figure 5-5: Model predictions of tracer sphere dynamics in Malmo samples. (■, tracer sphere data from field study, –, model prediction)

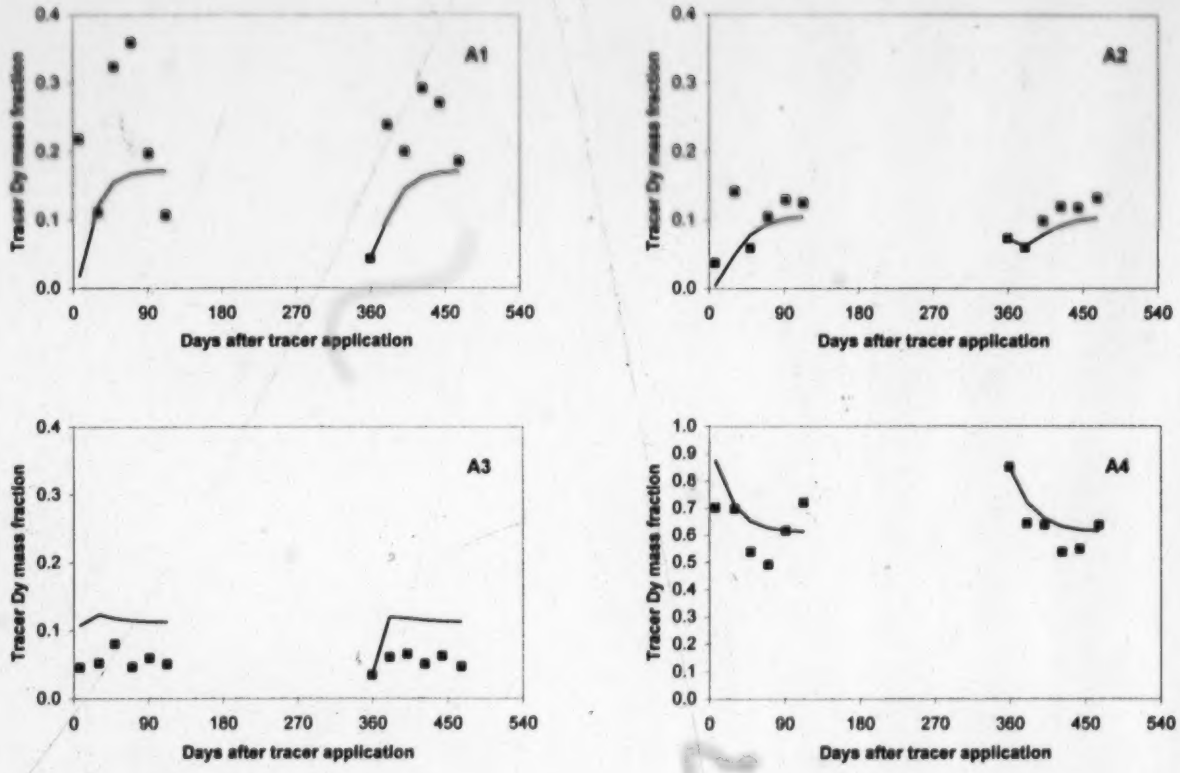

Figure 5-6: Model predictions of tracer sphere dynamics in Breton samples. (■, tracer sphere data from field study, –, model prediction)

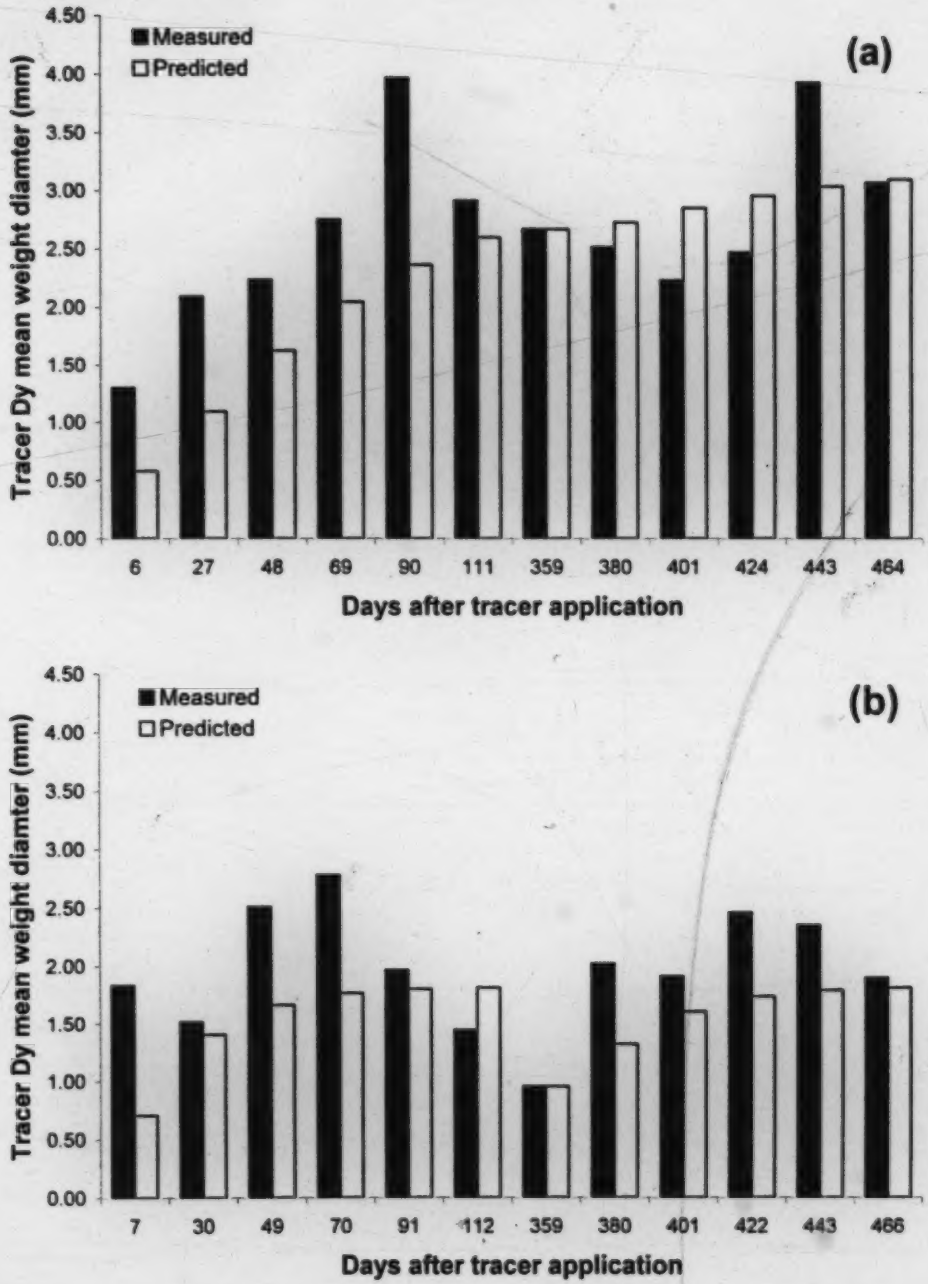

Figure 5-7: Measured and predicted tracer Dy mean diameters for (a) Malmo and (b) Breton soils.

References

Angers D.A., Samson N. and A. Légère. 1993. Early changes in water-stable aggregation induced by rotation and tillage in a soil under barley production. Can. J. Soil Sci. 73:51-59.

Balesdent J. Chenu C. and M. Balabane. 2000. Relationship of soil organic matter to physical protection and tillage. Soil Till. Res. 53:215-230.

Beare M.H., Hendrix P.F. and D.C. Coleman. 1994. Water-stable aggregates and organic matter fractions in conventional- and no-tillage soils. Soil Sci. Soc. Amer. J. 58:777-786.

Besnard E., Chenu C., Balesdent J., Puget P. and D. Arrouays. 1996. Fate of particulate organic matter in soil aggregates during cultivation. Eur. J. Soil Sci. 47:495-503.

Coughlan K.J., Fox W.E. and J.D. Hughes. 1973. Aggregation in swelling clay soils. Aust. J. Soil Res. 11:133-141.

Christensen B.T. 1986. Straw incorporation and soil organic matter in macroaggregates and particle size separates. J. Soil Sci. 37:125-135.

Chrsitensen B.T. 1996. Carbon in primary and secondary organomineral complexes. *In* M.R. Carter and B.A. Stewart (eds.) Structure and Organic Matter Storage in Agricultural Soils. CRC Press, Boca Raton FL.

Currie J.A. 1966. The volume and porosity of soil crumbs. J. Soil Sci. 17:24-35.

Dexter A.R. 1988. Advances in characterization of soil structure. Soil Till. Res. 11:223-238.

Dormaar J.F. 1983. Chemical properties of soil and water-stable aggregates after sixty-seven years of cropping to spring wheat. Plant Soil 75:51-61.

Edwards A.P. and J.M. Bremner. 1967. Microaggregates in soils. J. Soil Sci. 18:64-73.

Elliott E.T, Paustian K. and S.D. Frey. 1996. Modeling the measurable or measuring the modelable: A hierarchical approach to isolating meaningful soil organic matter

fractionations. *In* Evaluation of soil organic matter models. D.S. Powlson et al. (Eds.) NATO ASI Series Vol. 138.

Elliott E.T. 1986. Aggregate structure and carbon, nitrogen, and phosphorous in native and cultivated soils. Soil Sci. Soc. Amer. J. 50:627-633.

Golchin A., Oades J.M., Skjemstad J.O. and P. Clarke. 1994. Soil structure and carbon cycling. Aust. J. Soil Res. 32:1043-1068.

Hadas A. 1987. Long-term tillage practice effects on soil aggregation modes and strength. Soil Sci. Soc. Amer. J. 51:191-197.

Jastrow J.D. 1996. Soil aggregate formation and the accrual of particulate and mineral-associated organic matter. Soil Biol. Biochem. 28:665-676.

Jastrow J.D., Boutton T.W. and R.M. Miller. 1996. Carbon dynamics of aggregate-associated organic matter estimated by carbon-13 natural abundance. Soil Sci. Soc. Am . J. 60:801-807.

Oades J.M. 1984. Soil organic matter and structural stability: Mechanisms and implications for management. Plant and Soil. 76:319-337.

Oades J.M. and A.G. Waters. 1991. Aggregate hierarchy in soils. Aust. J. Soil Res. 29:815-828.

Parton W.J., Schimel D.S., Cole C.V. and D.S. Ojima. 1987. Analysis of factors controlling soil organic matter levels in Great Plains grasslands. Soil Sci. Soc. Am. J. 51:1173-1179.

Santos D., Murphy S.L.S., Taubner H., Smucker A.J.M. and R. Horn. 1997. Uniform separation of concentric surface layers from soil aggregates. Soil Sci. Soc. Am. J. 61:720-724.

Six J., Elliott E.T. and K. Paustian. 1999. Aggregate and soil organic matter dynamics under conventional and no-tillage systems. Soil Sci. Soc. Am. J. 63:1350-1358.

Six J., Elliott E.T., Paustian K. and J.W. Doran. 1998. Aggregation and soil organic matter accumulation in cultivated and native grassland soils. Soil Sci. Soc. Am. J. 62:1367-1377.

Solberg E.D., Nyborg M., Izaurralde R.C., Malhi S.S., Janzen H.H. and M. Molina-Ayala. 1997. Carbon storage in soils under continuous cereal grain cropping: N fertilizer and straw. *In* R. Lal et al. (eds.) Management of Carbon Sequestration in Soil. CRC Press, Boca Raton FL.

Staricka J.A., Allmaras R.R., Nelson W.W. and W.E. Larson. 1992. Soil aggregate longevity as determined by the incorporation of ceramic spheres. Soil Sci. Soc. Am. J. 56:1591-1597.

Tisdall J.M. and J.M. Oades. 1982. Organic matter and water-stable aggregates in soils. J. Soil Sci. 33:141-163.

Toth S.J. and R.B. Alderfer. 1960. Formation and breakdown of Co60-tagged water-stable aggregates in a Norton silt loam soil. Soil Sci. 90:232-238.

Van Veen J.A. and E.A. Paul. 1981. Organic carbon dynamics in grasslands soils: Background information and computer simulation. Can. J. Soil Sci. 61:185-201.

Chapter 6:

Linking active organic matter dynamics to soil aggregate dynamics in two contrasting field soils

1.0 Introduction

A large body of work has demonstrated that the sequestration of organic C requires, at least in part, the occlusion of the organic material into soil aggregates (see Chapter 1). As organic materials become occluded in aggregates they enter an environment less conducive to decomposition (e.g. anaerobic) or become physically inaccessible to degrading microorganisms. Physical protection provides the means by which organic matter contact with reactive surfaces (e.g. clay) is initiated and the process of stabilization occurs, thereby increasing the potential for long-term sequestration. However, as Besnard et al. (1996) point out "protection provided by the soil matrix should depend on the life expectancy of the arrangement of soil particles at protected sites". The process of aggregate disruption as an inferred cause for C losses in tilled soils was examined by several studies comparing conventional and no-tillage management practices (*e.g.* Beare et al. 1994a, 1994b; Six et al. 1998). These studies found that no-till soils had greater concentrations of total C and particulate organic matter (POM) C. Six et al. (1999) propose that OM losses under tillage are due to increased aggregate turnover in a "cultivation loop" versus a slower "decomposition loop" in no-till soils. They did not, however, directly measure aggregate turnover.

While the turnover of soil aggregates is thought to control organic matter turnover, the opposite is also observed. The importance of labile organic C in the stabilisation of soil aggregates has been widely demonstrated. Several researchers demonstrated strong correlations between aggregate stability and soil carbohydrates (e.g. Haynes and Swift 1990; Angers et al. 1993), microbial biomass (e.g. Capriel et al. 1990; Angers et al. 1992), and aliphatic C (e.g. Capriel et al. 1990). More recently, Beare et al. (1994a) and Golchin et al. (1994) proposed that particulate organic matter (POM) provides the nucleus for aggregate formation and the microbial colonization of the POM supplies

substrates for the stabilization of aggregates. Since organic matter contributes to the stability of soil aggregates, it can be expected to decrease aggregate turnover and lead to "self-protection" (Angers and Chenu, 1998; Balesdent et al. 2000).

1.1 Objectives

While many studies have observed differences in organic matter content and organic matter dynamics in differing soils and under differing management, few have made direct links between the observed organic matter dynamics and the dynamics of soil aggregates. The objectives of the current work were:

1. to observe the dynamics of the active organic carbon as measured by relative rates of respiration in two contrasting soils, and
2. to relate the observed organic matter dynamics to soil aggregate dynamics as previously reported.

The hypothesis to be tested is that a soil with rapid organic matter dynamics will also demonstrate rapid soil aggregate dynamics.

2.0 Materials and Methods

2.1 Experimental Field Sites

The experiment was conducted over the 1998 and 1999 growing seasons on long-term plots established in 1983 at the Ellerslie (53° 25'N, 113° 33'W) and Breton (53° 07'N, 114° 28'W) research stations (Solberg et al. 1997) as reported in Chapter 2. Soil properties at the two sites are reported in Table 6-1. The use of a Black Chernozem, Malmo series (Haplocryoll) at Ellerslie, and a Gray Luvisol, Breton series (Haplocryalf) at Breton permitted comparisons between soils with contrasting organic C contents and contrasting organic C dynamics (Dinwoodie and Juma 1988), but are located close enough together to be subject to similar climatic conditions (Solberg et al. 1997). At each site, only the treatments consisting of annual N additions of 56 kg ha^{-1}, with (T8) and without (T10) straw addition were used in the current experiment (Chapter 4).

Details of the ceramic tracer sphere characterization and application in the field plots are reported in detail in Chapter 4. Soil samples were taken by core sampler to a depth of 15

cm every three weeks beginning approximately 7 days after tillage and returned to the laboratory for analyses. Gravimetric water content was determined by overnight oven drying of ~10 g samples at 105°C. Separate sub-samples were also taken and used to determine soil respiration, microbial biomass C, water-stable aggregate size distribution, and tracer contents.

2.2 Soil biochemical analyses

2.2.1 Total soil organic C

Total soil organic C was determined on air-dried, ground samples by dry combustion using a Carlo-Erba NA 1500 elemental analyzer (Milan, Italy) after removal of carbonates with the addition of HCl.

2.2.2 Soil respiration

To determine soil respiration, 25 g (dry basis) of field moist soil were brought to 60% of WFP and incubated for 10 days in 100 mL beakers contained in 2 L canning jars. The lids of the jars were drilled and a septum inserted for gas sampling. On alternate days, CO_2 was measured every six hours by a Varian 3400 gas chromatograph equipped with a methanizer and flame ionization detector (FID) for detection, and a stream selector valve for handling multiple samples. The GC was controlled by a PC running Star Workstation v.5 control software (Varian Inc., Mississauga ON).

2.2.3 Soil microbial biomass C

Microbial biomass C was determined by the chloroform fumigation direct extraction method (Voroney et al. 1993). Essentially, 25 g field-moist samples were fumigated overnight with chloroform and subsequently extracted with 50 mL of 0.5M K_2SO_4. Non-fumigated control samples were also extracted. Soluble carbon in the K_2SO_4 extracts was measured using an Astro 2001 System II soluble carbon analyzer (Astro, League City TX). Microbial biomass C was determined using the equation:

$$MBC = \frac{C_f - C_{nf}}{k_{ec}} \qquad (18)$$

where C_f and C_{nf} are the C measured in the fumigated and non-fumigated samples, respectively and k_{ec} is the extraction coefficient (0.25; Voroney et al. 1993).

2.3 Soil physical analyses

Procedures for determining the water-stable aggregate size distribution and tracer sphere content of separated aggregate size classes are reported in detail in Chapter 4. In general, a 40 g air-dry sub-sample was placed on the top of a sieve stack for 2 min for rapid wetting and slaking, then wet sieved for 10 min. The soil retained on each sieve was oven dried at 105°C overnight, weighed, and prepared for tracer content analysis by INAA.

Distributions of soil aggregates or tracer sphere Dy in the size classes are reported using the mean-weight diameter (MWD) as an integrated representation. The formula used to calculate MWD is:

$$MWD = \sum_{i=1}^{n} x_i W_i \qquad (19)$$

where x_i is the mean diameter of the size fraction and W_i is the weight proportion of soil or tracer sphere Dy retained in the fraction.

In addition, the results of the physical analyses were previously used in a model of macroaggregate dynamics (Chapter 5). The model yielded first-order kinetic parameters that can be used to compare the rate of aggregate turnover in each of the two soils used in the experiment.

2.4 Statistical analyses

The biochemical data were analysed by univariate ANOVA as a split-plot design with sampling date as the split, and the selection of appropriate error and interaction terms (details available in Chapter 4). The condition of independence of within-subject observations was probably not violated because the samples were taken three weeks apart, when several physical and biological processes may occur to change the condition of the soil. Statistical analyses were performed using PROC GLM in SAS/STAT and a value of 5% was selected as the level of significance for all tests, unless otherwise noted.

3.0 Results

3.1 Soil physical analyses

Results of the wet sieving and tracer content analyses are previously reported in detail in Chapter 4. The results showed a cyclical pattern of soil aggregation (Figure 4-2) and rapid incorporation of tracer spheres into macroaggregates (Figure 4-3). The compartmental model of soil aggregate dynamics developed in Chapter 5 yielded mean residence times for the Breton soil two to three times shorter than those for the Malmo soil (Table 5-1). The results suggest that gross aggregate turnover in the Breton soil is more rapid than in the Malmo soil.

3.2 Soil biochemical analyses

Over the two growing seasons, a larger amount of CO_2 is respired from the Malmo soil than the Breton soil (Figure 6-1). The application of straw did not appear to have a significant effect on soil respiration in samples from Breton ($p = 0.268$), but did significantly increase respiration in samples from Malmo soil ($p = 0.003$). While the statistical significance is mixed, the general trend at both sites was for increased respiration in samples from plots with added straw versus those without.

The total organic C content was higher in Malmo samples (60.9 g C kg^{-1} soil) than in Breton samples (13.1 g C kg^{-1} soil). When expressed as a proportion of total soil organic C, samples from Ellerslie respired a much lower proportion compared to Breton samples (Figure 6-2).

Microbial biomass C was higher in Malmo soil compared to Breton (Table 6-2), and straw addition did not produce a significant difference at either site ($p = 0.623$ for Malmo, and 0.408 for Breton). When respiration is expressed normalized to microbial biomass C (Figure 6-3), the samples from Breton appear to have a more activate biomass, but no consistent trends are observed.

4.0 Discussion

4.1 Active organic matter dynamics

Dinwoodie and Juma (1988) used a 10-day laboratory incubation for measuring soil respiration in a study comparing organic C cycling in Black Chernozems and Gray Luvisols. The respiration measured over this period represents a pool of biologically active C in the soil that is not sequestered or physically protected in aggregates.

The soil respiration data in Figure 6-1 shows a higher amount of respired C in the Malmo soil compared to the Breton soil. However when expressed on a per-gram of organic C basis (Figure 6-2), the Breton soil respired a much larger proportion of the organic C in the soil, suggesting that a greater proportion of the C remains unprotected. Both the low total soil C measured and the high relative rate of respiration suggest that the Breton soil retains only a small proportion of its annual C inputs. Based on the hypothesis presented by Six et al. (1998) suggesting that rapid aggregate turnover contributes to organic matter losses, we would expect to observe more rapid aggregate turnover in the Breton soil compared to the Malmo soil.

4.2 Linking organic matter dynamics to aggregate dynamics

Studies performed to compare the C content in conventional- versus no-till soils have suggested that the increased disruption of aggregates associated with tillage results in the loss of organic C (e.g. Beare et al. 1994). It has also been suggested that a rapid aggregate turnover would result in a loss of particulate C (Six et al. 1998). The biochemical data and physical data from this field study support these findings. While both soils in this experiment were under tillage, the original hypothesis was that a rapid organic C turnover and low C content would be indicative of a high rate of aggregate turnover. The Breton soil respired a greater proportion of soil organic C and showed more rapid aggregate turnover, when compared to the Malmo soil.

Physical and tracer analyses indicate that aggregates in the Breton soil are easily slaked and turnover rapidly (Chapters 4 and 5), which would not provide a stable environment for the physical protection of incoming organic materials. This phenomenon may be attributed to both soil organic C and clay contents, which are both contributors to stable

soil aggregation (Kay 1998). While the aggregates in the Malmo soil were more stable (higher MWD), the kinetic modeling data suggests that macroaggregates in the Malmo soil have a residence time of only a few weeks (Chapter 5). If the process of organic C sequestration requires the occlusion of organic materials in aggregates as an initial step, there must be a means by which the organic materials enter the aggregate. Therefore, the periodic formation of new aggregates, i.e. aggregate turnover, likely provides an opportunity for not only the loss, but also the storage of organic C. This coupled with the high stability of the formed aggregates in the Malmo soil suggests that aggregate turnover provides the opportunity for the physical protection of incoming organic materials and its subsequent stabilization by chemical or physical sorption mechanisms, as reflected in the high organic C content and comparatively low rate of respiration. The relationship between soil aggregate turnover and organic C dynamics in the two soils observed in this experiment is perhaps the first direct evidence for the "self-protection" of organic matter proposed by Angers and Chenu (1998) and Balesdent et al. (2000), which suggests that the protection of organic matter in soil is enhanced in soils with higher organic matter content.

Puget et al. (1996) observed aggregate enrichment by relatively young organic matter and concluded that the organic matter contributed to aggregate stability such that only aggregates enriched in organic matter can resist slaking and the wet-sieving process. In addition to increased stability, organic matter enrichment may lead to increased aggregate resiliency (Kay 1998). Molope et al. (1987) suggest that aggregate disruption may be countered by a subsequent but transient increase in stability due to a flush in microbial activity after disruption. The physical protection of organic matter attributable to aggregate stability and resiliency promotes the long-term retention of organic matter in soil by increasing the contact time of organic matter with reactive surfaces such as clay or other organic matter, which increases the opportunity for chemical or physical sorption.

In a soil with lower organic C content, such as Breton, aggregates may lack resiliency such that the recovery from the disruption caused by tillage is insufficient to occlude organic materials resulting in higher relative rates of respiration. In a soil with higher organic matter content, aggregates are sufficiently resilient that after tillage, aggregates

are reformed and restabilized, and therefore can occlude and protect organic materials. Therefore, the self-protection of organic matter in soils is related to aggregate turnover. The increased aggregate stability afforded by increased soil organic matter content reduces aggregate turnover, which in turn increases the protection of the organic matter occluded within the aggregate. In addition, when aggregate turnover is increased, high soil organic matter content promotes the re-formation of stable aggregates that continue to occlude organic materials and protect them from mineralization.

5.0 Conclusion

Our results showed that the Breton soil not only contained less organic matter when compared to the Malmo soil from Ellerslie, but also respired a greater proportion of the soil organic C. In addition, the higher organic matter turnover in the Breton soil was reflected in previous measurements of more rapid aggregate turnover, when compared to the Malmo soil. While the lack of soil organic matter protection in the Breton soil may be attributed to the increased turnover of aggregates, observations of aggregate turnover in the soil from Ellerslie, with high organic matter content, suggests that aggregate turnover may also provide the opportunity for the occlusion of organic materials in aggregates and thus lower relative soil respiration. These results support the hypothesized feedback process of self-protection of organic matter proposed in the literature, which suggests that organic matter protection is enhanced in soils with high organic matter contents. The mechanism proposed for self-protection is a reduced aggregate turnover rate due to increased aggregate stability, which increases organic matter contact with reactive surfaces and provides the opportunity for long-term stabilization.

Table 6-1. Selected properties of surface layer (0-15 cm) of field soils used in experiment.

	Ellerslie	Breton
Classification	Black Chernozem (Malmo series) (Haplocryoll)	Gray Luvisol (Breton series) (Haplocryalf)
Texture (clay content, g kg^{-1})	360	220
Total Organic C (g kg^{-1})	60.9	13.1
Bulk Density (g cm^{-3})	1.1	1.4
Water-stable Aggregate Mean Weight Diameter (mm) †	2.42 ± 0.54	1.46 ± 0.37

† Mean ± SD, from all measurements made in 1998

Table 6-2. Microbial biomass C from 1998 subplots (mg C kg^{-1} OD soil) [†].

	Days after tracer addition										
	1998							1999			
	31	51	72	93	114	359	380	401	422	443	466
Malmo + straw	1438 ± 158	987 ± 79	1415 ± 87	1237 ± 117	1416 ± 147	673 ± 278	1196 ± 101	1159 ± 151	528 ± 262	754 ± 278	1244 ± 108
Malmo - straw	1280 ± 72	853 ± 38	1091 ± 117	1219 ± 70	1267 ± 116	646 ± 137	1144 ± 93	1112 ± 352	595 ± 104	631 ± 272	1112 ± 86
Breton + straw	740 ± 67	345 ± 18	650 ± 45	763 ± 77	706 ± 79	348 ± 94	609 ± 82	573 ± 117	427 ± 234	557 ± 101	783 ± 72
Breton - straw	690 ± 110	363 ± 69	641 ± 59	741 ± 110	684 ± 74	326 ± 5	522 ± 90	731 ± 38	412 ± 85	543 ± 172	739 ± 90

[†] Mean ± SD, n= 4 replicates

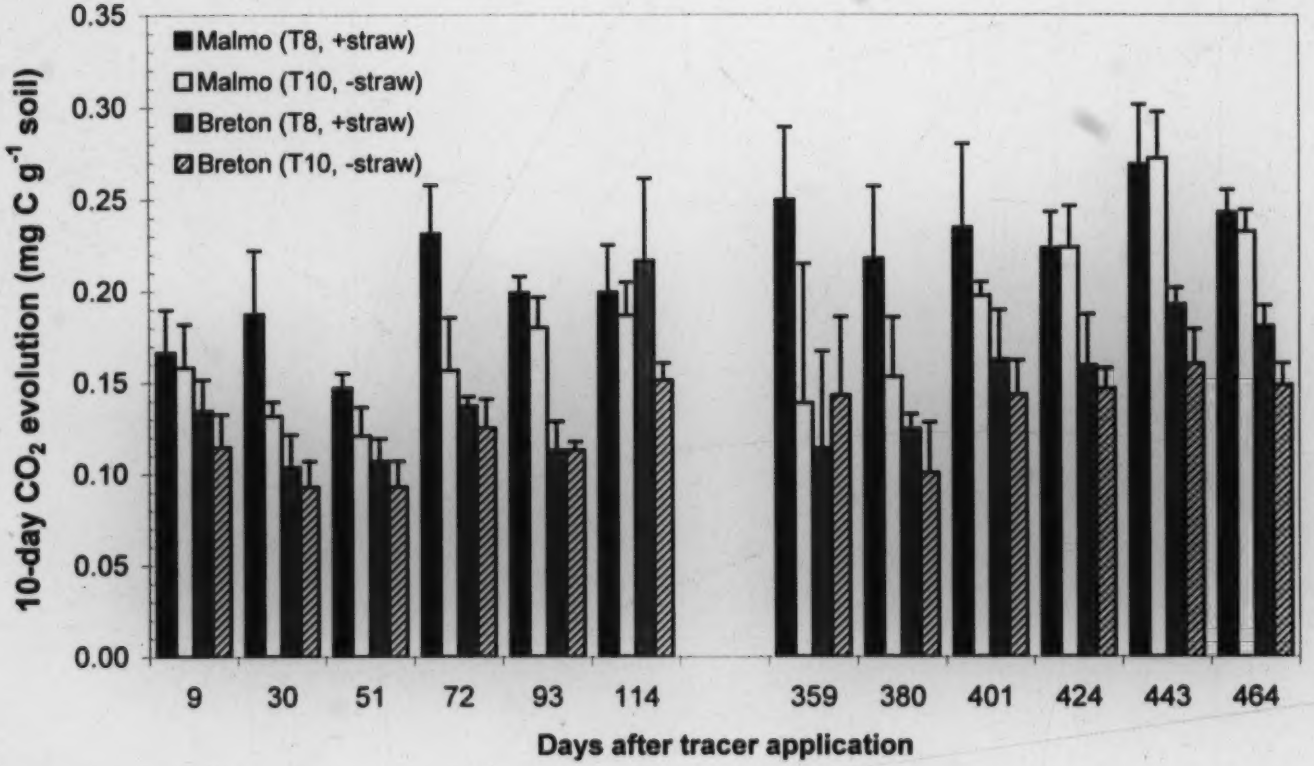

Figure 6-1. Carbon dioxide evolution in 10-day laboratory incubations on a per gram of soil basis.

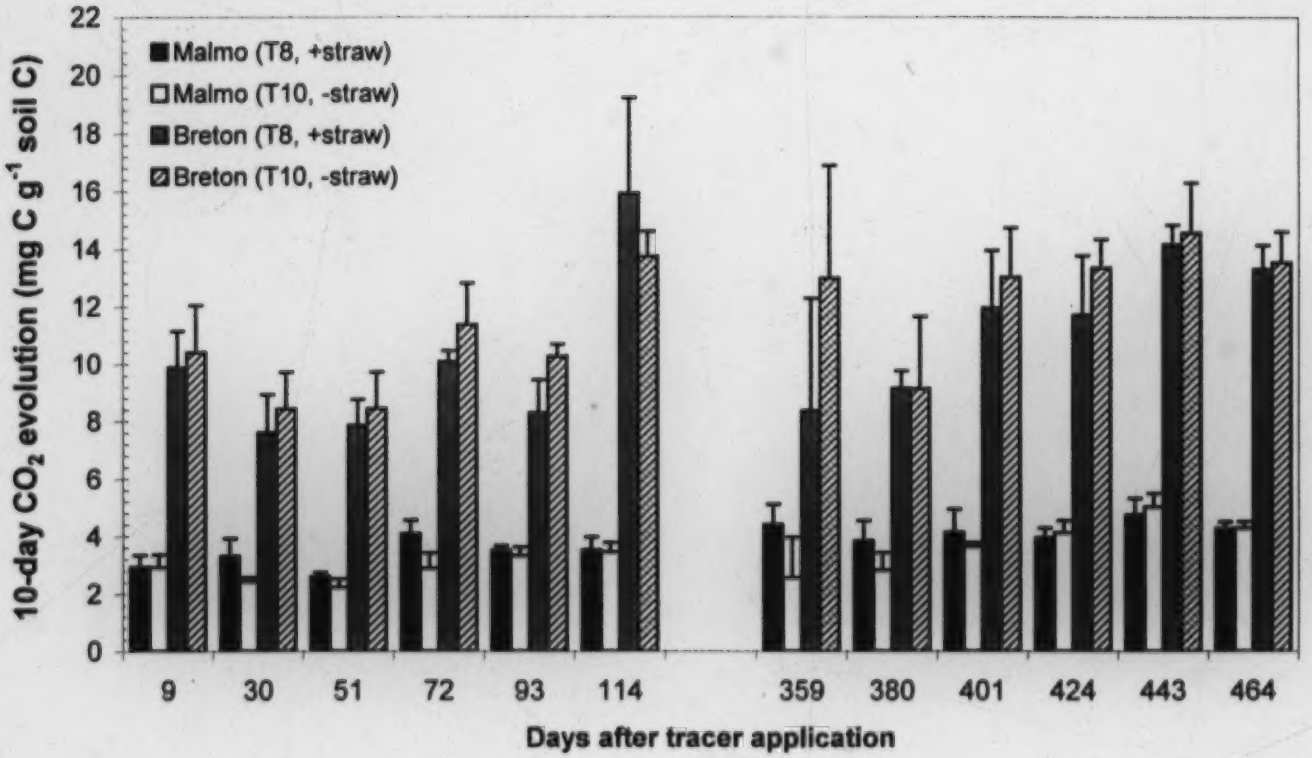

Figure 6-2. Carbon dioxide evolution in 10-day laboratory incubations on a per gram of organic carbon basis.

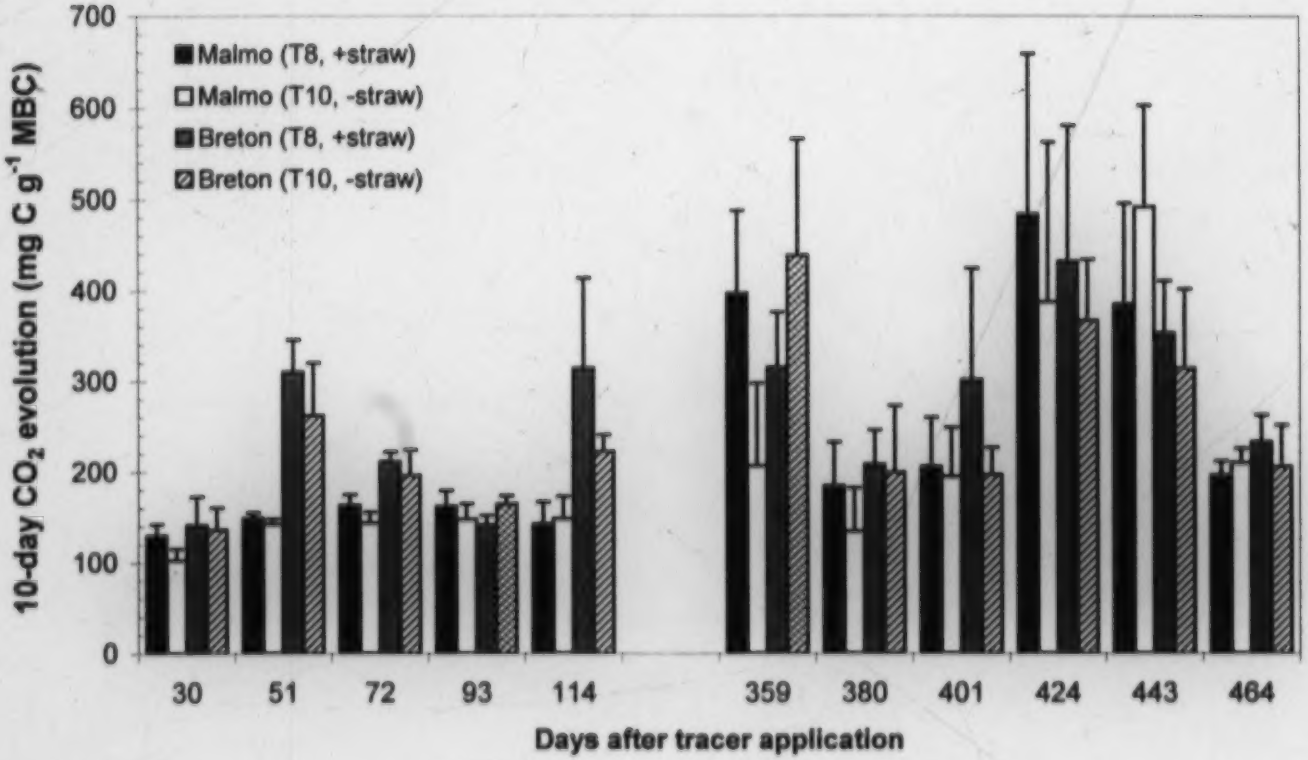

Figure 6-3. Carbon dioxide evolution in 10-day laboratory incubations on a per gram of microbial biomass carbon basis.

References

Angers D.A. and C. Chenu. 1998. Dynamics of soil aggregation and C sequestration. *In* R. Lal et al. (ed.) Soil processes and the carbon cycle. CRC Press, Boca Raton FL.

Angers D.A., Pesant A., and J. Vigneux. 1992. Early cropping-induced changes in soil aggregation, organic matter and microbial biomass. Soil Sci. Soc. Am. J. 56:115-119.

Angers D.A., Samson N. and A. Légère. 1993. Early changes in water-stable aggregation induced by rotation and tillage in a soil under barley production. Can. J. Soil Sci. 73:51-59.

Balesdent J. Chenu C. and M. Balabane. 2000. Relationship of soil organic matter to physical protection and tillage. Soil Till. Res. 53:215-230.

Beare M.H., Hendrix P.F. and D.C. Coleman. 1994a. Water-stable aggregates and organic matter fractions in conventional- and no-tillage soils. Soil Sci. Soc. Amer. J. 58:777-786.

Beare M.H., Cabrera M.L., Hendrix P.F. and D.C. Coleman. 1994b. Aggregate-protected and unprotected organic matter pools in conventional- and no-tillage soils. Soil Sci. Soc. Amer. J. 58:787-795.

Besnard E., Chenu C., Balesdent J., Puget P. and D. Arrouays. 1996. Fate of particulate organic matter in soil aggregates during cultivation. Eur. J. Soil Sci. 47:495-503.

Capriel P., Beck T., Borchert H. and P. Härter. 1990. Relationship between soil aliphatic fraction extracted with supercritical hexane, soil microbial biomass and soil aggregate stability. Soil Sci. Soc. Am. J. 54:415-420.

Dinwoodie, G.D. and N.G. Juma. 1988. Allocation and microbial utilization of C in two soils cropped to barley. Can. J. Soil Sci. 68:495-505.

Golchin A., Oades J.M., Skjemstad J.O. and P. Clarke. 1994. Soil structure and carbon cycling. Aust. J. Soil Res. 32:1043-1068.

Haynes R.J. and R.S. Swift. 1990. Stability of soil aggregates in relation to organic constituents and soil water content. J. Soil Sci. 41:73-83.

Kay B.D. 1998. Soil structure and organic carbon: A review. *In* R. Lal et al. (ed.) Soil processes and the carbon cycle. CRC Press, Boca Raton FL.

Molope M.B., Grieve I.C. and E.R. Page. 1987. Contributions by fungi and bacteria to aggregate stability of cultivated soils. J. Soil Sci. 38:71-77.

Puget P., Besnard E. and C. Chenu. 1996. Une méthode de fractionnement des matières organiques particulaires des sols en fonction de leur localization dans les agrégats. C.R. Acad. Sci. Paris. 322:965-972.

Six J., Elliott E.T. and K. Paustian. 1999. Aggregate and soil organic matter dynamics under conventional and no-tillage systems. Soil Sci. Soc. Am. J. 63:1350-1358.

Six J., Elliott E.T., Paustian K. and J.W. Doran. 1998. Aggregation and soil organic matter accumulation in cultivated and native grassland soils. Soil Sci. Soc. Am. J. 62:1367-1377.

Solberg E.D., Nyborg M., Izaurralde R.C., Malhi S.S., Janzen H.H. and M. Molina-Ayala. 1997. Carbon storage in soils under continuous cereal grain cropping: N fertilizer and straw. *In* R. Lal et al. (eds.) Management of Carbon Sequestration in Soil. CRC Press, Boca Raton FL.

Voroney, R.P., Winter, J.C. and R.P. Beyaert. 1993. Soil microbial biomass C and N. *In* M.R. Carter (ed.) Soil Sampling and methods of Analysis. Canadian Society of Soil Science, Lewis Publishers, Boca Raton FL.

Chapter 7:

Soil aggregate dynamics and the retention of organic matter in laboratory-incubated soil with differing simulated tillage frequencies

1.0 Introduction

The position of soil organic matter within the soil matrix is an important determinant of its fate (Elliott et al. 1996; Christensen 1996). Several researchers have devised methods to fractionate particulate organic matter based on its location with respect to soil aggregates, outside of aggregates (free POM), or occluded within aggregates (intraaggregate POM) (e.g. Golchin et al. 1994a; Puget et al. 1996). Golchin et al. (1994a, b) proposed that free and intraaggregate POM differ in composition, stability and dynamics, leading to the concept of "physical protection".

To a large degree, the existence of the physical protection of organic matter in soil aggregates has been inferred from experiments involving aggregate disruption. Several experiments measured increases in soil respiration after aggregate disruption by crushing (Craswell and Waring, 1972; Elliott, 1986) or by ultrasonic dispersion (Gregorich et al. 1989). Beare et al. (1994) supported the concept of physical protection by defining aggregate-protected C as the difference between C mineralized in intact aggregates and crushed aggregates. Balesdent et al. (2000) reviewed the crushing experiments and concluded that macroaggregates can protect against microbial decomposition, that the ability to protect increases with SOM and clay contents, and that a significant amount of SOM is also physically protected in microaggregates.

Recent studies have attempted to extend these observations to the field scale by measuring short-term increases in soil respiration after the physical disruption caused by tillage (e.g. Ellert and Janzen, 1999; Rochette and Angers, 1999). Both studies concluded that the short-term (< 24 h) flush of CO_2-evolution was primarily due to degassing of soil CO_2 already present. However, Rochette and Angers (1999) also found an extended period (80 d) following tillage where CO_2 evolution remained consistently higher. These differences were attributed to different decomposition rates of SOM rather than the

release of protected organic matter, as the study found emissions were strongly influenced by climatic conditions, which are known to be a principle mechanism by which tillage alters the decomposition of organic matter (Balesdent et al. 2000).

In general, long-term soil cultivation increases organic matter turnover, which Six et al. (1998) attributed to differences in the amount of aggregation and aggregate turnover. Six et al. (1999) summarized these trends in a conceptual model of soil aggregate dynamics for conventional- and no-till soils, where no-till soil aggregates cycle slowly through a "decomposition loop" while aggregates in tilled soils cycle more rapidly in a "cultivation loop". Our results showed a cyclical pattern of soil aggregation reset by the over-winter period and spring tillage (Chapter 4), which support the concept of aggregation loops. However, none of the studies cited above include observations of aggregate turnover along with soil respiration in an attempt to confirm the role of tillage in the disruption of physical protection. Our results showed rapid tracer incorporation into stable soil aggregates shortly after tillage, suggesting that tillage may promote the formation of new aggregates (Chapter 4). The relationship between soil aggregate turnover and the physical protection of organic matter needs to be further examined under controlled conditions.

1.1 Objectives

It is well accepted that aggregate dynamics are a significant control on the dynamics of organic C and that aggregate dynamics differ under cultivated and uncultivated (or no-till) conditions. The goal of this experiment was to observe aggregate dynamics under differing regimes of simulated tillage energy inputs and relate these to organic matter dynamics. The experiment will specifically examine the mechanism of "physical protection" by inducing a controlled rate of aggregate turnover. The hypotheses to be tested are:

1) that soils with increasing frequencies of simulated tillage will mineralize increasing amounts of added particulate organic matter, and
2) tracer spheres will be more rapidly incorporated in soils under higher simulated tillage frequencies.

2.0 Materials and Methods

The experiment consisted of an eight-week laboratory incubation with three treatments involving differing frequencies of simulated tillage energy inputs. Soil used in the experiment was surface soil (0-10 cm) collected by spade from the Breton series (Orthic Gray Luvisol) at the Breton Research Station (53° 07'N, 114° 28'W) and was kept in cold storage until the initiation of the experiment. Characteristic soil properties are reported previously in Chapter 4.

The experiment consisted of three applied treatments:

1) no applied tillage energy over the 8-week incubation period (no-till),
2) tillage at the initiation, midpoint, and end of the experiment (3x tillage), and
3) tillage performed every second week of the experiment (5x tillage).

Multiple samples were used for destructive sampling. For each sampling period, four replicate samples each consisted of 80 g moist soil, previously wetted to 60% WFP to maximize aerobic microbial activity, to which 100 mg of finely ground corn residues (POM) was added to provide a substrate for microbes and nuclei for aggregate formation. Tracer spheres (75 mg) from the small fraction of the 1998 full-scale batch were sieved to 125-250 μm and added to samples. Characteristic sphere properties are reported previously in Chapter 2. The soil, plant residues and tracer spheres were gently mixed in 125 mL Nalgene bottles to initiate the experiment. Samples under treatments 2 and 3 were then "tilled", and all samples were left for 24 h before initial analyses were performed. Samples were incubated in 2 L canning jars at room temperature (22 °C), in the dark.

2.1 Simulation of tillage energy

The process of tillage involves both combining and separating processes. The mixing of soil particles and aggregates can bring them together and combine them into larger aggregates, and conversely the application of shear forces may weaken or break aggregates apart. Soil tillage was simulated using an electric "egg-beater"-style hand mixer. This type of mixing best simulates rototillage, but may also simulate the action of

soil fauna. The mixer has a 100 W motor, was fitted with only one of the two mixing blades, and was used at the lowest of the five speed settings. The soil sample was placed in a 400 mL beaker and mixed in a circular fashion to ensure the soil was mixed homogeneously.

An initial trial was performed to examine the disruptive energy of the mixing. Soil samples were mixed for 10 s, 30 s, 1 min, 3 min and resulted in 14%, 34%, 43%, and 70% decreases in aggregate MWD. A mixing time of 15 s was subsequently selected for the experiment to prevent the extreme disruption of aggregates during the simulated tillage event.

2.2 Soil respiration and stable C isotope ratio of CO_2

Microbial activity and the "physical protection" of the added particulate organic matter were determined by measuring soil respiration on soil samples with and without POM amendment. Use of the ground corn residue POM amendment exploited variations of ^{13}C natural isotope abundance by adding C4-derived POM to a soil dominated by C3-derived organic matter. Soil samples were incubated in 2 L canning jars with an alkali trap containing 25 mL of 0.25 M NaOH. The alkali traps were used to measure both total CO_2 evolution, and the stable isotopic ratio ($\delta^{13}CO_2$) using a method described by Harris et al. (1997). After a period of incubation, the alkali solution was used to measure the total CO_2-evolution by precipitating the Na_2CO_3 to $SrCO_3$ using 4 mL of 1 *M* $SrCl_2$ and back-titrating the excess NaOH with 0.25 M HCl and 75 μL of phenolphthalein as the indicator. The resulting precipitate was washed with water to remove any Cl^- (which would otherwise rapidly consume the halogen scrubber of the preparation system on the mass spectrometer) by centrifugation (twice at 3000 rpm for 10 min), and oven dried overnight at 70°C to produce solid $SrCO_3$ that could be analyzed for $\delta^{13}C$ by mass spectrometry. Samples were analyzed for $\delta^{13}C$ using an NA1500 Carlo Erba Strumentazione N/C preparation system interfaced to a SIRA10 VG Isogas Mass Spectrometer. Oxalic acid was used as a working standard by calibration against a NIST NBS19 limestone primary standard.

Total CO_2 analyses were performed twice weekly over the course of the experiment. In addition, short-term CO_2-evolution was measured after the 24 h period following a tillage treatment. After the first tillage, $\delta^{13}C$ analysis was performed on the 24 h sample but subsequently on 3-day samples in order to recover enough $SrCO_3$ for analysis. Corrections for dilution by atmospheric CO_2 in the incubation jars were made using the following equation:

$$\delta^{13}CO_{2\ measured} = f \cdot \delta^{13}CO_{2\ atm} + (1-f) \cdot \delta^{13}CO_{2\ sample} \quad (20)$$

such that,

$$\delta^{13}CO_{2\ sample} = \frac{\delta^{13}CO_{2\ measured} - f \cdot \delta^{13}CO_{2\ atm}}{(1-f)} \quad (21)$$

where f is the fraction of the sample value contributed by atmospheric CO_2 which is calculated using a background concentration of 450 $\mu L\ L^{-1}$ CO_2 in the incubation jars. $\delta^{13}CO_{2\ measured}$ is the measured isotopic ratio, $\delta^{13}CO_{2\ sample}$ is the undiluted isotopic ratio of microbial respiration, and the $\delta^{13}CO_{2\ atm}$ is the isotopic ratio of atmospheric CO_2, which was set to -10‰ (Boutton, 1991).

$\delta^{13}C$ analyses were also performed once on reference samples of non-amended soil and the corn residue POM used as the amendment. The fraction of CO_2-evolution contributed by the mineralization of the added POM was calculated using:

$$\delta^{13}CO_{2\ measured} = f \cdot \delta^{13}CO_{2\ POM} + (1-f) \cdot \delta^{13}CO_{2\ SOM} \quad (22)$$

such that

$$f = \frac{\delta^{13}CO_{2\ measured} - \delta^{13}CO_{2\ SOM}}{\delta^{13}CO_{2\ POM} - \delta^{13}CO_{2\ SOM}} \quad (23)$$

Under conditions where isotopic fractionation is zero:

$$f = \frac{\delta^{13}CO_{2\ measured} - \delta^{13}CO_{2\ SOM}}{\delta^{13}C_{POM} - \delta^{13}CO_{2\ SOM}} \quad (24)$$

where $\delta^{13}C_{POM}$ is the isotopic ratio of the added POM and $\delta^{13}CO_{2\,SOM}$ is the isotopic ratio of CO_2 collected from the mineralization of native soil organic matter, determined from samples without added POM.

2.3 Water-stable aggregation

POM-amended soil samples were destructively sampled every other week for analysis. Soils were stored moist and cold (4 °C) until they could be wet-sieved (usually 2-3 days). Water stable aggregate size distributions and aggregate mean weight diameter (MWD) were determined on moist samples using the wet sieving protocol described in previous chapters.

2.4 Tracer content

After wet sieving, individual aggregate size fractions were transferred to 7 mL vials, the volume was adjusted with white granular sugar, and analysed for Dy using the INAA protocol described in previous chapters. The irradiation time was reduced from 240 s to 180 s due to higher concentrations of manganese in the soil, which interferes with Dy quantification. Results of the tracer Dy content of aggregate size fractions were used to calculate sample Dy MWD values as described in previous chapters.

2.5 Stable isotope ratios of C in aggregate fractions

The >1 mm water-stable aggregate fractions from the final sampling period were pooled and analysed for $\delta^{13}C$. The pooled >1 mm aggregates were homogenized and a sub-sample was analyzed for $\delta^{13}C$ using the mass spectrometry method outlined in Section 2.2. After the analysis, the light fraction organic matter (LF) of the remainder of the pooled aggregate samples was extracted using NaI (Gregorich and Ellert 1993). Samples were shaken in 50 mL of NaI adjusted to a density of 1.8 g cm^{-3} for a half-hour and allowed to settle overnight. The floating LF material was removed by suction onto a glass-fibre filter, rinsed using 0.01 M $CaCl_2$, oven-dried and weighed. The LF material was then analyzed for $\delta^{13}C$ using the same method as the whole aggregate samples. Non-amended soil samples were also included in the analyses.

3.0 Results

3.1 Soil respiration and stable C isotope ratio of CO_2

Additions of POM significantly increased soil respiration in the early part of the experiment (Figure 7-1, 7-2). However, the rate of CO_2 evolution in amended samples approached that of non-amended samples after approximately two weeks of incubation (Figure 7-1). Although the peaks were small, the tilled samples showed a flush of soil respiration shortly after simulated tillage (Figure 7-1). The flush occurred in both POM-amended and non-amended samples, suggesting that the simulated tillage may have temporarily increased the availability of both the added POM and other previously protected organic materials. Cumulative CO_2 data show that the treatment without simulated tillage evolved the most CO_2 while other treatments show slightly lower total amounts of CO_2 evolved (Figure 7-2).

Correction of $\delta^{13}CO_2$ data for atmospheric CO_2 did not significantly alter the measured values (data not shown) because the contribution of atmospheric CO_2 to the amount trapped in the incubation jars represented approximately 0.5%. In the early part of the experiment, $\delta^{13}C$ of trapped CO_2 was closer to values measured for the added corn POM than the native soil organic matter (Table 7-1), such that across all treatments 57% of the CO_2 evolved was contributed by the mineralization of the added POM (Table 7-2). As the experiment progressed, $\delta^{13}CO_2$ approached values similar to the CO_2 respired from non-amended Breton soil (Table 7-1). At the end of the experiment, the added POM contributed less than 10% to the soil respiration (Table 7-2). The results suggest that the labile portion of the added POM was completely decomposed in all treatments.

3.2 Water-stable aggregation and tracer content

Soil aggregate MWD showed a significant response to both simulated tillage and the supply of labile organic matter (Figure 7-4). Samples with only initial tillage showed increased aggregation through the early part of the experiment, but decreased slightly as the added labile organic matter was consumed. Samples subjected to more frequent simulated tillage showed decreased, but more dynamic aggregation. Simulated tillage significantly reduced aggregate MWD at each event (before vs. after), however

aggregates were rapidly reformed and stabilized in the interim periods between tillage events.

Higher tracer Dy MWD values for frequently tilled samples versus samples with only initial mixing show that more rapid aggregate turnover associated with frequent simulated tillage increased the incorporation of tracer spheres into newly formed soil aggregates (Figure 7-5). Similar to the aggregation data, tracer incorporation was highest after the first two weeks of the experiment when the decomposition of the added POM provided a large supply of labile microbial products that contribute to the stabilization of aggregates. The reduced Dy MWD values after tillage suggest that tracers were released when aggregates were disrupted. While the disruption of aggregates after simulated tillage, as evidenced by reduced soil aggregate MWD (Figure 7-4) reduces the opportunity for tracers to be found in larger sieve fractions, the tracer Dy enrichment of macroaggregates is significant higher in the frequently tilled treatments (Figure 7-6). The results clearly show that the mixing of soil and tracer spheres by simulated tillage formed new aggregates that included incorporated tracers.

3.3 Stable isotope ratios of C in aggregate fractions

No significant differences were found in the $\delta^{13}C$ of >1 mm aggregates or the LF contained in the aggregates at the end of the 8-week experiment (Table 7-3). The results suggest that the added POM is no longer detectable because of rapid association with the mineral fraction, or due to dilution by native SOM. Physical protection of the added POM in macroaggregates was not significantly different in any of the treatments. These results concur with the $\delta^{13}C$ analysis of respired CO_2, which showed little contribution by the added POM at the end of the experiment.

4.0 Discussion

4.1 Mineralization of added POM

In addition to contamination by atmospheric CO_2, $\delta^{13}C$ of soil respiration trapped in alkali solutions is subject to fractionation by the soil microbial population (Santruckova et al. 2000) and by differential diffusion of the respired CO_2 through soil (Cerling et al. 1991), sometimes resulting in observations of isotopic depletion of the trapped CO_2

compared to the original substrate (Mary et al. 1992; Schweizer et al. 1999). However, the trapped CO_2 from the non-amended soil samples showed isotopic enrichment, averaging -21.2‰ versus -26.6‰ for the whole soil C (Table 7-1). These results lead us to believe that fractionation may also result from the incomplete precipitation or combustion of calcium or barium carbonates versus strontium carbonates as suggested by Harris et al. (1997).

The rate of soil respiration in POM-amended samples approached that of non-amended samples after two weeks of incubation. In addition, the largest changes in $\delta^{13}CO_2$ occurred during the first two weeks of the incubation, after which the isotopic ratios remained consistently similar to those of non-amended samples. These observations suggest that the labile portion of the added POM was decomposed within the first two weeks of the experiment. For this reason, only the simulated tillage upon the initiation of the experiment had any bearing on the protection or mineralization of the added POM. The divergence of total CO_2 respiration after 3 weeks of incubation, as observed in Figure 7-2, suggests that the native soil organic matter rather than the added POM was affected by subsequent tillage events.

4.2 Retention of SOM under differing frequencies of tillage

Much of what is understood about the physical protection of organic matter is based on increases in soil respiration, and the associated decrease in organic matter content, after the physical disruption of aggregates containing some amount of already "protected" organic material. Balesdent et al. (2000) summarized several studies that demonstrated increases in C mineralization after aggregate disruption by crushing. In cultivated systems, tillage is a significant mechanism by which aggregates are disrupted and several authors have shown decreases in soil aggregate MWD under tillage (e.g. Puget et al. 1995). For this reason, we originally hypothesized that mineralization would increase with increased tillage frequency. The flush of CO_2 observed after simulated tillage appears to support this hypothesis. However, the tilled treatments showed lower total amounts of respiration, which does not support our hypothesis.

The observed flushes in CO_2 after tillage events were not likely due to degassing since this would have occurred during the transfer of the soil from the incubation jar to the mixing beaker and during mixing. The released gasses would not have been captured in the subsequent incubation period. The flushes are likely the results of mineralization of both the added POM and previously protected native soil organic matter because the flushes were observed in both POM-amended and non-amended samples. The sustained elevated respiration after 21 days in the 1x tillage samples may be due to the "priming effect" where the mineralization of native soil organic matter is accelerated by the addition of labile material (Kuzyakov et al. 2000). Jans-Hammermeister et al. (1997) previously observed that a pulsed addition of labile C resulted in increased microbial biomass and increased mineralization of native organic matter, when compared to smaller daily additions. In our experiment, the addition of POM in the 1x tillage treatment simulated a pulsed addition, while the more frequent tillage in the other treatments may have simulated lower and slower additions of labile C. The primary mechanism proposed for the priming effect is the activation and growth of the soil microbial biomass because of the addition of a labile substrate (Kuzyakov et al. 2000). We propose that the added POM residue was rapidly colonized and decomposed without disruption in the 1x tillage treatment, resulting in a larger priming effect. In more frequently mixed treatments, microbial colonization of the added POM may have been disrupted and the contact between the POM and reactive surface may have increased, thereby reducing the availability of the POM and reducing the potential priming effect. In this experiment simulated tillage created new aggregates that occluded the initially free POM and provided short-term protection from decomposition. Conversely, the 1x tillage treatment left the residue consistently unprotected and available for microbial attack resulting in increased mineralization.

Several authors have shown that the association of an organic material with aggregates reduces mineralization. Bartlett and Doner (1988) measured the mineralization of labelled amino acids and found that the substrates incorporated into aggregates were decomposed more slowly. However, the evidence for tillage-enhanced physical protection is limited. Puget et al. (1996) measured proportionally more free-POM in no-

till versus tilled samples, and suggested that organic C was incorporated into aggregates by tillage. The tracer Dy data of this experiment showed that tillage increased the incorporation of tracer spheres, and by extension may have promoted the occlusion of POM. Measurements of decreased soil respiration in tilled versus non-tilled samples support the hypothesis of increased retention of SOM.

Observations of tillage-enhanced organic matter retention, and previous observations of aggregate turnover in two cultivated field soils with contrasting organic matter dynamics (Chapters 4 and 6) lead us to hypothesize that threshold rates of aggregate turnover may exist where organic matter is either protected or released. The sequestration of organic matter in soil requires either the reduction of the extent of mineralization of the incoming material, or a sufficient reduction in the rate of decomposition to extend its lifetime in the soil. Several studies reported in the literature have demonstrated that organic matter occluded in aggregates is mineralized more slowly than organic matter that is not occluded. The relationship between organic matter mineralization and soil aggregate turnover rate differs for incoming organic matter such as crop residues, and for native soil organic matter. The relationships are illustrated conceptually in Figure 7-7.

Incoming organic materials such as crop residues can only be occluded in aggregates when a new aggregate forms around the organic material. This does not require net soil aggregate formation in the soil, but only gross aggregate turnover such that some new aggregates are formed. If the soil aggregate turnover rate is too slow, the incoming organic materials will be rapidly mineralized before the opportunity for occlusion presents itself. Hypothetically, a threshold aggregate turnover rate exists where aggregates turnover rapidly enough to begin occluding organic materials before they are mineralized outside the aggregates, thereby increasing sequestration because of the decrease in mineralization in the occluded state due to increased interaction of the organic matter with reactive surfaces. This first threshold aggregate turnover rate is marked as R_1 in Figure 7-7a. As aggregate turnover increases, an increasing proportion of the organic material will be occluded before it is mineralized, resulting in decreasing mineralization. However, as soil aggregate turnover increases there is an increasing opportunity for the re-exposure of the organic matter. Therefore a second threshold

aggregate turnover rate (R_2) is proposed where the incoming organic matter is no longer occluded for a sufficient period time before re-exposure, reducing the opportunity for interaction with reactive surfaces and increasing the rate of mineralization.

In addition to occluding initially free organic materials, aggregate turnover also exposes previously occluded or otherwise protected soil organic matter making it accessible for mineralization. A second relationship between SOM mineralization and aggregate turnover is proposed for native SOM (Figure 7-7b), as opposed to recently added materials (Figure 7-7a). Without soil aggregate turnover, aggregates provide the maximum protection for organic matter by providing contact with reactive surfaces, a poor (e.g. anaerobic) environment for decomposition, and physical separation between substrates and decomposers in closed pores. Therefore mineralization is at a minimum. As aggregate turnover increases, a threshold aggregate turnover rate (R_3) is proposed where previously protected organic matter begins to be exposed to conditions favourable for decomposition. Mineralization of organic matter continues to increase with increasing soil aggregate turnover rates, until a maximum is reached where aggregation no longer provides any protection for SOM, and mineralization is at a maximum.

There is currently insufficient data to estimate how the mineralization patterns for recently added organic matter and native soil organic matter are related in terms of soil aggregate turnover rate. The absolute aggregate turnover rates represented by R_1, R_2 and R_3 are expected differ between soils and to be a function of soil organic matter and clay contents. In general, it is hypothesized that a soil with an aggregate turnover rate that is: below R_1 will release C, between R_1, R_2 and R_3 will maintain or sequester C, and above R_2 or R_3 will release C.

In addition to the frequency of tillage, a severe limitation in our knowledge of how tillage alters the physical protection of organic matter afforded by aggregates is the lack of quantification of the energy applied to the soil during tillage. The soil MWD data clearly shows that the simulated tillage did not disrupt aggregates beyond an unrecoverable threshold, and did not approach the same degree of disruption as crushing. The applied simulated tillage may not have exposed the protection sites in small macroaggregates and

microaggregates, where a significant portion of organic matter is protected (Gregorich et al. 1989; Jastrow et al. 1996). Tillage under field conditions, where temperature and moisture are variable, may apply a disruptive energy significantly greater or smaller than those simulated in the laboratory.

5.0 Conclusions

An eight-week laboratory experiment showed that more frequent simulated tillage increased the incorporation of tracer spheres and reduced the total amount of CO_2 evolved during the experiment. We suggest that organic matter protection was enhanced through a reduction of the priming effect afforded by the increased aggregate turnover and the formation of new aggregates that occluded added POM thereby reducing its availability for mineralization by the microbial population and increasing its association with reactive surfaces. While they appear contrary to the common observation that cultivation reduces soil aggregation and increases the turnover of organic matter, these results and previous observations of aggregate turnover in cultivated soils with contrasting organic matter contents suggest that for a given soil and environmental conditions, there may be threshold rates of aggregate turnover that will protect rather than release organic C.

Table 7-1. Stable isotope ratio, $\delta^{13}C$ (‰), of reference samples and atmospheric CO_2-corrected soil respired CO_2.

	Week 0	Week 2	Week 4	Week 6	Week 8
Breton soil reference			-26.6322		
POM reference			-12.1314		
Non-amended	-21.16	-21.14	-21.15	-20.96	-21.79
No-till	-15.86	-19.13	-19.81	-20.47	-21.20
3x tillage	-15.98	-18.36	-20.56	-20.03	-21.18
5x tillage	-16.21	-18.74	-20.66	-20.60	-20.85

Table 7-2. Proportion of soil respired CO_2 attributable to the mineralization of added POM (%)

	Week 0	Week 2	Week 4	Week 6	Week 8
No-till	58.7	22.3	14.9	5.6	6.1
3x tillage	57.4	30.8	6.5	10.6	6.3
5x tillage	54.8	26.6	5.4	4.1	9.7

Table 7-3. Stable isotope ratio of C, $\delta^{13}C$ (‰), in the pooled >1 mm aggregate fraction at the end of 8-week incubation.

	> 1 mm aggregates	Light Fraction
Non-amended Breton soil	-25.83	-27.28
1x tillage	-25.74	-25.99
3x tillage	-25.66	-25.40
5x tillage	-25.60	-25.72

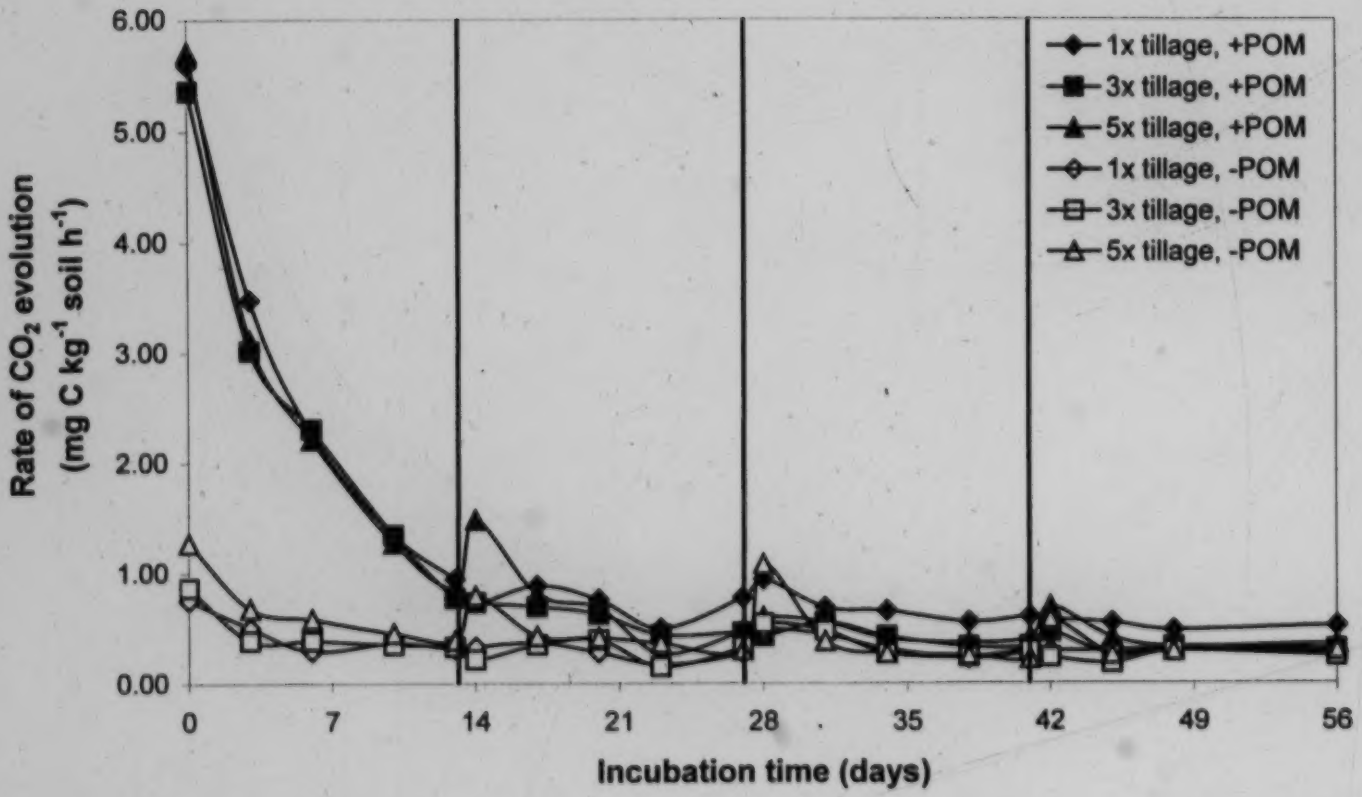

Figure 7-1. Rate of CO_2 evolution from samples incubated under differing tillage frequencies. (Vertical lines represent timing of simulated tillage events.)

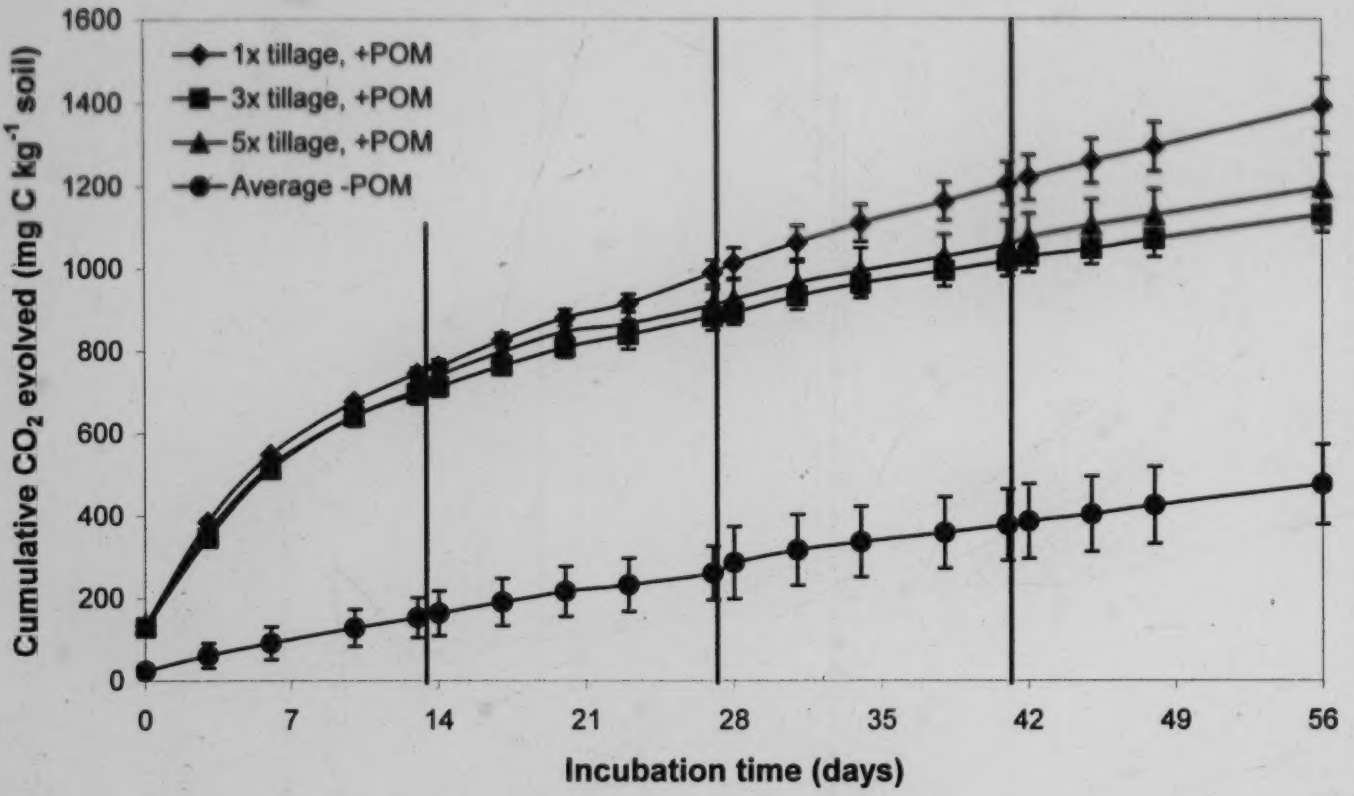

Figure 7-2. Cumulative CO_2 evolved from samples incubated under differing tillage frequencies. (Vertical lines represent timing of simulated tillage events.)

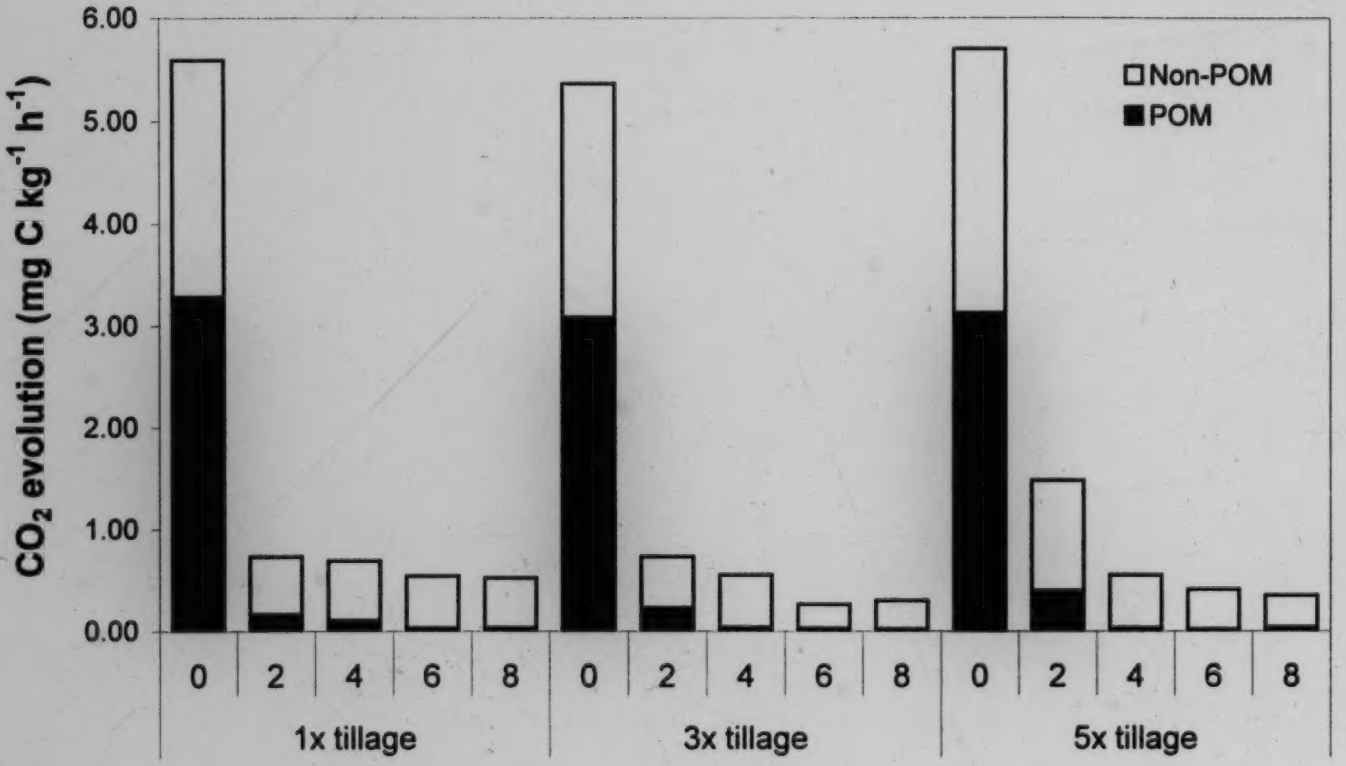

Figure 7-3 Soil respiration from POM and non-POM sources of organic C.

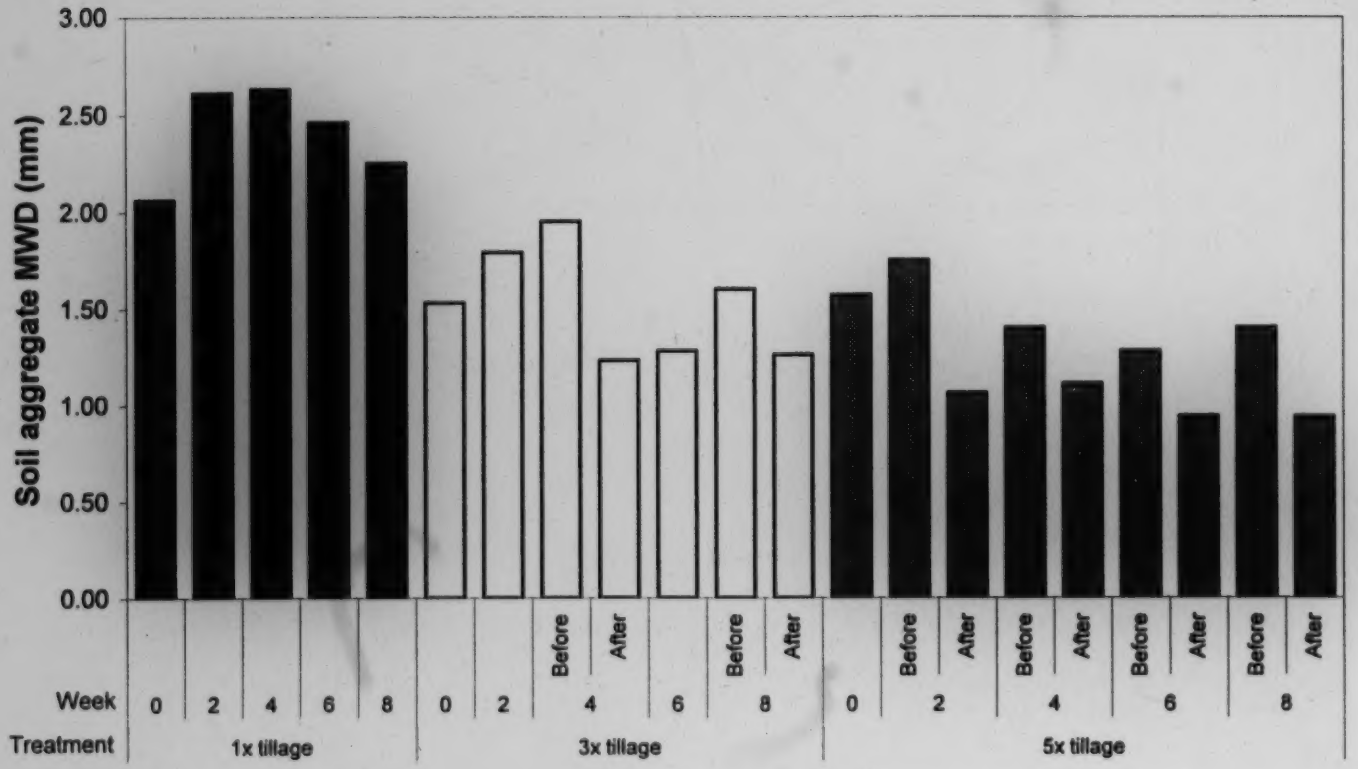

Figure 7-4. Water-stable soil aggregate mean weight diameters.

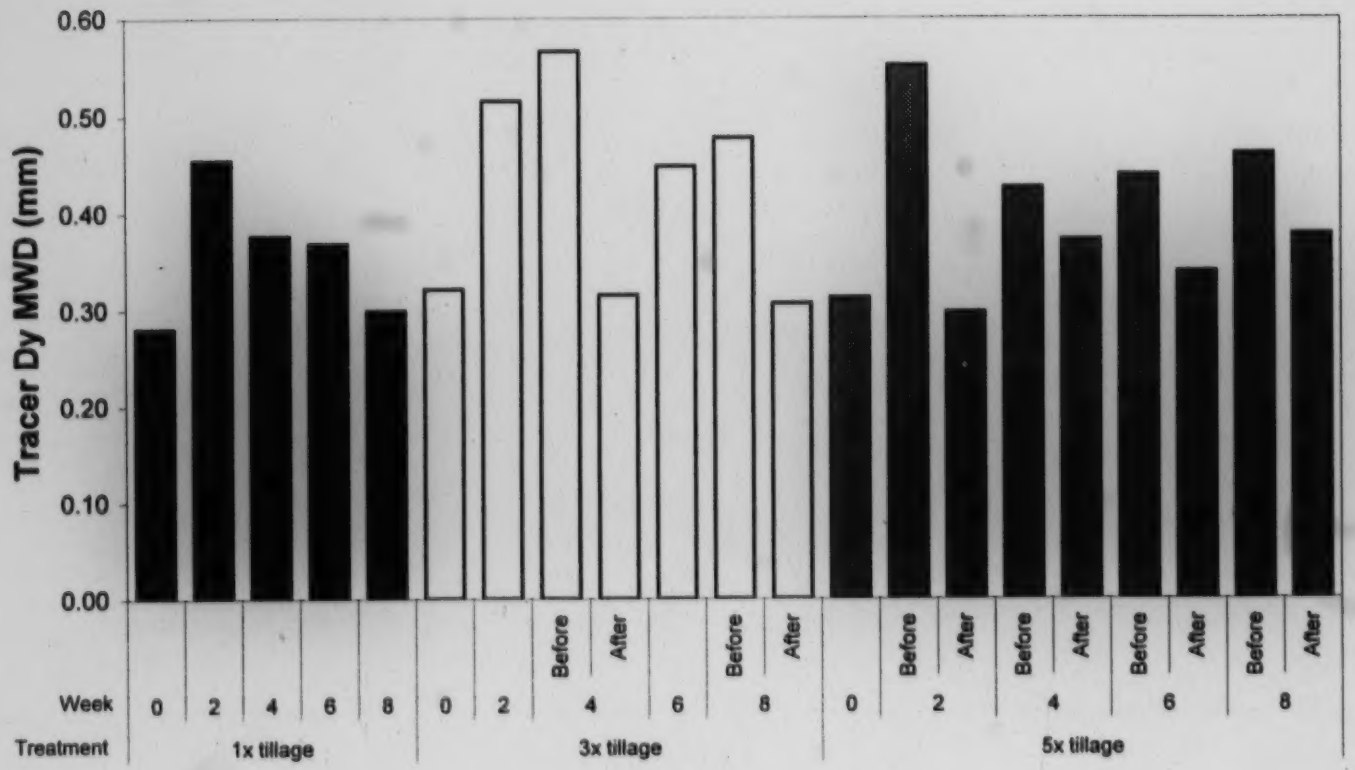

Figure 7-5. Tracer sphere Dy mean weight diameters.

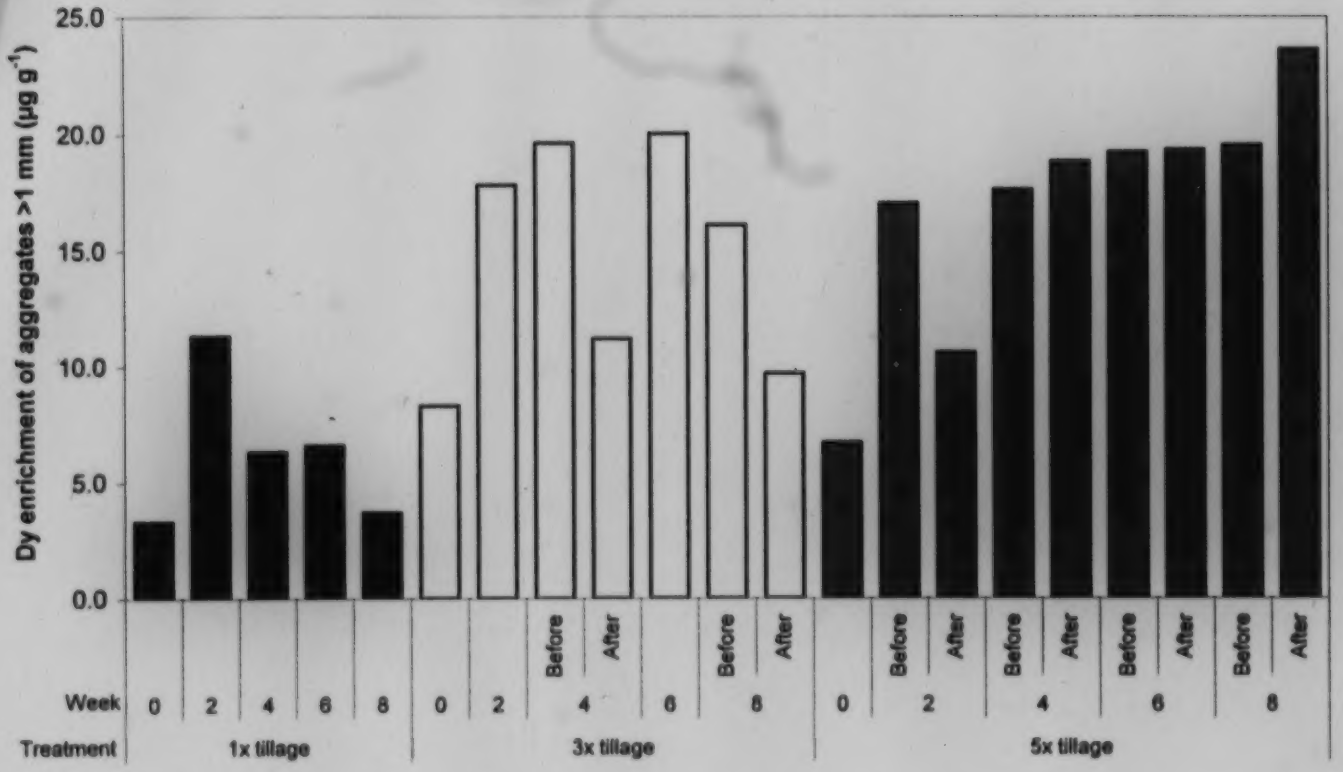

Figure 7-6. Tracer Dy enrichment of pooled water-stable aggregates >1 mm.

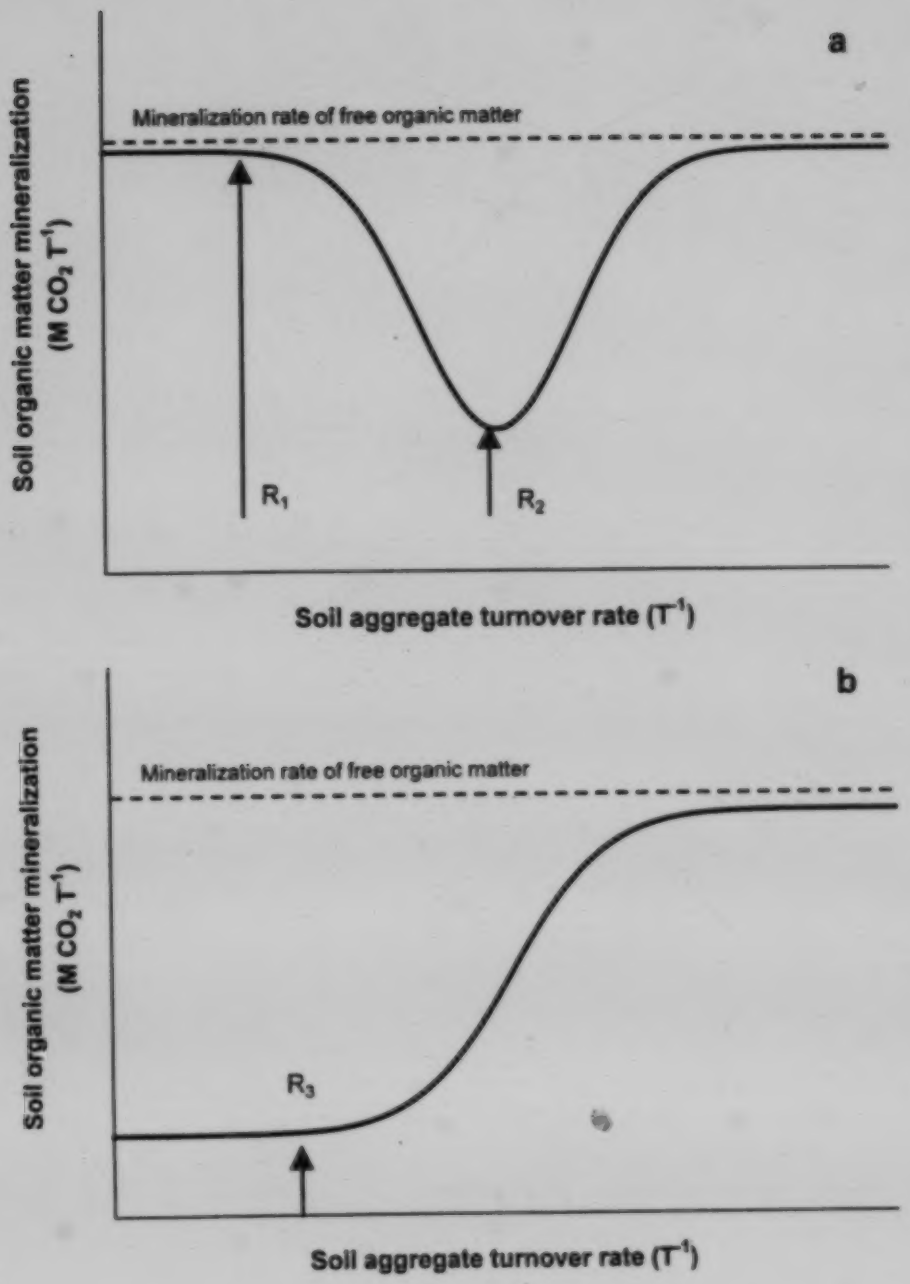

Figure 7-7. Conceptual representation of the relationships between soil aggregate turnover and organic matter mineralization for (a) incoming, initially free organic matter, and (b) native, protected organic matter.

References

Balesdent J., Chenu C. and M. Balabane. 2000. Relationship of soil organic matter dynamics to physical protection and tillage. Soil Till. Res. 53:215-230.

Barlett J.R. and H.E. Doner. 1988. Decomposition of lysine and leucine in soil aggregates: adsorption and compartmentalization. Soil Biol. Biochem. 20:755-759.

Beare M.H., Cabrera M.L., Hendrix P.F. and D.C. Coleman. 1994. Aggregate-protected and unprotected organic matter pools in conventional- and no-tillage soils. Soil Sci. Soc. Am. J. 58:787-795.

Boutton T.W. 1991. Stable C isotope ratios of natural materials: II. Atmospheric, terrestrial, marine, and freshwater environments. p. 173-185. *In* D.C. Coleman and B. Fry (ed.) Carbon isotope techniques. Academic Press, San Diego, CA.

Cerling T.E., Solomon D.K., Quade J. and J.R. Bowman. 1991. On the isotopic composition of carbon in soil carbon dioxide. Geochim. Cosmochim. Acta. 55:3402-3405.

Christensen B.T. 1996. Matching measurable soil organic matter fractions with conceptual pools in simulation models of carbon turnover: Revision of model structure. p. 143-159. *In* D.S. Powlson et al. (ed.) Evaluation of soil organic matter models. NATO ASI Series, Vol. I 38. Springer-Verlag, Berlin Heidelberg.

Craswell E.T. and S.A. Waring. 1972. Effect of grinding on the decomposition of soil organic matter. II. Oxygen uptake and nitrogen mineralization in virgin and cultivated soils. Soil Biol. Biochem. 4:435-442.

Ellert B.H. and H.H. Janzen. 1999. Short-term influence of tillage on CO_2 fluxes from a semi-arid soil on the Canadian prairies. Soil Tillage Res. 50:21-32.

Elliott E.T. 1986. Aggregate structure and carbon, nitrogen and phosphorous in native and cultivated soils. Soil Sci. Soc. Am. J. 50:627-633.

Elliott E.T., Paustian K. and S.D. Frey. 1996. Modeling the measurable or measuring the modelable: A hierarchical approach to isolating meaningful soil organic matter fractions. p. 161-179. *In* D.S. Powlson et al. (ed.) Evaluation of soil organic matter models. NATO ASI Series, Vol. I 38. Springer-Verlag, Berlin Heidelberg.

Golchin A., Oades J.M. Skjemstadt J.O. and P. Clarke. 1994a. Study of free and occluded particulate organic matter in soils by solid state ^{13}C CP/MAS NMR spectroscopy and scanning electron microscopy. Aust. J. Soil Res. 32:285-289.

Golchin A., Oades J.M. Skjemstadt J.O. and P. Clarke. 1994b. Soil structure and carbon cycling. Aust. J. Soil Res. 32:1043-1068.

Gregorich E.G. and B.H. Ellert. 1993. Light fraction and macroorganic matter in mineral soils. *In* M.R. Carter (ed.) Soil Sampling and methods of Analysis. Canadian Society of Soil Science, Lewis Publishers, Boca Raton FL.

Gregorich E.G., Kachanoski R.G. and R.P. Voroney. 1989. Carbon mineralization in soil size fractions after various amounts of aggregates disruption. J. Soil Sci. 40:649-659.

Harris D., Porter L.K. and E.A. Paul. 1997. Continous flow isotope ratio mass spectrometry of carbon dioxide trapped as strontium carbonate. Commun. Soil Sci. Plant Anal. 28:747-757.

Jans-Hammermeister D.C., McGill W.B. and R.C. Izaurralde. 1997. Management of soil C by manipulation of microbial metabolism: Daily vs. pulsed C additions. p. 321-333. *In* R. Lal et al. (ed.) Soil processes and the carbon cycle. CRC Press, Boca Raton FL.

Jastrow J.D., Boutton T.W. and R.M. Miller. 1996. Carbon dynamics of aggregate-associated organic matter estimated by carbon-13 natural abundance. Soil Sci. Soc. Am. J. 60:801-807.

Kuzyakov Y., Friedel J.K. and K. Stahr. 2000. Review of mechanisms and quantification of priming effects. Soil Biol. Biochem. 32:1485-1498.

Mary B., Mariotti A. and J.L. Morel. 1992. Use of ^{13}C variations at natural abundance for studying the biodegradation of root mucilage, roots and glucose in soil. Soil Biol. Biochem. 24:1065-1072.

Puget P., Besnard E. and C. Chenu. 1996. Une méthode de fractionnement des matières organiques particulaires des sols en fonction de leur localization dans les agrégats. C.R. Acad. Sci. Paris. 322:965-972.

Puget P., Chenu C. and J. Balesdent. 1995. Total and young organic carbon distributions in aggregate of silty cultivated soils. Eur. J. Soil Sci. 46:449-459.

Rochette P. and D.A. Angers. 1999. Soil surface carbon dioxide fluxes induced by spring, summer, and fall moldboard plowing in a sandy loam. Soil Sci. Soc. Am. J. 63:621-628.

Santruckova H. Bird M.I. and J. Lloyd. 2000. Microbial processes and carbon-isotope fractionation in tropical and temperate grassland soils. Functional Ecol. 14:108-114.

Schweizer M., Fear J. and G. Cadish. 1999. Isotopic (^{13}C) fractionation during plant residue decomposition and its implications for soil organic matter studies. Rapid Comm. Mass Spec. 13:1284-1290.

Six J., Elliott E.T. and K. Paustian. 1999. Aggregate and soil organic matter dynamics under conventional and no-tillage systems. Soil Sci. Soc. Am. J. 63:1350-1358.

Six J., Elliott E.T., Paustian K. and J.W. Doran. 1998. Aggregation and soil organic matter accumulation in cultivated and native grassland soils. Soil Sci. Soc. Am. J. 62:1367-1377.

Chapter 8:

General Discussion and Conclusions

1.0 Synthesis

Recent literature on the turnover of soil aggregates suggests that rapid aggregate turnover, such as in cultivated soil, promotes soil organic matter turnover and a concomitant decrease in soil aggregation. However, a significant deficit of direct measurements of soil aggregate dynamics exists in the literature. The overall objective of the research reported in this thesis was to observe and quantify soil aggregate dynamics to better understand the role that aggregation plays in the physical protection of soil organic matter. This research has achieved the stated objective by reporting results from several experiments. We have reported on the development of a particle tracer method that can be used to observe and measure soil aggregate dynamics. Observations in field and laboratory experiments have provided data on the gross turnover of soil aggregates. Finally, these data have been used in an attempt to quantify and compare the turnover of soil aggregates in soils with contrasting organic matter turnover. Results have shown that aggregate turnover results in not only the release of organic matter, but also its protection through occlusion in newly formed aggregates. Threshold rates of aggregate turnover are proposed such that a soil will protect rather than release organic matter.

2.0 Summary of findings

2.1 Chapter 2: A tracer particle method for the study of soil aggregate dynamics

Macrolite® ceramic spheres enriched with Dy were selected as tracer analogues for soil particles and aggregates. The use of the ceramic spheres is preferred over other tracers because the tracer simulates soil aggregate properties. The dysprosium label permits the use of a rapid, routine, and non-destructive INAA detection technique. Coefficients of variance for various measured sphere characteristics ranged from 5% to 54%. Such high variability caused some concern, however results of detection limit trials indicate that the over-all variability was insufficient to affect the quantification of tracer spheres. The inert tracer approach, with detection and quantification by INAA, offers the specificity of a

radiotracer approach to directly observe soil aggregate dynamics without the need for tracer extraction.

2.2 Chapter 3: Calibration of a wet sieving procedure to study aggregate dynamics

Wet sieving is a standard procedure for determining the size distribution of water-stable soil aggregates. Results of the procedure can be subject to variability caused by moisture content at time of sieving, sieve loading, and to a lesser degree antecedent soil moisture content. However, calibration trials showed that the distribution of tracer spheres in aggregate size fractions was unaffected by these factors. While some tracer impedance occurred in all cases, tracer incorporation occurred only in pre-treatments involving mixing and incubation of soil samples. Simulated tillage created new tracer Dy-containing aggregates even though many aggregates were destabilized and a decreased soil MWD was measured.

2.3 Chapter 4: Soil aggregate turnover in two contrasting field soils

During a two-year field study performed at the Ellerslie and Breton research stations, tracer spheres were detected in larger aggregate fractions than allowed by their size, providing a direct observation of aggregate formation during the internal cycling, or turnover, of soil aggregates occurring within a growing season. During incorporation, the tracers moved directly into the largest aggregate fraction suggesting that macroaggregates are formed first and subsequently degrade to form smaller aggregates. Soil aggregation, as represented by soil aggregate mean weight diameter, followed a cyclical pattern that is reset by the over-winter period and tillage. Tracer incorporation approached equilibrium with soil aggregates within the study period, reflecting a rapid turnover of aggregates in both soils studied. Based on observations of aggregate turnover in soils with contrasting organic matter contents, we suggest that rapid aggregate turnover may not always result in the loss of organic matter but may also provide a mechanism for physical protection.

2.4 Chapter 5: A quantitative model of soil macroaggregate dynamics

We developed a quantitative compartmental model of water-stable soil macroaggregate dynamics because the quantification of aggregate turnover is essential to testing any hypothesis concerning the relationship between aggregate turnover and organic matter

decomposition. Aggregate dynamics were modelled using four compartments representing three macroaggregate fractions (> 4, 2-4, 1-2 mm) and a pooled fraction (< 1 mm). The flow of soil aggregate components into and out of macroaggregate size fractions was described using first order kinetics. The best fitting model structure was a non-random arrangement of aggregate components and soil-specific patterns of aggregation. Mean residence times of the model aggregate components ranged from 4 to 95 days, and were generally 2-3 times more rapid in the Breton soil than in the Malmo soil. Model prediction of the pattern of tracer sphere incorporation was poor for the Malmo soil and good for the Breton soil, however the model was able to predict tracer Dy MWD. While the model has limitations, it makes no assumptions about flows of soil materials, it fits temporal changes in measured soil aggregate size distributions, and we believe it is the first attempt to quantitatively describe soil aggregate dynamics reported in the literature.

2.5 Chapter 6: Linking active organic matter dynamics with aggregate dynamics

Results of biochemical analyses on two contrasting field soils have shown that the Breton soil respired a greater proportion of its organic C. Results showed that higher organic matter turnover in a low C soil is reflected in a more rapid aggregate turnover, when compared to a high C soil. Observations of lower relative respiration in the Malmo soil suggest that aggregate turnover occluded organic materials, thereby reducing its mineralization. These results support the hypothesized feedback process of self-protection of organic matter proposed in the literature, which suggests that organic matter protection is enhanced in soils with high organic matter content. The mechanism proposed for self-protection is a reduced aggregate turnover rate due to increased aggregate stability afforded by organic matter enrichment of aggregates.

2.6 Chapter 7: Physical protection of organic matter under simulated tillage

An eight-week laboratory experiment showed that increased frequency of simulated tillage increased the incorporation of tracer spheres into stable aggregates, and reduced the total amount of CO_2 evolved during the experiment. We proposed that organic matter retention through a reduction of the priming effect afforded by the increased aggregate

turnover and the formation of new aggregates that occluded added POM thereby reducing its availability for mineralization by the microbial population and increasing its association with reactive surfaces. While there appears to be a disparity between short-term tillage-enhanced organic matter protection and the long-term decreases in organic matter content observed in cultivated soils, the results suggest that there may be threshold rates of aggregate turnover that will protect rather than release organic C.

3.0 Implications and speculations

3.1 Measuring aggregate and organic matter turnover

There is an apparent disparity between the hypotheses in the literature that attribute organic matter losses in cultivated soils to aggregate turnover, and our suggestion that aggregate turnover promotes the physical protection of organic matter. However, the lack of a consistent relationship between aggregate turnover and organic matter storage in soils is perhaps because inferences concerning aggregation have an implicit net aggregate process, or "direction".

Under net soil aggregate disruption conditions, organic matter is usually released if it is already stored within the aggregates. Several experiments have demonstrated an increase in soil respiration from macroaggregates crushed to microaggregate size compared to intact macroaggregates and intact microaggregates (e.g. Elliott 1986). Other experiments have shown a decrease in soil aggregation and losses of organic matter in conventional-tilled soils compared to no-till (e.g. Six et al. 1998). On the other hand, organic matter is usually occluded if it is currently free under net soil aggregate formation conditions. In a prairie restoration experiment, Jastrow (1996) showed a rapid increase in macroaggregation and a slower increase in organic matter. The results led Jastrow to conclude that aggregate formation was a precursor to organic matter accrual.

However, other patterns of organic matter exchange with aggregates occur in soils in addition to the two simplified extremes described above. Puget et al. (1996) reported that a greater proportion of particulate organic matter was occluded in tilled soils compared to no-till soils, even though the total amount of POM recovered in the tilled soil was lower. Wander and Yang (2000) also reported a higher proportion of occluded POM under

tillage, and slower C turnover rates in the tilled treatment compared to no-till. In the current study, we found that tracer particles, and hypothetically particulate organic materials, were occluded into newly formed aggregates even when the overall level of aggregation in the soil was decreasing (Chapters 3 and 7). Clearly, both aggregate formation and disruption can occur simultaneously, but only the net difference can be observed over the long-term. Therefore, measuring gross aggregate turnover may be more important than the net direction of aggregation to elucidate the capacity of a soil to protect organic matter.

Because a given aggregate MWD can describe an infinite number of aggregate size distributions, a soil may posses a rapid rate of gross aggregate turnover without any detectable change in soil aggregate MWD and therefore periodic measurements of MWD provide data only on net aggregation and no information about gross turnover. Measurements of gross aggregate turnover provide an insight into the opportunities for the exchange of organic materials between free and occluded states and therefore on the potential for a soil to protect or release organic matter. While the measurement of gross soil aggregate turnover is more intensive than temporal measurements of aggregate MWD, any conclusions about the ability of a soil to physically protect organic matter can only be achieved by knowing the gross dynamics of soil aggregate formation and disruption, and not simply net aggregation. A labelled particle tracer approach is the best method to date for measuring gross soil aggregate turnover.

3.2 Soil aggregate turnover and the protection of organic matter

Section 6.2 of Chapter 1 reviewed some of the studies that have examined the change in organic matter decomposition by association with soil aggregates. Jastrow and Miller (1998) illustrated three categories of mechanisms responsible for the stabilization of organic matter in soils: 1) biochemical recalcitrance, 2) chemical stabilization, and 3) physical protection (see Fig. 1 in Jastrow and Miller (1998)). Labile organic matter is "physically protected" through a soil matrix (aggregate) control over microbial access to the substrate. The most common evidence proposed for this phenomenon is the increase in respiration measured after the disruption of soil aggregates (e.g. Elliott 1986; Beare et

al. 1994). These studies proposed that crushing macroaggregates released occluded organic matter and made the substrate available for decomposition. The relationship between soil aggregate turnover and this mechanism of organic matter protection is evident. The turnover of aggregates provides the opportunity for organic matter occlusion into aggregates (this is currently underemphasized in the literature), and the opportunity for the exposure of previously occluded organic matter. However, what remains unknown is the extent to which aggregate turnover alter the spatial relationship between the microbial biomass, labile substrates, and more humified soil organic matter, and the potential to create positive or negative "priming effects" through the spatial reorganization of these components.

While soil aggregate turnover clearly provides a mechanism for physical protection, it may also play a significant role in the chemical stabilization of organic matter; the second mechanism proposed for organic matter stabilization. Physical protection of organic matter by occlusion in aggregates is likely only the first step toward long-term organic matter stabilization. Jastrow (1996) showed that most of the organic C accumulated in a field experiment was rapidly associated with the mineral fraction. Occlusion into aggregate may not only physical separate organic matter from decomposers, but may also provide the opportunity for the organic matter to interact with the reactive surfaces of organo-mineral complexes and clay domains. While the physical mechanism of protection is temporary (as evidenced by crushing experiments), interaction with reactive surface while the organic matter is occluded may provide a longer-term stabilization mechanism. Soil aggregate turnover may provide the opportunity for organic matter to periodically interact with different, and potentially more reactive surfaces, thus provided a greater opportunity for long-term stabilization.

The lack of a single relationship between soil aggregate turnover and the protection of soil organic matter is likely because the response of organic matter turnover to aggregate turnover is a balance between the physical separations between substrates and decomposers, and the interactions of organic materials with reactive surfaces.

3.3 The potential for tillage-enhanced physical protection of organic matter to maximize C sequestration

The location of organic matter within the soil matrix has a profound effect on its fate. At the pedon scale, tillage greatly alters the distribution of organic C through the depth profile. Generally, no-till systems concentrate organic residues at, or just below the soil surface (0-5 cm) while tilled systems distribute organic residues more homogeneously through the soil profile (0-30 cm) (Balesdent et al. 1990, Wander et al. 1998). Tillage also alters the spatial distribution of organic C at the aggregate scale. Several researchers (e.g. Golchin et al. 1994; Puget et al. 1996) have developed physical fractionation schemes of soil and organic matter that distinguish between particulate organic matter that is outside of aggregates (free POM) or occluded within them (iPOM). As previously noted, studies have shown that even when total soil POM decreases under tillage, the proportion of iPOM is usually higher (Puget et al. 1996; Wander and Yang 2000).

The implementation of no-till management systems has been recommended as a measure to sequester soil organic C in the aim of reducing CO_2 emissions from soil (Kern and Johnson 1993). However, some soils cannot be managed under no-till conditions, and other soils have not sequestered more C under no-till management (Wander et al. 1998). If the aim is to maximize organic C sequestration in soils, then increases in the soil volume involved in the sequestration will be required. One way to achieve this is to till the soil in order to place more organic C deeper. In addition, one might speculate that C sequestration via the concentration of organic residues above the soil surface may come at a cost of decreased soil quality and fertility, as 300-year old experiments have shown that the incorporation of crop residues increases soil fertility (Warkentin 2000).

In addition to increasing the soil volume involved in C sequestration, the biophysical means by which organic C is sequestered must be considered. Jastrow et al. (1996) showed that accrued C is rapidly associated with the mineral fraction. Based on changes in the carbon content of different soil particle size classes, Hassink (1997) proposed that organic matter association with soil minerals is limited and the protective capacity of the silt and clay fraction can be saturated. Therefore, further increases in sequestered C will

likely have to be in the particulate form and the incoming POM will need to be protected from mineralization. Aggregate occlusion will become an important process in maximizing C sequestration.

Based on differences in organic matter and soil aggregate turnover in two contrasting soils and the increased incorporation of materials under increased tillage frequency in laboratory incubated soils, we have proposed that a given soil may have threshold rates of aggregate turnover or set of conditions under which aggregate turnover will result in a gain versus a loss of stored organic C (Chapters 6 and 7). However, the required tillage frequency of a given soil that will induce the desired soil aggregate turnover rate to promote organic matter protection remains unknown. We speculate that if occlusion in aggregates reduces organic matter turnover, and if tillage promotes occlusion of materials in aggregates (based on our observations), then the physical protection of organic matter, and therefore C sequestration, will be maximized under a scheme of periodic- rather than no-tillage or that the targeted increases in soil C may be achieved more rapidly under a scheme of periodic tillage, rather than conversion to no-till. A no-till system may have too slow an aggregate turnover, such that any incoming organic materials are mineralized before they can be protected. A single tillage event may release some C, but several may induce an aggregate turnover rate that protects a greater proportion of the incoming C[1].

4.0 Future research

The work reported in this thesis provides a first attempt at directly observing soil aggregate dynamics, including aggregate formation, disruption, and internal cycling or turnover. Further work should seek to compliment the findings reported in previous chapters by performing some of the following investigations.

4.1 Observing particle tracer dynamics from initially complete incorporation

Both the field study and laboratory incubation reported in previous chapters used initially free tracer particles and observed their subsequent incorporation into aggregates as new

---

[1] Of course none of these speculations accounts for the C cost of the fuel consumption for tillage.

aggregates were formed. Tracer incorporation into new aggregates may occur under conditions of net aggregate formation in the soil, or under conditions of internal turnover without net aggregate formation or disruption. Experiments observing the redistribution of tracer particles from initial complete incorporation in the largest aggregates would provide observations of the behaviour of soil particles and aggregates under conditions of degradation, or again internal turnover with no net formation or disruption. The combination of these data with those generated from experiments with initially free tracer should provide a complete description of aggregate dynamics without the bias of "direction" described above.

4.2 Simultaneous observations of different sized particle tracers

A significant limitation in the work using the tracer particle method reported in previous chapters is that the tracer had a defined size and therefore can represent only a fraction of the soil aggregates that the tracers are meant to analog. It is hypothesized that soil particles, aggregates, and therefore tracers of differing size will have differing dynamics of formation and disruption in soil. Studies need to be performed to simultaneously observe the differing dynamics of tracers of differing sizes, which can be achieved using different elemental labels (e.g. "colours") for each size fraction and INAA for their detection. For instance, the largest tracers may be labelled with Dy, an intermediate size labelled with Eu, and the smallest fraction labelled with Sm. Label selection should use similar criteria as those outlined in Chapter 2, and insure that the energies of decay are sufficiently resolved to prevent interference during detection and quantification by INAA.

4.3 Comparing particle tracer dynamics in tilled versus no-till field soils

Perhaps the most significant challenge to the acceptance of the findings reported in the previous chapters is corroborating the increased retention of organic matter under frequent simulated tillage found in short-term incubation studies, with the observations of long-term decreases in organic matter and aggregation with continuous cultivation reported in the literature. Several authors have proposed that the rate of soil aggregate turnover in conventional versus no-till soils is a significant contributor to the loss of

organic matter in conventionally tilled soils, however none of these authors report direct measurements of soil aggregate turnover. The solution proposed is to apply a tracer particle method in a field experiment comparing tilled versus no-till soils. The challenge to this approach is to properly apply tracers to the no-till soil such that they are homogeneously distributed through the soil volume of interest without disturbing the equilibrium established by no-till management.

References

Balesdent J., Mariotti A. and D. Boisgontier. 1990. Effect of tillage on soil organic carbon mineralization estimated from ^{13}C abundance in maize fields. J. Soil Sci. 41:587-596.

Beare M.H., Cabrera M.L., Hendrix P.F. and D.C. Coleman. 1994. Aggregate-protected and unprotected organic matter pools in conventional- and no-tillage soils. Soil Sci. Soc. Amer. J. 58:787-795.

Elliott E.T. 1986. Aggregate structure and carbon, nitrogen, and phosphorous in native and cultivated soils. Soil Sci. Soc. Am. J. 50:627-633.

Golchin A., Oades J.M., Skjemstad J.O. and P. Clarke. 1994. Study of free and occluded particulate organic matter in soils by solid state ^{13}C CP/MAS NMR spectroscopy and scanning electron microscopy. Aust. J. Soil Res. 32:285-309.

Hassink J. The capacity of soils to preserve organic C and N by their association with clay and silt particles. Plant Soil. 191:77-87.

Jastrow J.D. and R.M. Miller. 1998. Soil aggregate stabilization and carbon sequestration: Feedbacks through organomineral associations. *In* R. Lal et al. (eds.) Soil Processes and the Carbon Cycle. CRC Press, Boca Raton FL.

Jastrow J.D., Boutton T.W. and R.M. Miller. 1996. Carbon dynamics of aggregate-associated organic matter estimated by carbon-13 natural abundance. Soil Sci. Soc. Am. J. 60:801-807.

Jastrow J.D. 1996. Soil aggregate formation and the accrual of particulate and mineral-associated organic matter. Soil Biol. Biochem. 28:665-676.

Puget P., Besnard E. and C. Chenu. 1996. Une méthode de fractionnement des matières organiques particulaires des sols en fonction de leur localization dans les agrégats. C.R. Acad. Sci. Paris. 322:965-972.

Six J., Elliott E.T., Paustian K. and J.W. Doran. 1998. Aggregation and soil organic matter accumulation in cultivated and native grassland soils. Soil Sci. Soc. Am. J. 62:1367-1377.

Wander M.M. and X. Yang. 2000. Influence of tillage on the dynamics of loose- and occluded-particulate and humified organic matter fractions. Soil Biol. Biochem. 32:1151-1160

Wander M.M. Bidart-Bouzat G. and S. Aref. 1998. Tillage impacts on depth distribution of total and particulate organic matter in three Illinois soils. Soil Sci. Soc. Am. J. 62:1704-1711.

Appendix A:

Tracer sphere application rates to field plots

Applications rates were operationally set to 0.65 kg spheres plot^{-1}, due to limited availability of tracers.

$$= 0.65 \frac{\text{kg sphere}}{\text{plot}} \times \frac{1 \text{ plot}}{2.75 \text{ m} \times 2.29 \text{ m}}$$

$$= 0.103 \frac{\text{kg sphere}}{\text{m}^2} \times \frac{1}{0.15 \text{ m (tillage depth)}}$$

$$= 0.688 \frac{\text{kg sphere}}{\text{m}^3}$$

at Ellerslie
Bulk density = 1.1 Mg m^{-3}

$$= 0.688 \frac{\text{kg sphere}}{\text{m}^3} \times \frac{1 \text{ m}^3}{1.1 \text{ Mg}}$$

$$= 0.626 \frac{\text{kg sphere}}{\text{Mg}}$$

$$= 0.626 \frac{\text{mg sphere}}{\text{g soil}}$$

In 1998:

$$= 0.626 \frac{\text{mg sphere}}{\text{g soil}} \times \frac{0.158 \text{ mg Dy}}{\text{mg sphere}}$$

$= 0.0989$ mg Dy g^{-1} soil

And in 1999:

$$= 0.626 \frac{\text{mg sphere}}{\text{g soil}} \times \frac{0.133 \text{ mg Dy}}{\text{mg sphere}}$$

$= 0.0833$ mg Dy g^{-1} soil

at Breton
Bulk density = 1.4 Mg m^{-3}

$$= 0.688 \frac{\text{kg sphere}}{\text{m}^3} \times \frac{1 \text{ m}^3}{1.4 \text{ Mg}}$$

$$= 0.491 \frac{\text{kg sphere}}{\text{Mg}}$$

$$= 0.491 \frac{\text{mg sphere}}{\text{g soil}}$$

In 1998:

$$= 0.491 \frac{\text{mg sphere}}{\text{g soil}} \times \frac{0.158 \text{ mg Dy}}{\text{mg sphere}}$$

$= 0.0776$ mg Dy g^{-1} soil

And in 1999:

$$= 0.491 \frac{\text{mg sphere}}{\text{g soil}} \times \frac{0.133 \text{ mg Dy}}{\text{mg sphere}}$$

$= 0.0653$ mg Dy g^{-1} soil